



JFS Turbine Engine for Cal Poly Mechanical Engineering Department

Final Design Review
Sponsor: Dr. Patrick Lemieux
06/15/17

Dorian Capps
dcapps@calpoly.edu

Zoe Tuggle
jtuggle@calpoly.edu

JFS Turbine Engine for Cal Poly Mechanical Engineering

by

Zoe Tuggle
Dorian Capps

Project Advisor: Peter Schuster

Instructor's Comments:

Instructor's Grade: _____

Date: _____

Statement of Disclaimer

Since this project is a result of a class assignment, it has been graded and accepted as fulfillment of the course requirements. Acceptance does not imply technical accuracy or reliability. Any use of information in this report is done at the risk of the user. These risks may include catastrophic failure of the device or infringement of patent or copyright laws. California Polytechnic State University at San Luis Obispo and its staff cannot be held liable for any use or misuse of the project.

Table of Contents

List of Figures	7
List of Tables	8
Abstract/Executive Summary.....	10
Chapter 1: Introduction	10
Sponsor Background	10
Problem Definition	10
Objectives/Specification Development	10
Chapter 2: Background	13
The JFS-100 Engine	13
The JFS Turbine Lab at Cal Poly	15
Benchmarking	20
Pulse Detonation Combustors at University of Cincinnati.....	20
JFS Hobbyist Projects	20
Cal Poly BRAE Turbine Senior Project	22
MiniLab and TurboGen	23
Gas Turbine Laboratory Activities.....	25
Benchmarking Summary	26
Chapter 3: Design Development	27
Turbine Disassembly	27
Material Characterization	28
Design Point Thermodynamic and Stress Models	29
3-D CAD Model.....	32
Instrumentation	33
Stage 1: Compressor Inlet.....	33
Stage 2: Compressor Exit	33
Stage 3: Gas Generator Turbine Inlet	33
Stage 4: Power Turbine Inlet.....	35
Stage 5: Engine Exhaust	40
Redundant Throttle Position Sensor.....	40
Laboratory Activity.....	43
Design Development Summary	44
Chapter 4: Description of Final Design.....	45

Instrumentation	45
Stage 1: Compressor Inlet	45
Stage 2: Compressor Exit	45
Stage 3: Gas Generator Turbine Inlet	46
Stage 4: Power Turbine Inlet.....	46
Stage 5: Engine Exhaust	48
General Instrumentation Information	49
JFS Primary Starter	49
Software Programming and Shutoff Algorithms.....	50
Redundant Throttle Position Sensor	51
System Overview.....	51
Position Sensor.....	52
Helical Coupling.....	53
Sensor Bracket	53
Base Plate.....	54
Cost Analysis and BOM	54
Laboratory Activity.....	55
Chapter 5: Manufacturing and Assembly	55
Manufacturing	55
Stage 4 Sensor Housing	55
Containment Ring	56
Power Turbine Housing.....	59
Throttle Position Sensor.....	60
Assembly	61
Chapter 8: Testing and Design Verification	68
Thermocouple Testing	68
Sensor Calibration.....	69
Shutoff Algorithms	70
Engine Startup.....	70
Chapter 9: Conclusions and Recommendations	71
APPENDIX A.....	72
House of Quality	72
Design Safety Hazard Checklist	73

APPENDIX B	75
Drawing Packet	75
JFS-100 Engine	75
Stage 4 Instrumentation	77
Throttle Position Sensor.....	79
APPENDIX C.....	82
Vendor List	82
McMaster-Carr	82
DigiKey	82
Omega.....	82
Grainger	82
Honeywell Sensing	82
APPENDIX D.....	83
Vendor Specification Sheets	83
Thermocouples	83
Pressure Transducers.....	84
Potentiometer.....	90
APPENDIX E	91
Supporting Analysis.....	91
Test Data	92
APPENDIX F	94
Gantt Chart	94
APPENDIX G.....	96
Indented BOM.....	96
Design Verification Plan	97
APPENDIX H.....	98
References	99

List of Figures

Figure 1. LTV A-7 Corsair II in flight [2]	14
Figure 2. Cutaway schematic of the JFS-100 engine [4]	15
Figure 3. Close-up of the compressor intake after the JFS was installed in Cal Poly's Engines Lab	16
Figure 4. Completed installation of the JFS in the test cell.....	17
Figure 5. Schematic of JFS-100 Turbine Engine	17
Figure 6. Stator for the power turbine, almost completely disintegrated	19
Figure 7. Gas-generator turbine blades after over-temperature condition	19
Figure 8. Pulse Detonation Combustion test rig	20
Figure 9. The original Turbokart, powered by a JFS-100 engine [9]	21
Figure 10. JFS-100 engine driving the propeller of a home-built aircraft [10].....	21
Figure 11. GTP350-51 turbine engine upon completion of the 2012 senior project work[11]	22
Figure 12. TurboGen laboratory unit sold by Turbine Technologies[12]	23
Figure 13. User interface of the TurboGen laboratory engine [12]	24
Figure 14. Instrumentation on the SR-30 turbojet engine [12]	24
Figure 15. Energy balance of the SR-30 turbojet engine [13]	25
Figure 16. JFS-100 Engine.....	27
Figure 17. P.T. rotor.....	27
Figure 18. Containment Ring Front.....	27
Figure 19. Containment Ring Rear	27
Figure 20. P.T. Inlet Guide Vanes.....	27
Figure 21. Gas Generator Turbine.....	28
Figure 22. Portable XRF Analyzer [17]	28
Figure 23. 3-D model of the JFS hot section, exploded view	32
Figure 24. Cross section of JFS assembly, gas flow-path is right to left.....	32
Figure 25. Air-start rakes at Stage 3.....	34
Figure 26. Stage 3 Initial Design Instrumentation Assembly	35
Figure 27. Target Stage 4 instrumentation location	36
Figure 28. Stage 4 instrumentation layout	36
Figure 29. Stage 4 temperature instrumentation.....	37
Figure 30. Stage 4 Thermocouple Port	37
Figure 31. Stage 4 pressure instrumentation	38
Figure 32. Stage 4 Pressure Port	39
Figure 33. Radial location of the stage 4 instrumentation, upstream of the air-start rakes	40
Figure 34. Existing fuel control system	41
Figure 35. Close-up of fuel plunger	41
Figure 36. Soft-jaw coupling (left) versus helical coupling (right). [McMaster-Carr]	42
Figure 38. JFS Intake System.....	45
Figure 39. Stage 1 Instrumentation	45
Figure 40. Stage 2 Instrumentation	46
Figure 42. CAD Model of Stage 4 Sensor Housing.....	46
Figure 43. Internal Geometry of the Sensor Housing	47

Figure 44. Final drawing of sensor housing for stage 4	48
Figure 45. Stage 5 Instrumentation	49
Figure 46. Inside of dyno control Box.....	49
Figure 47. Inputs to dyno control box.....	49
Figure 41. Photo of electrical starter installed on JFS.....	50
Figure 48. Entire TPS assembly	52
Figure 49. Exploded view of TPS assembly	52
Figure 50. CTS Series 026 Rotary Potentiometer, Panel-Mount.....	53
Figure 51. Cost Analysis	54
Figure 52. Final Sensor Housing Part with Drawing.....	55
Figure 53. Sensor Housing Installed on Tee fitting w/ Thermocouple.....	56
Figure 54. End of sensor housing with the thermocouple and copper crush washer installed	56
Figure 55. Power Turbine Containment Ring.....	57
Figure 56. Spare Containment Ring Being Machined on Jim's TM-1	58
Figure 57. Straight-Flute Drill Bit.....	58
Figure 58. Final Machining of Actual Containment Ring.....	59
Figure 59. Aluminum vice jaws.....	60
Figure 60. Power Turbine Machining Setup.....	60
Figure 61. Base plate machining setup	60
Figure 62. Stage 3 instrumentation port.....	61
Figure 63. Stage 3 thermocouple inserted through the air-start rakes.....	61
Figure 64. Power turbine IGV ring ready for installation	62
Figure 65. IGV ring installed in the gas-generator assembly, with the bolts safety-wired	62
Figure 66. Thermal insulation wrapped around containment ring prior to installation.....	63
Figure 67. Containment ring installed in power turbine housing	63
Figure 68. Stage 4 instrumentation installed in power turbine.....	64
Figure 69. Stage 4 thermocouple location.....	65
Figure 70. Preparing to mate the gas generator and power turbine assemblies	65
Figure 71. Fully assembled and instrumented engine	66
Figure 72. Installing the engine on the dynamometer	67
Figure 73. Engine fully installed and hooked up to the dynamometer	68
Figure 74. Controller interface including Hypercell display	69
Figure 75. Testing over-speed shutoff conditions using a signal generator	70
Figure 76. The dream team!	71

List of Tables

Table 1. Technical Specifications	11
Table 2. Summary of benchmarking efforts	26
Table 3. Summary of XFR Results.....	29
Table 4. Summary of thermodynamic analysis results	31
Table 5. Design point stress analysis.....	31
Table 6. Summary of stress analysis at design point	31
Table 7. Summary of Important Design Decisions.....	44

Table 8. Programmed warning and shut-off limits	51
Table 9. Worst-case stress analysis results at shut-off conditions	51
Table 10. Results from preliminary thermocouple testing	68

Abstract/Executive Summary

This project concerns the development of a gas turbine engine laboratory activity for use in one of Cal Poly's technical elective courses in the Mechanical Engineering Department, ME 444: Combustion Engine Design. The class is taught by Dr. Patrick Lemieux, who is also in charge of the on-campus engines lab where the turbine engine will be installed. The engine itself is a JFS-100-13A turboshaft engine that will be coupled to an electric dynamometer inside of the dyno test cell. Students taking the ME 444 class, likely starting in Winter Quarter of 2018, will be able to perform hands-on experiments using the JFS-100 to gain insight into the types of components, operating theory, and critical parameters of gas turbine engines.

Chapter 1: Introduction

Sponsor Background

One of Cal Poly Mechanical Engineering's popular technical elective courses, ME 444: Combustion Engine Design, includes a laboratory portion where students work in the Engines Lab to test and characterize real engines. In order to enhance this hands-on learning experience, a laboratory activity is being developed to investigate the performance of small gas turbine engines. A JFS-100-13A turboshaft engine, originally used as an Auxiliary Power Unit (APU) in the A-7 Corsair fighter, is the subject of this activity. This project first involved instrumenting the small turbine engine and designing the control system such that it can be run safely and reliably. Secondly, the engine was installed on one of the lab's dynamometer test stands and its individual components characterized. Lastly, the laboratory exercise that allows for conceptual understanding of how the turbine operates was outlined for incorporation into the lab portion of the class. The three primary stakeholders in this project were:

1. Dr. Lemieux, the Engines Lab coordinator and instructor of ME444
2. The students who will take ME444 in the future.
3. Jim Gerhardt, who is responsible for lab maintenance and technical support.

Problem Definition

Cal Poly students that enroll in the internal combustion engine design class, ME 444, focus on analyzing different thermodynamic cycles. Currently, the lab is limited to studying reciprocating, piston-style engines. The implementation of a JFS-100 gas turbine lab activity would allow students to have a unique learning experience while also applying fundamental concepts from previous thermodynamics courses to gas turbine engines. Previously, the JFS-100 engine instrumentation did not provide adequate control and monitoring of critical turbine conditions for a laboratory setting.

Objectives/Specification Development

The goal of this project was to aid in the development of an insightful and engaging laboratory activity that allows ME 444 students to gain hands-on experience with gas turbine engines and become familiar with their performance parameters. To safely implement the JFS-100 into the ME combustion engine design class, proper instrumentation of the engine was required to safely monitor engine conditions. Backup safety algorithms were added to the engine control unit that shut down the engine if any of the

temperature or pressure readings exceed pre-determined thresholds. After both of these tasks were completed, the engine was reinstalled on the dynamometer to allow for safe and reliable operation. Startup, shutdown, and testing procedure documents were created to ensure all future users are familiar with the necessary process and that the turbine can be used in this lab for many years to come.

Table 1. Technical Specifications

No.	Description	Target	Tolerance	Risk	Compliance
1	Instrumentation capable of accurate measurements at local conditions	varies	min	M	A,I
2	Temperate and Pressure Instrumentation at Stages 1-5	All	min	H	T,I
4	Externally-cooled oil system	65.5	n/a	L	T,I
5	Thermocouples throughout oil circuit	200 ° C	+/- 10 °C	L	I
6	Maximum engine temperature	800 ° C	+/- 10 °C	H	T,I
7	Instrumentation interface with Digalog Controller	yes	n/a	L	T,I
8	Accurate mechanical interface with Digalog Dyno	1 deg	max	M	I
9	System Durability	10 years	min	H	A

L = Low
M = Medium
H = High

T = Testing
I = Inspection
A = Analysis

Customer Requirements:

- Safety
- Reliable
- Ease of operation
- Cost efficient (inexpensive)
- Serviceable
- Educational

The technical specifications for this project were derived from the customer requirements. These were based on Cal Poly lab safety standards and practical measures that could be taken to extend the life of the engine. The general objective that was gathered from these requirements was to make an interesting and educational lab that would be reliable and cost efficient from the standpoint of the instructor, serviceable for the mechanic, and safe for students to operate.

Each of the specifications listed above were used to determine if we successfully met our objectives at the conclusion of the project. These are defined with a target value, an estimated tolerance, the associated risk, and compliance. The target goal is the value we were aiming to reach for system performance. The tolerance is how far we could deviate from the goal and still count it as being met. Risk evaluates how essential the requirement was to the project. Compliance defines how we planned

on assessing the completion of each design objective. A comprehensive description of each of specifications is listed below.

Instrumentation capable of accurate measurements at local conditions.

The sensors needed to have a high degree of accuracy and reliability to monitor the turbine during operation and provide critical data for the lab activity. The sensors for each stage were chosen based off their temperature limitations, and certainty in data measurements. We conducted a thermodynamic analysis to determine the temperature and pressure at each stage, to ensure that the sensors were rated to the appropriate values. The sensors are replaceable and can be changed if necessary, which is why this was assessed as low risk.

Temperature and pressure instrumentation at stages 1-5.

The instrumentation of the turbine itself was one of the most crucial portions of the project. We only have one operating engine, and the integration of sensors required machining close to critical components. This was a high-risk specification because without these sensors, the turbine could exceed the temperature limitations of the materials and ultimately damage the power turbine blades.

Externally-cooled oil system

An externally-cooled oil system ensured proper lubrication of the bearings in the gas generator and power turbine assemblies. This was accomplished by keeping the oil being delivered to the systems at a low temperature, providing greater heat absorption from each component. Failure of this system presents a medium risk level. If the bearings do not receive sufficient cooling, the heat generated from the rotational friction could lead to potential damage of the main components of the turbine. Future testing will involve running the engine for various lengths of time and recording the oil circuit thermocouple readouts.

Installation of thermocouples throughout oil circuit

By integrating thermocouples throughout the oil circuit, we can determine if the gas generator and power turbine bearings are appropriately cooled. If the oil temperature reaches above 200 degrees C, the heat being generated by the rotational friction could damage the bearings and lead to failure of the turbine. The thermocouples used to measure these temperatures are rated to well above the maximum oil temperature.

Maximum engine temperature

The maximum engine temperature is directly related to the material limits of the power turbine, where the highest temperature is located. This was determined from the 1-dimensional thermodynamic analysis of the engine. This was assessed to be high risk because if the engine was to exceed this temperature, significant damage of the turbine blades could result.

Instrumentation interface with Digalog Controller

After the turbine was mounted on the dynamometer, instrumentation interface with the Digalog controller needed to be configured. This involved calibration of sensor readings and mechanical components to ensure the accuracy of the data displayed by the Digalog software. This was first visually

inspected to verify that all connections were in place and attached properly. Secondly, the interface was tested while the engine was running.

Accurate mechanical interface with Digalog Dyno

The accuracy of the instrumentation interface largely depends on how quickly the sensors respond to changes in temperature and pressure. If there is any lag in the transmission of this data to the program interface, the operator could accidentally run the engine incorrectly. An automatic shut off algorithm for the Digalog dynamometer controller was implemented to act as a cut-off switch if the turbine temperature values reach predetermined limits. This system also needed to have accurate inputs in order to operate correctly. The accuracy of the interface was tested by running the engine and determining how quickly the program responds to operation changes. This has been regarded as medium risk, because an inaccurate interface could lead to improper use of the turbine.

System Durability

We have set the turbine life to be close to ten years, based off frequency of use and serviceability. The system durability risk assessment is high due to the fact that if the engine was to fail prematurely, then the entire lab could be compromised. This was verified via stress analysis on critical components and a routine maintenance plan to keep each system running optimally.

Chapter 2: Background

The JFS-100 Engine

The background of this project should begin with a discussion of the JFS-100 engine itself, including original application and design intent. Most military aircraft use large gas turbine engines as their primary propulsion method due to their high power-to-weight ratios and excellent reliability. Considering the scale of these engines, designing a reliable but light-weight starting mechanism can often be a difficult problem. Using only electric motors (similar to automotive starting systems) would require a very large electric machine that would be unlikely to meet flight-weight targets. Another option is to utilize highly compressed air from ground sources to air-start the engines, however this means that the engines could not be re-started once in flight should a flameout or other anomaly occur. The common solution to this problem is known as an Auxiliary Power Unit (APU).¹ These APU's generally consist of a small (50-150 HP range) turboshaft engine that is geared to the shafts of the main engines. The turboshaft itself is started by a small and compact electric motor which is generally integrated into the APU package. This arrangement employs the excellent power-to-weight characteristics inherent to gas turbine engines, and results in a compact, reliable, and relatively light-weight starting unit. The JFS-100 engine, which is the main subject of this project, was designed as one of these APUs. Built by Allied Signal, who was later acquired by Honeywell, the JFS-100 was installed in the LTV A-7 Corsair II (shown in Figure 1), a light attack aircraft primarily used by the United States Air Force and Navy during the Vietnam War. Approximately 1,569 of these planes were made before production ended in 1984. They were officially retired from the U.S. military in 1991.² Upon decommission, many of the APU's were uninstalled and sold to private parties, and over the years most of the JFS engines have been circulating amongst hobbyists.



Figure 1. LTV A-7 Corsair II in flight [2]

The JFS-100 is a two-spool turboshaft engine rated to approximately 90 shaft horsepower. It consists of a single-stage centrifugal (radial outflow) compressor and two axial-flow turbines. The first turbine is on a common shaft with the compressor; when combined with the combustor, this assembly is known as the gas generator and functions as the engine's first "spool." The combustor is of the annular type with five fuel nozzles symmetrically arrayed around the common shaft. A single capacitive ignitor serves to light the engine once it is brought to self-sustaining speed by the electric starter.³ The second turbine, called the "power turbine," is placed in series directly after the gas-generator turbine, but is mounted on a completely separate shaft (spool). This power turbine is connected to the splined output shaft through an integrated 18.3:1 gear reduction, and functions to extract useful work from the hot gases produced by the gas generator. The exhaust exits the power turbine housing radially³. These components can be seen in the cutaway schematic of Figure 2.

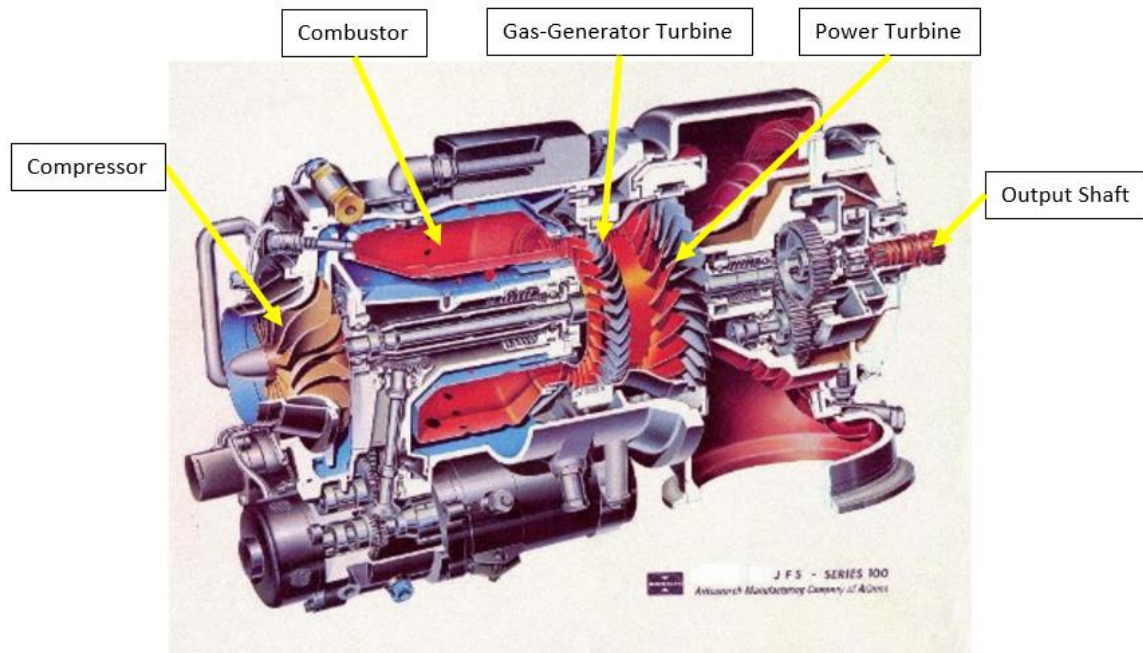


Figure 2. Cutaway schematic of the JFS-100 engine [4]

As the JFS was designed solely as a starter motor, it was never intended to run for longer than 30 seconds at a time. Many sacrifices were made in this regard, namely lower-quality turbine materials (rated for a lower fatigue life) and a low-capacity, uncooled lubrication system. These pose a challenge to anyone seeking to use the engine for continuous-use applications.

The JFS Turbine Lab at Cal Poly

A few years ago at Cal Poly, Professor Lemieux first conceived the idea of integrating a gas turbine-based laboratory activity into the ME 444 technical elective. This class, officially titled "Combustion Engine Design," introduces students to the theory and design of reciprocating (automobile-style) engines, gas turbines, as well as rockets. Unfortunately, however, the hands-on laboratory portion of the class studies primarily reciprocating engines, largely due to their low cost and high availability. In the interest of giving students a broader variety of hands-on experience, Dr. Lemieux endeavored to introduce a practical activity investigating the performance parameters of a real gas turbine engine. The engine would be coupled to a large eddy-current dynamometer already installed in the Engine Lab's test cell, and students would be able to collect experimental data and correlate it to the theory learned in class.

In pursuing this goal of a turbine engine installation in the engines lab, Dr. Lemieux had a variety of engines to choose from. For practicality purposes, and to avoid exceeding the capacity of the dynamometer, the engine had to be a turboshaft engine in the 50-150 HP range (these engines are technically classified as "microturbines"). The JFS-100 quickly became a top contender due to its availability, adequate size, and convenient mounting points. However it was not without competition; for example the T62 engine manufactured by Solar Turbines was strongly considered as well. Unlike the JFS, the T62 is a single-spool engine, in which the drive output, compressor, and turbine are all mounted

to a common shaft, resulting in no separate power turbine. Rated to 80 horsepower, the size, cost, and simplicity matched that of the JFS, and in terms of long-term reliability the T62 appeared superior. However there was a big problem with the T62: the engine's air intake was arrayed around the entirety of the core. Since connecting the air intake to the lab's mass air-flow sensor (with a single pipe outlet) was a necessity in order to accurately characterize the engine, the T62's layout proved very inconvenient and unwieldy. The single pipe inlet leading to the compressor on the JFS created no such problem, and that proved to be the deciding factor when the JFS was selected. After acquiring one of the engines, Dr. Lemieux and Jim Gerhardt began the modifications necessary for the engine to be integrated in the test cell and coupled to the dynamometer. Among many small details, this included design and fabrication of a large-capacity, externally cooled oil system. This was necessary to ensure long-term reliability of the JFS, as the stock lubrication system was undersized for continuous use. After many months of fabrication, the engine was finally installed on the dyno, and initially it ran very well. Figures 3 and 4 show the completed JFS installation in the Cal Poly engines lab.



Figure 3. Close-up of the compressor intake after the JFS was installed in Cal Poly's Engines Lab



Figure 4. Completed installation of the JFS in the test cell.

At this point in the discussion, a short discourse is required on the variation in temperature throughout the different stages of a gas turbine engine, and the importance of monitoring temperature as a critical operating parameter. We will consider specifically the JFS-100 as an example, however many of these principles apply to all gas turbine engines. We will use the numbering convention outlined in Figure 5 to describe the five stages of the JFS, starting with ambient air entering the compressor at Stage 1 and ending with burnt gasses exhausting from the power turbine at Stage 5.

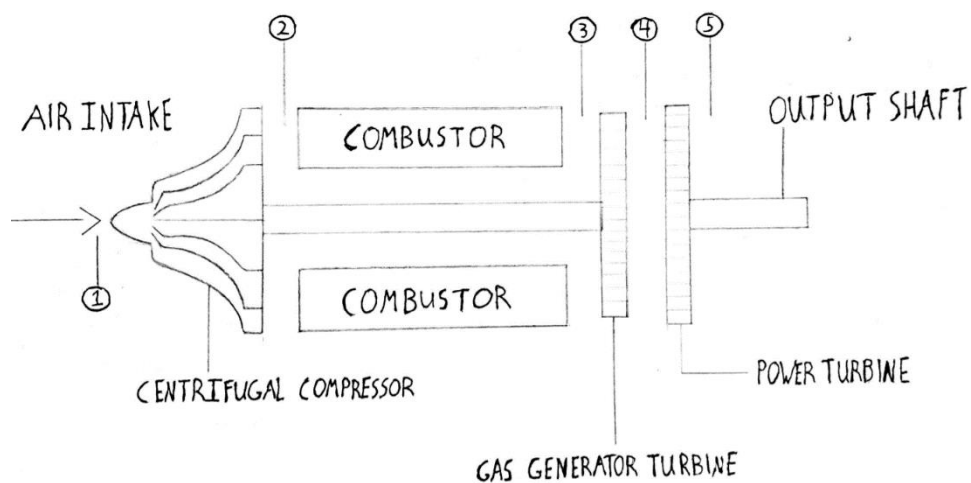


Figure 5. Schematic of JFS-100 Turbine Engine

Following a simple model for compressible flow, air exits the compressor (Stage 2) at both an elevated pressure and temperature. Even for the ideal case of isentropic compression, the temperature is raised proportional to the stage pressure ratio.⁵ Inefficiencies resulting from friction effects, tip clearances, and other details generally cause the temperature to increase further.⁶ This compressed and heated air

enters the combustor where it is mixed with atomized fuel and ignited. The rapid heat release from this reaction causes a drastic temperature spike, and the hot gases are then expanded through the turbines to produce useful work. The first turbine drives the compressor and the second turbine drives the output shaft. From a thermodynamic perspective, a higher temperature at the turbine inlet (T_3) results in a large increase in both power output and thermal efficiency.⁶ Thus, as one would expect, general turbine engine design usually involves maximizing the temperature at this particular location within the limits of the material used for the turbine and housing. Blade cooling using compressor bleed air, ceramic materials, and advanced high-temperature coatings have been very active areas of research in the turbine industry, all with the goal of increasing this temperature capability.⁶ Because the operating temperature at Stage 3 is usually very close to the material limit, it is important for the survival of the engine that this temperature be carefully controlled. Note that there are many more complexities to this, and depending on the application, different engines are designed with varying degrees of safety margin with respect to this temperature parameter.

From the factory, the JFS-100 is instrumented with an Exhaust Gas Temperature (EGT) sensor located at Stage 5. The output from this sensor is used in the integrated control architecture to indicate when an over-temperature condition occurs, by means of illuminating a warning light in the plane's cockpit.² However, from the discussion above it is clear that the temperature at Stage 5 is rarely the peak temperature in the engine, nor does this value directly indicate how close the engine is to its limit.

Returning to the discussion on installing the JFS in Cal Poly's engines lab, the original setup utilized the same EGT sensor as the primary indicator of engine temperature. Assuming careful monitoring and control, this likely would have been entirely sufficient. Unfortunately, however, during a student experiment not long after the JFS was set up, a series of prolonged start attempts distracted attention away from the temperature gauge. By the time Dr. Lemieux, who was overseeing the experiment, noticed that the students were not watching the gauge, the temperature had far exceeded the limit. The engine was shut off immediately, however unfortunately the damage had been done. Figures 6 and 7 shows the gas-generator turbine that was exposed upon subsequent disassembly, indicating catastrophic heat damage throughout.



Figure 6. Stator for the power turbine, almost completely disintegrated



Figure 7. Gas-generator turbine blades after over-temperature condition

It was immediately obvious that the engine either required a complete overhaul or a full replacement. Dr. Lemieux initially pursued the first option, however was unable to come to an agreement with the mechanic who was to perform the work. Ultimately, the decision was made to purchase a brand new engine, which after years of logistical delays arrived at Cal Poly in the Spring of 2016. This new engine, which has logged a remarkably few number of hours and is in excellent condition, is the subject of our project. Through careful design, instrumentation, and control methods, we hope to prevent it from meeting the same fate as its predecessor.

Benchmarking

Pulse Detonation Combustors at University of Cincinnati

Throughout our background research on the JFS-100, we found very little reference to the engine in scientific journals or other peer-reviewed literature. The main exception is a series of studies and experiments performed by the Department of Aerospace Engineering at the University of Cincinnati starting in 2005.^{7,8} The primary goal of this work, which is ongoing, is to study the effects of using pulse detonation combustors (PDC) in place of traditional steady-flow combustors to increase the power and fuel efficiency of aircraft engines. The PDC concept is being considered for direct thrust-based propulsion (where the combustion products are simply expanded through a nozzle), as well as a hybrid propulsion system where the combustors are integrated with an axial power turbine that extracts shaft work. Regarding the latter, since the supersonic combustion shock waves that characterize pulse detonation behave very differently than steady-flow combustion, the researchers needed a way to study the interaction between the PDCs and the power turbine. To do this, they constructed a test rig that incorporated a circular array of six PDC tubes exhausting into an axial-flow power turbine, with the turbine's output shaft coupled to a water-brake dynamometer (Figure 8).

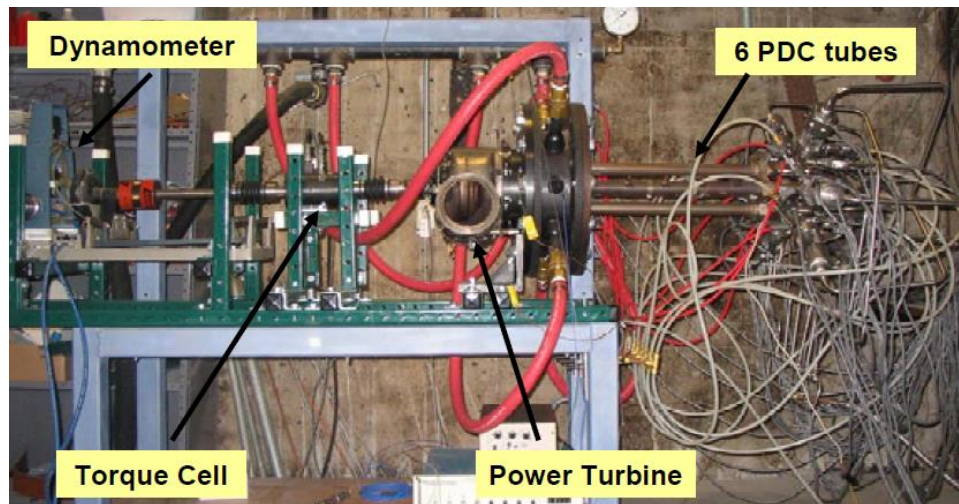


Figure 8. Pulse Detonation Combustion test rig

The relevance to our project involves the particular power turbine that they decided to use: that of a JFS-100. Since the power turbine is a separate assembly that can easily be unbolted from the gas generator portion of the JFS, it was simple and convenient for them to integrate the single turbine into their test setup. The PDC tubes could be operated in both pulse-detonation and steady-flow combustion modes, which allowed for direct comparison of turbine performance under both conditions. This resulted in a thorough characterization of the power turbine itself, data that will be very useful to us for comparison and benchmarking purposes.

JFS Hobbyist Projects

The most common results returned when performing cursory internet searches on the JFS-100 engine generally involve home-built, hobbyist projects using the engine to power some sort of customized vehicle. For example, an ambitious go-kart racer once decided to install a JFS-100 into a heavily modified

kart frame (Figure 9). This project, affectionately named Turbokart, took over four years to complete but resulted in a go-kart that could easily outrun a Ferrari 360 Modena in a quarter-mile drag race.⁹



Figure 9. *The original Turbokart, powered by a JFS-100 engine [9]*

An equally adventurous and significantly more dangerous venture was the installation of a JFS-100 as the primary powerplant for a homebuilt aircraft (Figure 10). While the early stages of this particular build were documented fairly well, it is unclear if the plane was ever flown more than once or twice



Figure 10. *JFS-100 engine driving the propeller of a home-built aircraft [10]*

While documentation and reliable data was often thin on the ground when it came to these projects, they nonetheless provided valuable insight into the performance of the JFS-100 under operating conditions vastly different than what it was designed for. Since most of these applications required continuous operation, the primary obstacle that needed to be overcome was the power turbine's inadequate lubrication system. Some builds (I.e. Turbokart) avoided the problem entirely by removing the power turbine and replacing it with a simple thrust nozzle. This effectively converted the engine from a turboshaft to a turbojet, and simplified the installation significantly. An alternative solution, followed by the aircraft builder shown above and closely matching the work of Dr. Lemieux and Jim Gerhardt on the original Cal Poly JFS setup, involved adding a higher capacity, externally cooled oil system. Additionally, a number of ingenious fuel systems, mounting methods, and other supporting hardware were devised during the course of these individual projects, which will be helpful references as we work out similar details ourselves.

Cal Poly BRAE Turbine Senior Project

Although the JFS program has definitely been the most thorough and detailed work on gas turbines at Cal Poly, there has been another effort at the school to develop and experiment with a real turbine engine. Completely separate from the Engines Lab, and largely unbeknownst to the Mechanical Engineering Department, a BRAE senior project in 2012 involved setting up and characterizing a Garrett AiResearch GTP350-51 turbine (Figure 11).¹¹



Figure 11. GTP350-51 turbine engine upon completion of the 2012 senior project work[11]

The engine was sourced from Avon Aero Supply, however was purchased with little knowledge of the specific condition of the unit. The main goals of the project were to simply get the engine running (which ultimately involved two complete rebuilds) and to design a new control system allowing for more accurate monitoring of engine parameters. While these objectives were met, the engine was never tested on a dynamometer or truly characterized in any way. Nevertheless, the work completed on this engine will provide a good source of information on control methods and general turbine questions. In

fact, we hope to meet with Kyle Smith, the student involved with the project, and have him show us the engine first hand.

MiniLab and TurboGen

The internal combustion engine, including the gas turbine variety, is a subject frequently studied at various educational institutions. Since the end goal of this project is a laboratory activity to be used for teaching purposes, we conducted a thorough investigation of other turbine engine installations used primarily for research or education. Although there are many of these programs, mostly in the engineering departments of well-known universities, there is relatively little variety when it comes to which specific engines they use. In fact, the majority of educational gas turbine labs (at least with any degree of documentation) involved one of two products sold by a small, Wisconsin-based company called Turbine Technologies, LTD.¹² This company manufactures and sells a variety of educational laboratory equipment, designed to help teach many different engineering subjects including structures, controls, and fluid mechanics. However, one of their most popular products, MiniLab, consists of a completely self-contained turbojet engine, complete with fuel system, controls, and a high degree of instrumentation to allow continuous monitoring the engine's operating parameters. A spinoff of this product is called TurboGen (Figure 12), and utilizes the same turbojet engine core (operating as a gas generator) combined with a power turbine and electric generator to measure shaft power.



Figure 12. TurboGen laboratory unit sold by Turbine Technologies[12]

Both of these products are very convenient (although costly) for educational programs that are seeking to introduce a gas turbine laboratory but don't have the time or inclination to build a custom setup from

scratch. As we work to implement a comparable degree of instrumentation into the JFS, the methodology followed by Turbine Technologies provides an excellent source of information and benchmarking. Figure 13 shows the user interface displayed while the TurboGen engine is running, while Figure 14 shows the instrumentation locations on the SR-30 turbojet engine.

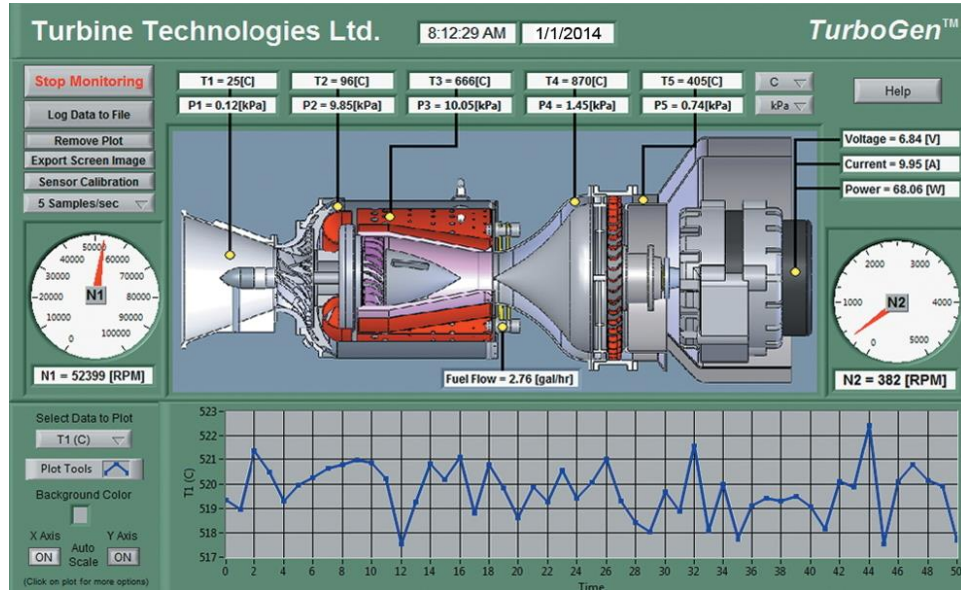


Figure 13. User interface of the TurboGen laboratory engine [12]

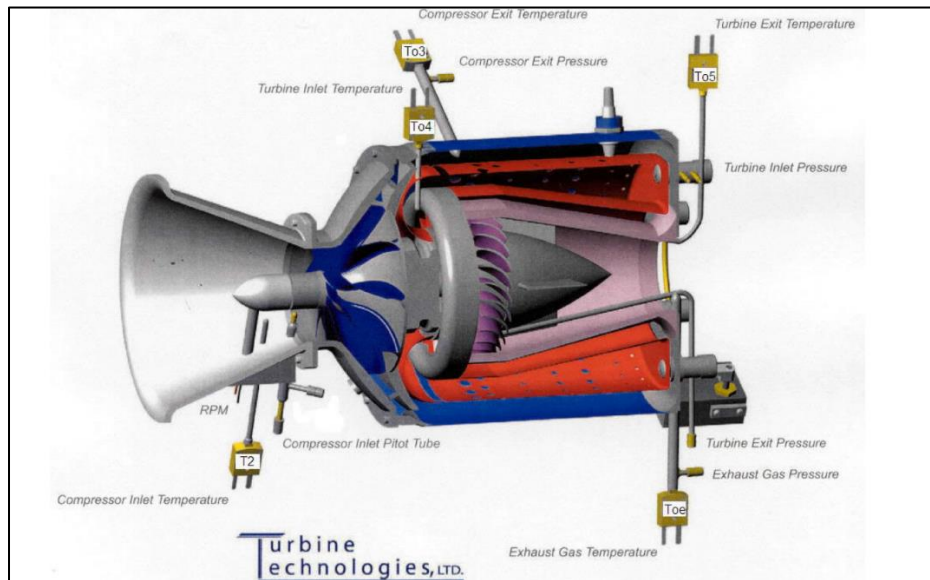


Figure 14. Instrumentation on the SR-30 turbojet engine [12]

Note the similar stage numbering convention as discussed earlier, as well as the temperature and pressure sensors located at all five stages. Gas-generator shaft speed as well as output shaft speed are also carefully monitored, which will be a necessity on the JFS as well. All of this data is used both to ensure safe, reliable operation, and to allow accurate analysis and engine characterization as part of the learning objectives.

Gas Turbine Laboratory Activities

It was made clear from the outset of this project that developing the specific laboratory exercise for ME 444 would be a key deliverable. Accordingly, we performed a large amount of background research on gas turbine labs at other educational institutions. Initially this research proved difficult, however we later found a page on Turbine Technology's website that included links to 20+ papers detailing the laboratory procedure that a variety of schools use in combination with the TurboGen and MiniLab products described above. For example the University of Minnesota performs a series of experiments called "Characterizing the Performance of the SR-30 Turbojet Engine" with undergraduate engineering students¹³. The primary objectives of this exercise are to perform a thermodynamic analysis on the SR-30 engine, investigate the impact of sensor location on experimental results, and characterize component efficiencies. One of the lab's deliverables is a visual aid known as an "energy balance," which shows exactly how the fuel energy is converted into other forms of energy. This graphic is depicted in Figure 15. Additionally, while many of the activities followed similar investigations of thermal efficiency and performance, this particular laboratory performed an interesting investigation into the effect of temperature sensor location. Since a one-dimensional thermodynamic analysis requires bulk average fluid properties, care must be taken to ensure that the obtained data closely represents these average properties. To highlight this importance, the lab initially placed the compressor outlet temperature probe too close to the combustion chamber. This caused very high temperature readings in this location, and when the data was used for the thermodynamic analysis the results made little sense. Students were then tasked with finding the best radial location for the temperature sensor such that the measurements most accurately reflected the average fluid properties.

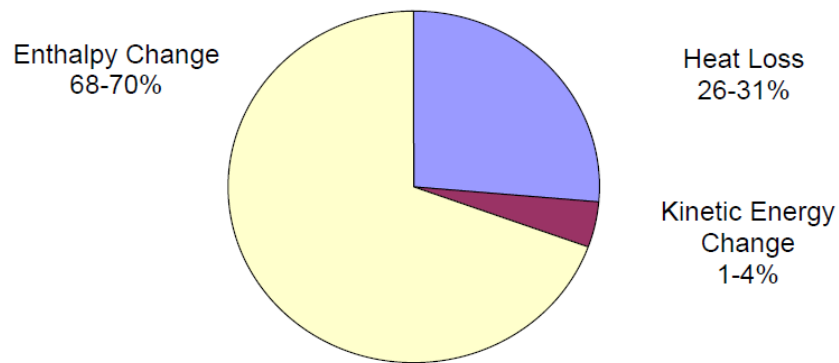


Figure 15. Energy balance of the SR-30 turbojet engine [13]

Benchmarking Summary

Table 2 shows a summary of our benchmarking process. It cites the specific reference and summarizes the main points that we took away from each project. Both hardware and lab activity benchmarking are included.

Table 2. *Summary of benchmarking efforts*

Reference	Highlights
University of Cincinnati Pulse Detonation Combustors ^{7,8}	<ul style="list-style-type: none"> • Characterized JFS power turbine under both steady flow and pulse detonation conditions • Average turbine-inlet temperature did not exceed 900 degrees F
JFS Hobbyist Projects ^{9,10}	<ul style="list-style-type: none"> • Installed JFS Engine in kart, homebuilt aircraft • Almost universally replaced the power turbine with a thrust nozzle for simplicity and cooling reasons • Some temperature limits were established, but no test data or validation available
Cal Poly BRAE Turbine Senior Project ¹¹	<ul style="list-style-type: none"> • BRAE department at Cal Poly has some experience instrumenting gas turbine engines • Not specifically relevant to the JFS
Minilab and Turbogen ¹²	<ul style="list-style-type: none"> • Self-contained, fully instrumented gas turbine laboratory equipment • Good inspiration for how to develop our user interfaces • Temperature/pressure instrumentation at all stages
Lab Activity - University of Minnesota ¹³	<ul style="list-style-type: none"> • SR-30 Turbojet • Sensitivity of Stage 2 thermocouple placement (compressor outlet) • Detailed turbomachinery analysis (geometry) – agreed with data well • Energy balance
Lab Activity - Penn State ¹⁴	<ul style="list-style-type: none"> • SR-30 Turbojet • Details on installation – exhaust, fuel, power, etc... • Good startup checklist
Lab Activity - Georgia Tech ¹⁵	<ul style="list-style-type: none"> • SR-30 Turbojet • Thorough coverage of thermocouple theory • PR_c vs m_{air}, $\eta_{s,comp}$ vs m_{air}, $\eta_{thermal}$ vs PR_c
Lab Activity - US Naval Academy ¹⁶	<ul style="list-style-type: none"> • SR-30 Turbojet • Thorough discussions of theoretical vs. real thermal efficiency • Cycle analysis, turbomachinery characterization

Chapter 3: Design Development

The following sections will review each stage of our design development process. In each section, we will discuss the decisions we made and layout the process we followed to reach our final design.

Turbine Disassembly

Following the approval of the project scope, we began evaluating potential locations for the sensors at each stage. The primary objective was to find integration points that would not obstruct the gas path or interfere with rotating components. After thoroughly reviewing the manual, it was determined that the turbine would need to be disassembled to get a closer look at flow paths and the internal geometry. Figures 16 through 21 show pictures taken during the disassembly process.

The first step was to remove any external lines blocking access to the bolts connecting the gas generator assembly to the power turbine assembly. Once the necessary accessories were taken off, the two sections were separated.



Figure 16. JFS-100 Engine

Next, the power turbine containment ring and gasket were detached from the gas generator assembly.



Figure 17. P.T. rotor



Figure 18. Containment Ring Front



Figure 19. Containment Ring Rear

The final step was to unscrew the power turbine stator from the gas generator.



Figure 20. *P.T. Inlet Guide Vanes*



Figure 21. *Gas Generator Turbine*

This process took about half a day, with each initial part location photograph and labeled. The completion of the turbine disassembly was crucial in making the first design decisions.

Material Characterization

Although we were provided with the engine's manual containing detailed diagrams and assembly drawings, we had difficulty finding any information pertaining to the material composition of each component. This information is crucial for turbine life due to the material being the limiting factor of turbine operation.

After contacting the MATE department, we were notified Dr. Trevor Harding was in possession of a portable XFR, or X-ray Fluorescence Spectrometer (Figure 22). The XRF works by emitting an X-ray beam from the front end of the analyzer that has enough energy to excite electrons that will in turn release X-ray photons. By analyzing these photons, the XRF can then identify the element percentages in an unknown metal, thus determining the composition and alloy.



Figure 22. *Portable XRF Analyzer [17]*

Using the XFR, we were able to determine what each part of the turbine was made of; the results can be seen in Table 3. This allowed us to find the temperature limits of each part, and estimate the maximum operating temperatures for each stage.

Table 3. *Summary of XFR Results*

Component	Material	Percentage of elements
Power Turbine Rotor	Waspaloy	Ni 56.83, Cr 18.61, Co 12.09, Ti 3.04, Fe 1.405, Mo 4.63, V 0.06, Mn 0.04, No 0.13, Ta 0, W 0.03
Gas Generator Rotor	Unknown	Ti 25.19, Co 11.94, Ni 33.8, Zinc, 0.02, Pggp 0.01
Power Turbine Housing	Nitronic 40	Fe 62.38 %, Cr 20.81, Mn 8.40, Ni 7.15, Ti 0.07, V 0.03, Co 0.33, Cu 0.07
Power Turbine Inlet Guide Vanes	ST 25, L6 05	Co 49.56, Cr 19.49, Mn 1.71, Fe 2.31, Ni 10.72, No 0.02, Mo 0.66, W 14.58
Power Turbine Containment Ring	Ti 64	88.25 Ti, 4.46 V, Cr 0.31, Fe, 0.27, Cu .02, Tin 0.5
Diffuser	347 Stainless Steel	Ti 0.09, V 0.04, Cr 17.54, Mn 1.94, Fe 66.93, Co 0.8, Ni 10.99, Cu 0.24, No 0.75, Md 0.18, W 0.02

The only inconclusive results were from the gas generator rotor. This was due to the XRF not having a flat surface to perform the test on. We were still able to identify some of the elements, and determined from these that the gas generator rotor was most likely Waspaloy, the same alloy as the power turbine rotor.

Design Point Thermodynamic and Stress Models

Although we had come up with a preliminary idea of which sensors we were going to use, we needed a way to determine specifically what temperatures and pressure the instruments would be exposed to. This involved performing a one-dimensional thermodynamic analysis on the engine, and developing what we call the “design point.” The design point is the steady-state operating point that we plan on running the engine at during laboratory experiments, and includes full state descriptions (defined by two properties) for the working fluid at all five stages of the engine. Defining this design point also specifies parameters such as engine speed (both gas-generator and power turbine), power output, and fuel flow. The ultimate goal was to set this design point very conservatively, such that the engine components are operating far from their maximum working temperatures and stress levels.

Additionally, determining this design point allowed us to more confidently choose which thermocouples and pressure transducers to utilize in the different engine stages.

Upon beginning the analysis, we quickly realized that our lack of specific technical information about the JFS-100 would be very limiting and inconvenient. We were not able to find parameters such as rated mass flow rate, pressure ratios, or isentropic efficiencies anywhere in the literature or in the maintenance manual. We did have a few data logs from the initial JFS installation at Cal Poly, however the vast majority of that data was not taken at truly “steady-state” conditions (i.e. conditions not changing with respect to time), making it difficult to use for an idealized steady-state analysis. Ultimately, we used a combination of the few available technical specifications, the old Cal Poly test data, and some certain assumptions to complete the thermodynamic analysis. This model was programmed in Microsoft Excel to allow us to easily change parameters and iterate until desired conditions were achieved.

Once the steady-state thermodynamic model was finished, the next step was to estimate the maximum stress experienced by the engine to ensure that our chosen operating point did not exceed the material limits. Of the many components in the gas turbine engine, the turbine rotor blades are generally considered the weakest points. They are essentially thin, cantilevered beams subjected to high rotational speeds, torque-induced bending moments, and extreme temperatures. Thus, our objective was to estimate the minimum safety-factor based on yield strength for the blades of both the gas generator turbine rotor and the power turbine rotor. This analysis required three crucial pieces of information:

1. The approximate temperature of the blade at our design point
2. The rotational speed and power output of each turbine at our design point
3. The yield-strength vs. temperature curve for the blade material

Fortunately, we possessed all of this required information. The thermodynamic analysis described above provided us with the gas temperatures at each turbine stage. Because this is a steady-state analysis, we made the assumption that the blades themselves operate at exactly the same temperature as the gas. Although not strictly true, this assumption will yield a conservative, “worst-case” result. The same analysis described the work output and rotational speed of the two turbines, which can be easily converted to a torque exerted on the turbine blades by the expanding gases. From this torque value, the average force acting at the centroid of each blade could be estimated. Modeling each blade as a simple cantilevered beam, this force acting perpendicular to the blade face (at the centroid) resulted in a maximum bending moment at the blade root, which was determined to be the critical location (maximum stress). This bending stress was combined with centrifugal loading from the rotational speed to create a relatively simple, 2-dimensional stress state.

As previously explained, we had used the XRF Spectrometer to determine that both turbine rotors are likely made out of Waspaloy, a nickel-based superalloy frequently used for extreme temperature applications. We were able to find significant test data showing the yield strength of Waspaloy at multiple elevated temperatures, allowing us to apply a curve fit equation to the data and estimate the strength at our design point¹⁸. With the yield strength and the stress state fully defined, we calculated safety factors at the blade root of each rotor.

Detailed versions of both the thermodynamic and stress analyses can be found in Appendix E, along with the test data that was used and a comprehensive list of results for our design point. A summary of the results pertinent to sensor selection are shown in Tables 4, 5, and 6, below.

Table 4. Summary of thermodynamic analysis results

Compressor			Gas Generator Turbine			Power Turbine		
N	74000	RPM	N	74000	RPM	N	60400	RPM
W_{in}	88	kW	W_{out}	87.6	kW	W_{out}	16.4	kW
η_s	55%	-	η_s	86%	-	η_s	80%	-
P_1	0.10	Mpa	P_3	0.26	Mpa	P_5	0.10	Mpa
T_1	25.0	degC	T_3	685	degC	T_5	500	degC
P_2	0.26	MPa	P_4	0.11	Mpa			
T_2	198	degC	T_4	803	K			

Table 5. Design point stress analysis

G.G. Stress Analysis			P.T. Stress Analysis		
W_{out}	88	kW	W_{out}	16.4	kW
Speed	74000	RPM	Speed	60400	RPM
Torque	11.310	N*m	Torque	2.59	N*m
# of blades	34	-	# of blades	36	-
Bending Force Per Blade	6.37	N	Bending Force per Blade	1.1214	N
Bending Moment	0.053	N m	Bending Moment	0.016	N m
Centripetal Force	8249	N	Centripetal Force	24480	N
Bending Stress	3284996	Pa	Bending Stress	259436	Pa
Axial Stress	420849527	Pa	Axial Stress	596166255	Pa

Table 6. Summary of stress analysis at design point

G.G. Stress Analysis			P.T. Stress Analysis		
Sigma Max	424134523	Pa	Sigma Max	596425691	Pa
Temperature	684	°C	Temperature	510	°C
Yield Strength [Mpa]	786398000	Pa	Yield Strength [Mpa]	1053499801	Pa
Factor of Safety	1.8541	-	Factor of Safety	1.766	-

3-D CAD Model

After the engine was disassembled we immediately began trying to determine a plan for installing the required instrumentation. However even with the engine apart, it was still very difficult to visualize how effective the different ideas would be. To further help the design process, we decided to create a 3-D CAD model in SolidWorks of the components that we had just disassembled. That way we could virtually assemble the engine and look at various cross-section views to help determine where there might be space for instrumentation. The model is shown in Figures 23 and 24.

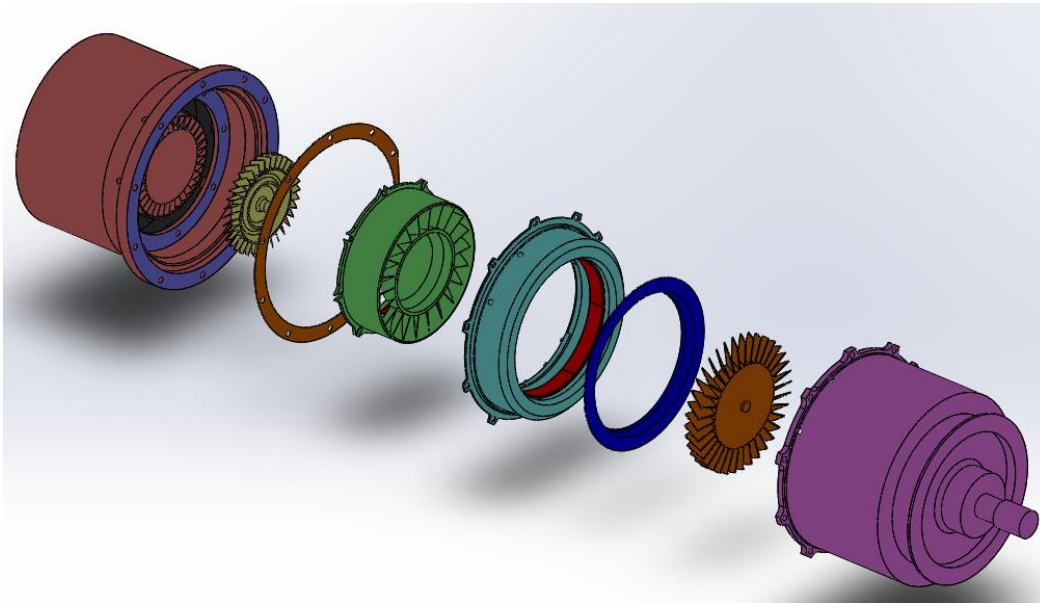


Figure 23. 3-D model of the JFS hot section, exploded view

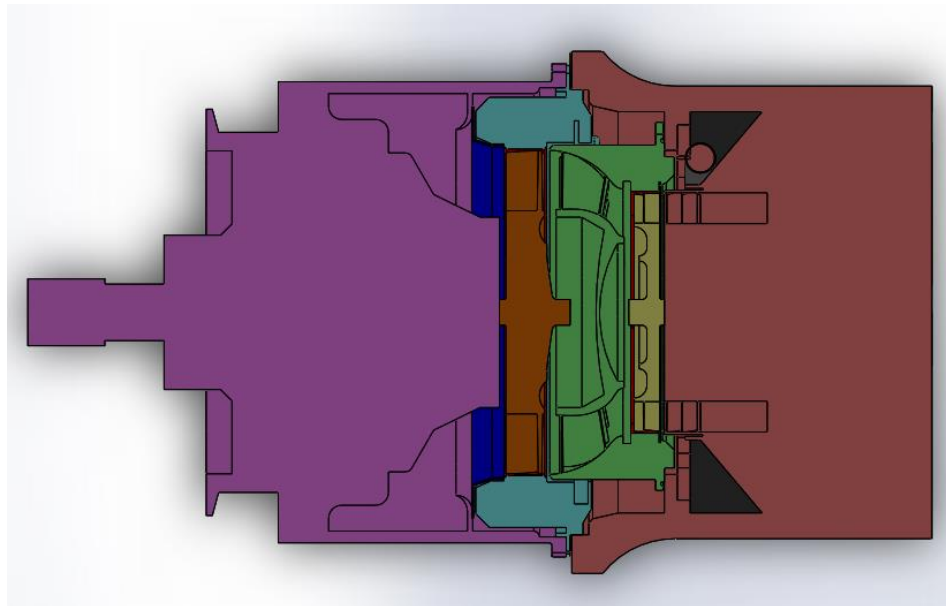


Figure 24. Cross section of JFS assembly, gas flow-path is right to left

Because we are primarily concerned with the turbine “hot section” (i.e. all components downstream of the combustor), those were the only components that were drawn in detail. Similarly, in reality the Power Turbine housing (purple in Figure 24) contains a complex gear reduction system and exhaust routing, however because these components are not relevant to our instrumentation plans, they were not modeled.

Instrumentation

With the above development activities completed, we were then able to fully begin instrumentation plans at each of the five engine stages. The following sections describe the design development process for the instrumentation at each stage.

Stage 1: Compressor Inlet

Due to the previous installation of the JFS-100 in the engines lab, Stage 1 instrumentation had already been implemented by Jim Gerhardt. No further design development was necessary. More details can be found in Chapter 4.

Stage 2: Compressor Exit

Due to the previous installation of the JFS-100 in the engines lab, Stage 2 instrumentation had already been implemented by Jim Gerhardt. No further design development was necessary. More details can be found in Chapter 4.

Stage 3: Gas Generator Turbine Inlet

After the combustor, the combustion products flow through a set of inlet guide vanes that direct the mixture into the gas generator turbine rotor. Stage 3 is located at inlet to this turbine, right after the inlet guide vanes. The instrumentation plans for this stage initially involved drilling and tapping into the casing at a single point, directly in front of the gas generator. By using a T-fitting equipped with both a thermocouple and pressure transducer, we were planning to collect both temperature and pressure data at this point. This would decrease machining time, while also reducing the potential for an error to occur in the manufacturing process.

Upon turbine disassembly, we realized that this plan was not possible. We discovered that the power turbine stator seals directly over the gas generator blades, which are also partially covered by the nozzle leading from the combustor. If we were to drill into the housing through the outer walls of the stator, we run a risk of creating a creating another place for the gas to flow, potentially reducing the power output of the turbine.



Figure 25. Air-start rakes at Stage 3

However, there was a much easier solution. As the engine is designed to be started using compressed air in case of loss of electrical, there are a set of existing rakes that lead from an air-start port on the outside of the engine (Figure 25). These rakes direct the compressed air directly at the gas generator turbine rotor in order to spin it up, and are located exactly at the Stage 3 location. Thus, the decision was quickly made to use these air start rakes as the access point for both temperature and pressure. They would provide a housing for a thermocouple, as well as a gas path that could lead back out of the start port to a pressure transducer. This solution requires no machining, and provides access to an area close to the gas generator blades. The calculated maximum temperature and pressure from the thermodynamic analysis was determined to be 1264°F and 37.7 psi. Based on these values, a 1/16" diameter Super OMEGACLAD XL Thermocouple and a Honeywell Sensym ICT pressure transducer rated to 50 PSI were specified. Figure 26 shows the CAD model developed for this design. A detailed description of the final design can be found in Chapter 4.

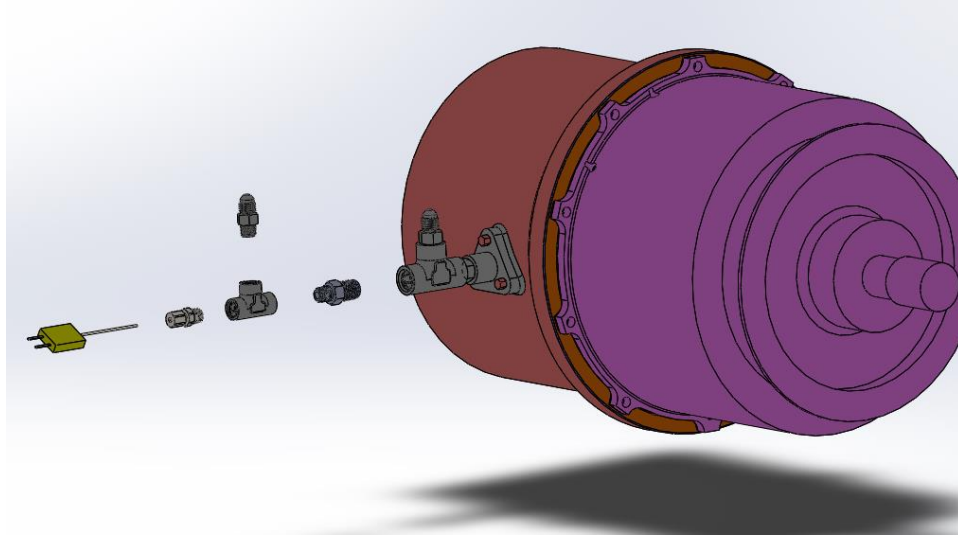


Figure 26. Stage 3 Initial Design Instrumentation Assembly

Stage 4: Power Turbine Inlet

When we began looking carefully at the disassembled engine and CAD model, it soon became clear that Stage 4 would be the most challenging location to implement temperature and pressure sensors. To measure temperature, the goal was to insert a thermocouple into the gas flow-path immediately downstream of the power turbine inlet guide vanes, just in front of the power turbine rotor (see Figure 27). To measure pressure, we needed to provide a small passageway (gas-path) leading from that same location to a port on the outside of the engine. From this port, a length of steel braided hose would connect to the pressure transducer, itself mounted in the electrical control box a few feet away from the engine.

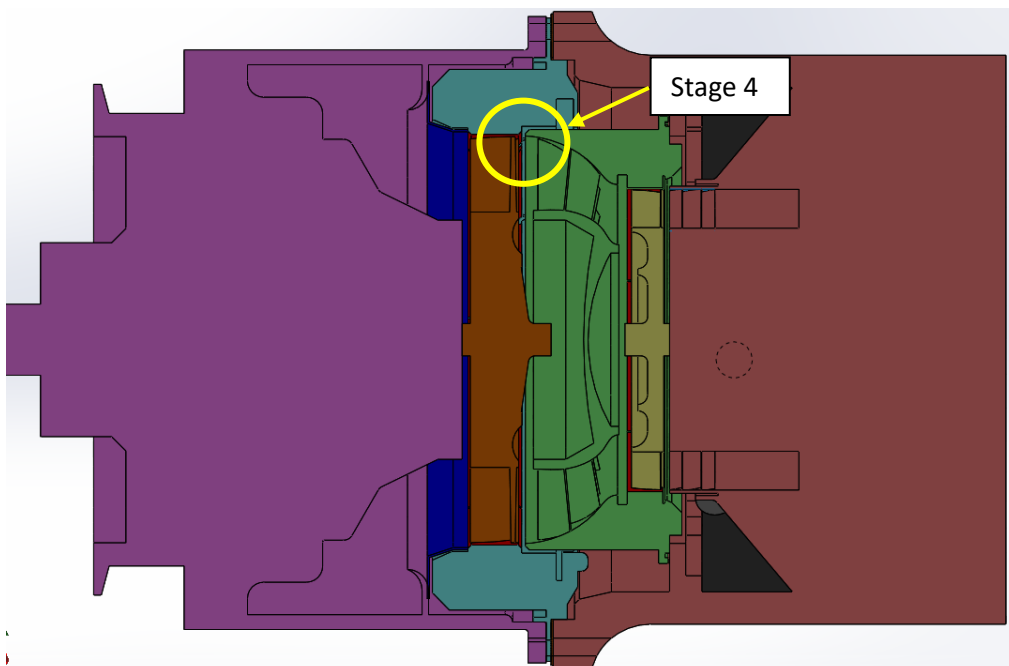


Figure 27. Target Stage 4 instrumentation location

For this stage, the first step was to determine specifically which sensors we would be using. From the thermodynamic design point analysis detailed earlier, the gas at this point in the engine was predicted to be at a temperature of 985 degrees F and a pressure of 16.5 psi. We initially specified an Omega sheathed thermocouple of 1/32" diameter, which was rated to 1600°F. However we decided to switch to a 1/16" diameter thermocouple from the same Omega product line because we were unable to find compression fittings that fit 1/32" thermocouples. For simplicity and cost reasons, we decided to use the same line of Sensym ICT pressure transducers for Stage 4, and thus specified the model rated to 50 psi.

With the sensors for Stage 4 specified, we tackled the problem of installation. There is only approximately .15" of clearance between the guide vanes and the rotor, and direct radial access to this location necessitates drilling through both the Power Turbine Housing and the Power Turbine Containment ring. Because of these difficulties, we initially hoped that there might be another way of accessing the location of interest, perhaps by fishing a thermocouple through the guide vanes from further towards the front of the engine. However even if this approach would have worked for the thermocouple, it would not have been an effective solution to provide the gas path necessary to measure pressure, and wouldn't have made the manufacturing process any easier. Ultimately, we decided that the best approach for both sensors was to simply drill holes radially inwards. This approach meant that we needed to design some sort of port or housing that would be installed in the engine and allow for a thermocouple to be fed down into the Stage 4 location. We also needed to provide a small gas path leading to the outside of the engine in order to measure pressure. Figure 28 shows the instrumentation layout for the initial design.

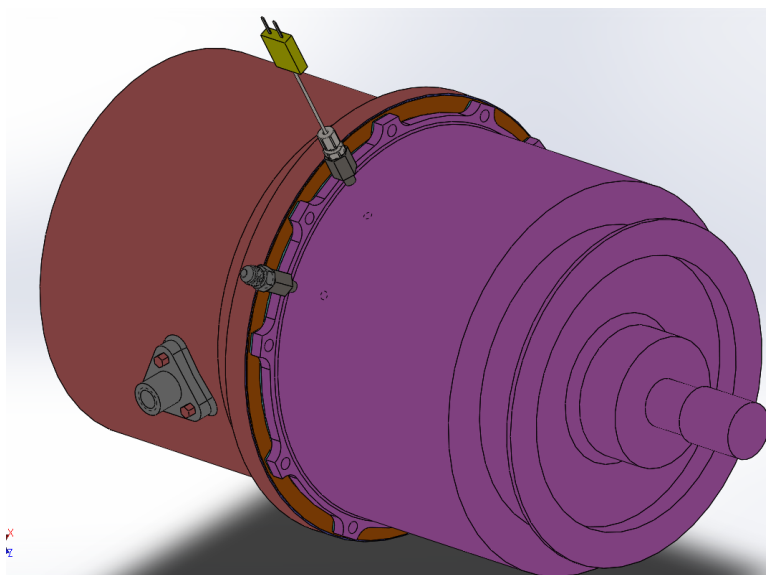


Figure 28. Stage 4 instrumentation layout

The temperature instrumentation consisted of 3 primary components: the 1/16" diameter sheathed thermocouple (made by Omega), the compression fitting to fit the thermocouple (also made by Omega), and the Stage 4 Thermocouple Port, a component that we designed ourselves. These components can be seen in Figure 29, and a detailed view of the Stage 4 Thermocouple Port can be seen in Figure 30.

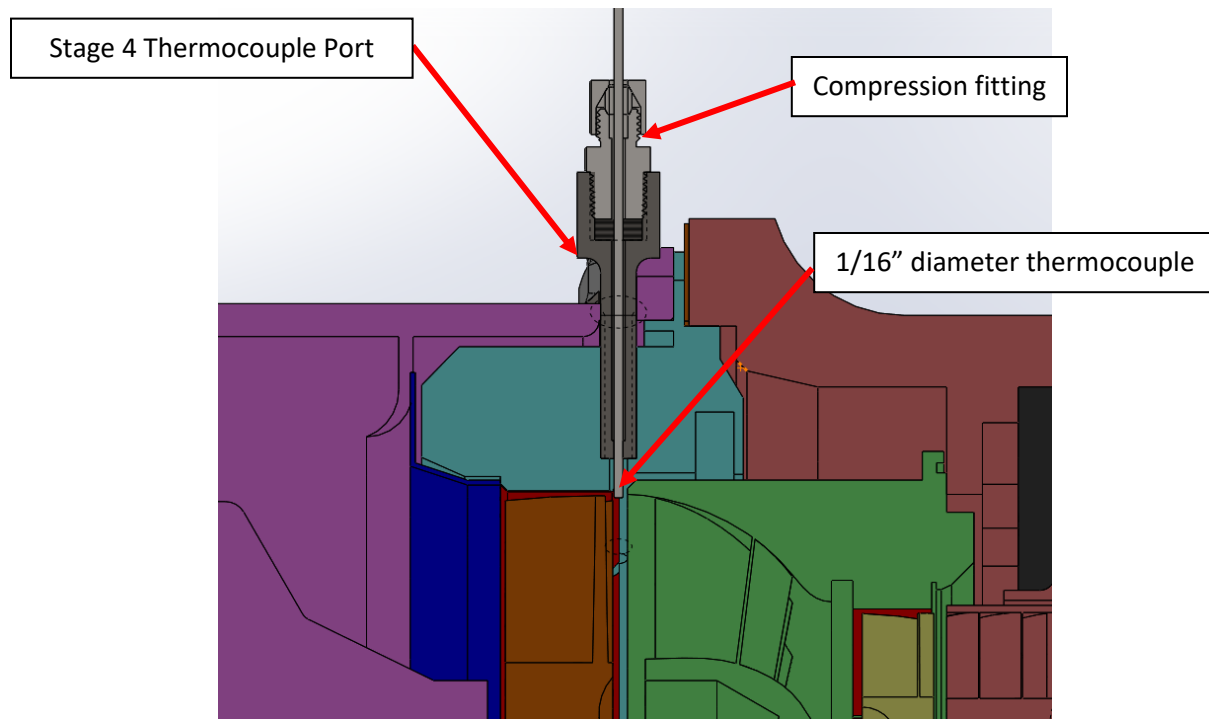


Figure 29. Stage 4 temperature instrumentation

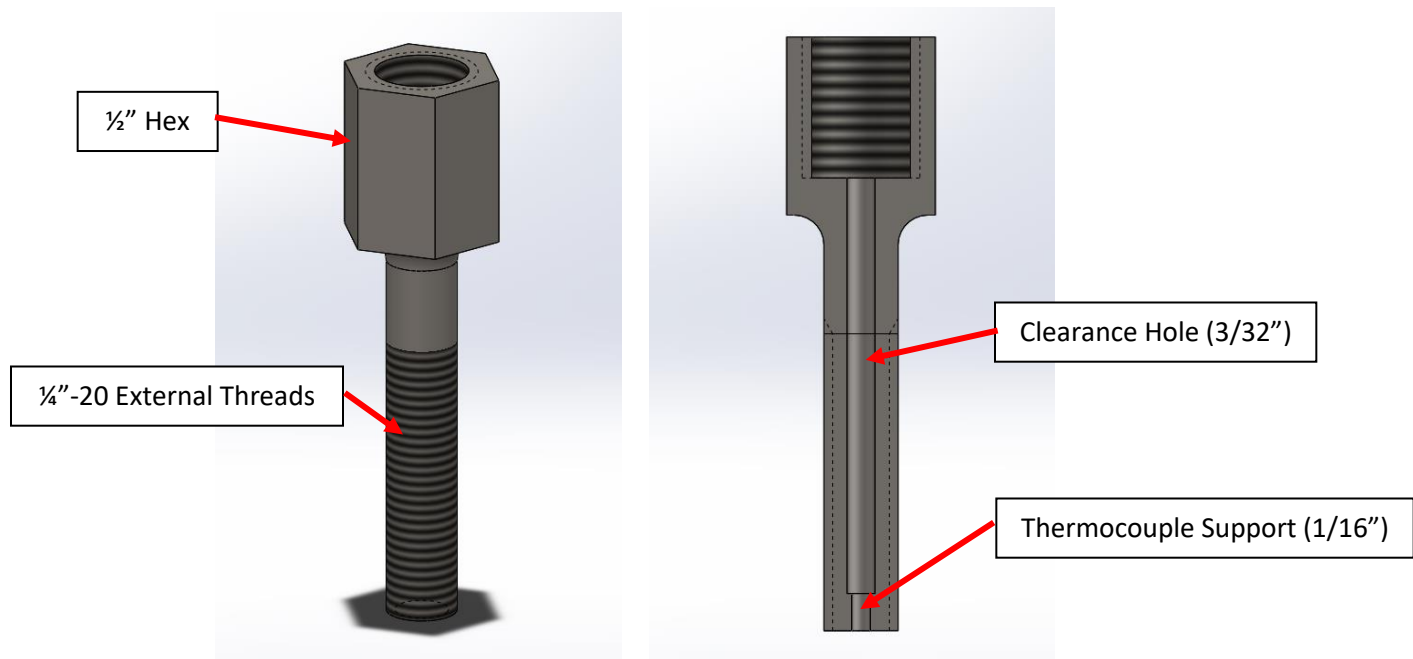


Figure 30. Stage 4 Thermocouple Port

The Stage 4 Thermocouple port screws into the containment ring (shown in light blue/turquoise in Figure 29) through a clearance hole in the Power Turbine Housing (shown in purple). The thermocouple

is then inserted down through the center of the port into the Stage 4 gas path. An OMEGAllok series compression fitting sized for a 1/16" thermocouple is then screwed into the female 1/8-27 NPT threads in the thermocouple port. When tightened, this compression fitting clamps down around the thermocouple probe, securing it in place and sealing off the gas path.

The Stage 4 pressure instrumentation was designed to be very similar to the temperature instrumentation. Thus, many of the redundant details are omitted in the following discussion.

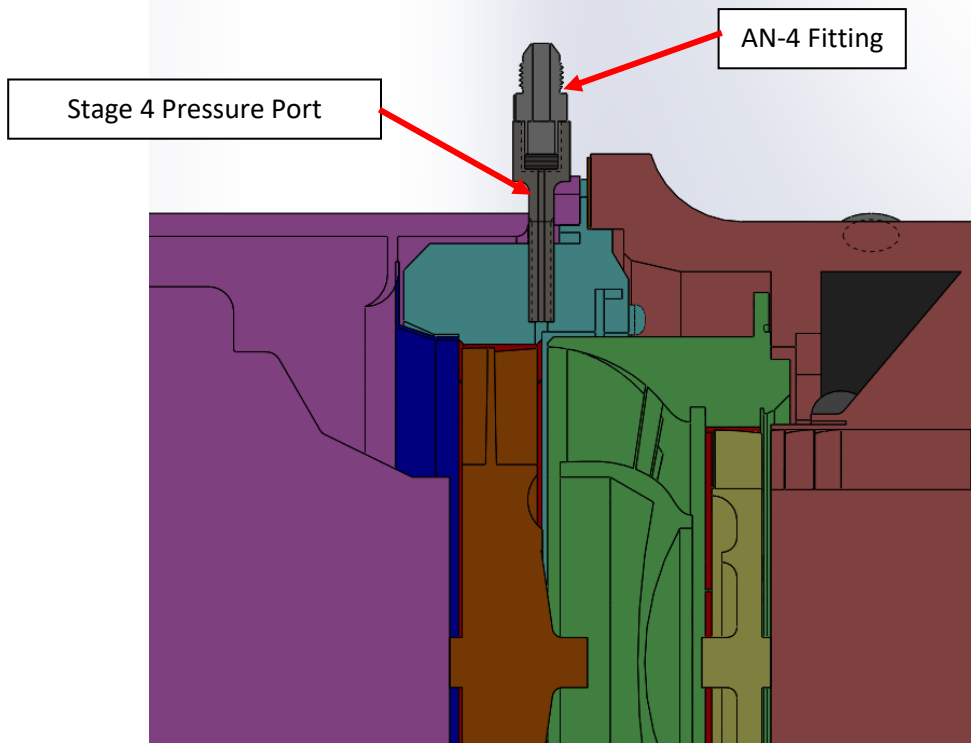


Figure 31. Stage 4 pressure instrumentation

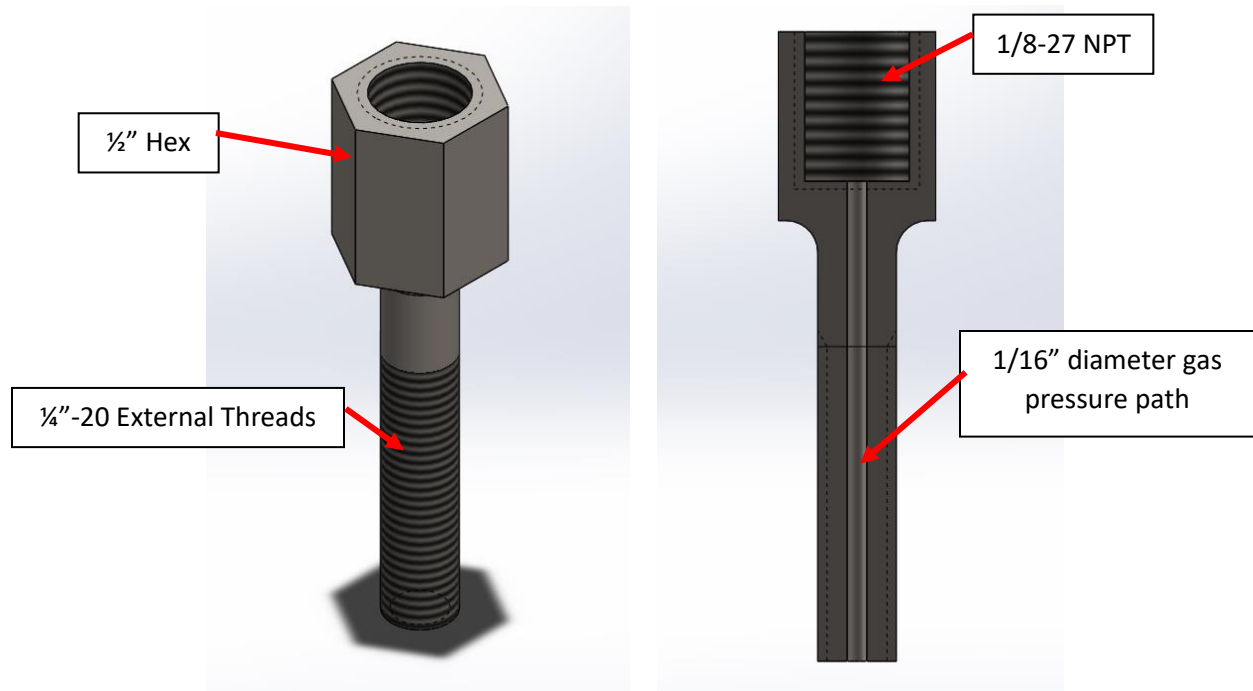


Figure 32. Stage 4 Pressure Port

Just like the thermocouple port, the pressure port (Figures 31 and 32) would have been threaded into the containment ring through a clearance hole in the power turbine housing. An AN-4 pipe fitting would have been screwed into the female 1/8-27 NPT threads, which will provide an easy connection point for an AN-style hose, which is already provided in the lab. The hose would have then fed to the Sensym ICT pressure transducer mounted in the dyno control box.

Both sensors would have been radially arranged “upstream” of the air-start rakes, as shown in Figure 33. This would have ensured that any unsteady-flow conditions caused by these rakes do not affect the Stage 4 temperature and pressure readings.

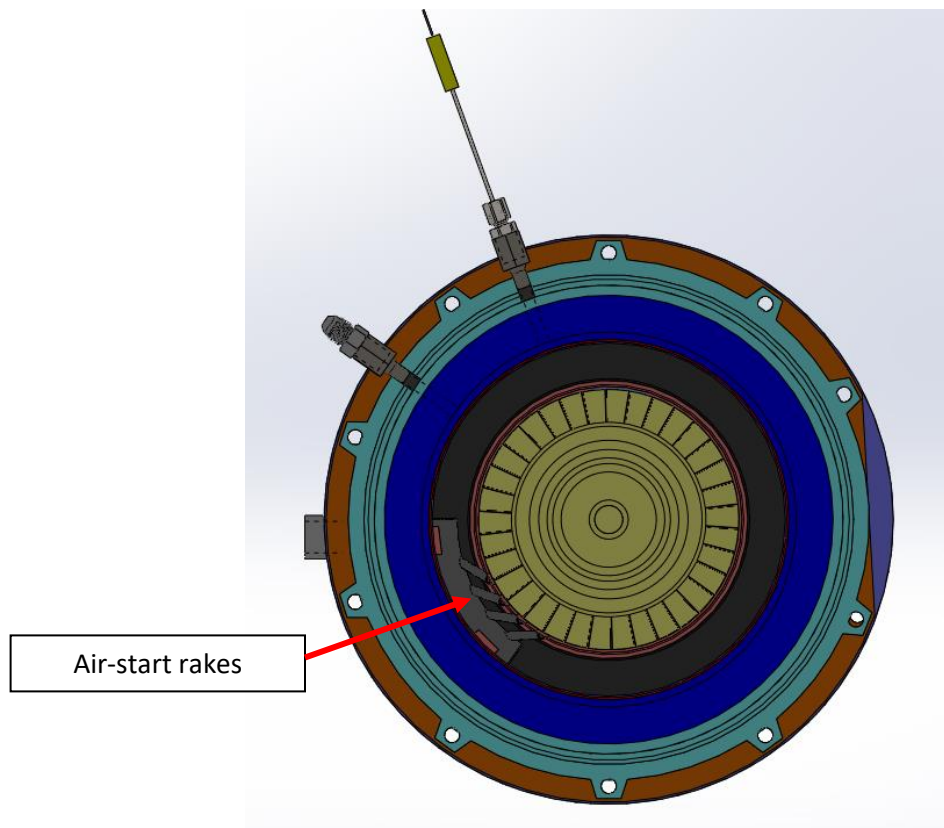


Figure 33. Radial location of the stage 4 instrumentation, upstream of the air-start rakes

Stage 5: Engine Exhaust

Due to the previous installation of the JFS-100 in the engines lab, Stage 5 instrumentation had already been implemented by Jim Gerhardt. No further design development was necessary. More details can be found in Chapter 4.

Redundant Throttle Position Sensor

The second subsystem development outlined in the objectives above involves the design and implementation of a redundant throttle position sensor. The existing fuel system in the dyno cell is relatively robust and effective at delivering fuel to the engine. However, its main weakness is that the only indication of throttle position for the operator outside of the engine cell comes from the electric throttle actuator itself (which is installed inside of the cell). Thus, should this built-in position sensor fail (as it has done in the past), there is no way for the operator to know. This can result in the operator unknowingly opening the throttle too much, causing excess fuel to be injected into the engine and resulting in a very unsafe condition. To remedy this problem, a secondary, independent throttle position sensor will be installed on the throttle actuation linkage to ensure that the throttle is working properly. This redundancy will help prevent engine failure and once again increase system reliability.

The first step in the design process is to truly understand the problem, which required a thorough understanding of how the current throttle system works. While spark-ignition reciprocating engines (like in many consumer vehicles) control power by means of throttling the *air* entering the engine, gas

turbine engines (as well as diesel engines) achieve the same effect by throttling the *fuel* flow. Our JFS-100 engine is no exception, however because it was designed only to start the main engines of an aircraft, in stock form there is no manually-operated throttle. The pilot needs only to press a single “start” button, and the fuel control unit automatically delivers the appropriate amount of fuel based on engine speed. However, a manual throttle is critical for a laboratory application, and thus in the original installation much effort went into designing a system that could repeatedly deliver varying amounts of fuel and be controlled by a user outside of the dyno cell. This system is outlined in Figures 34 and 35.

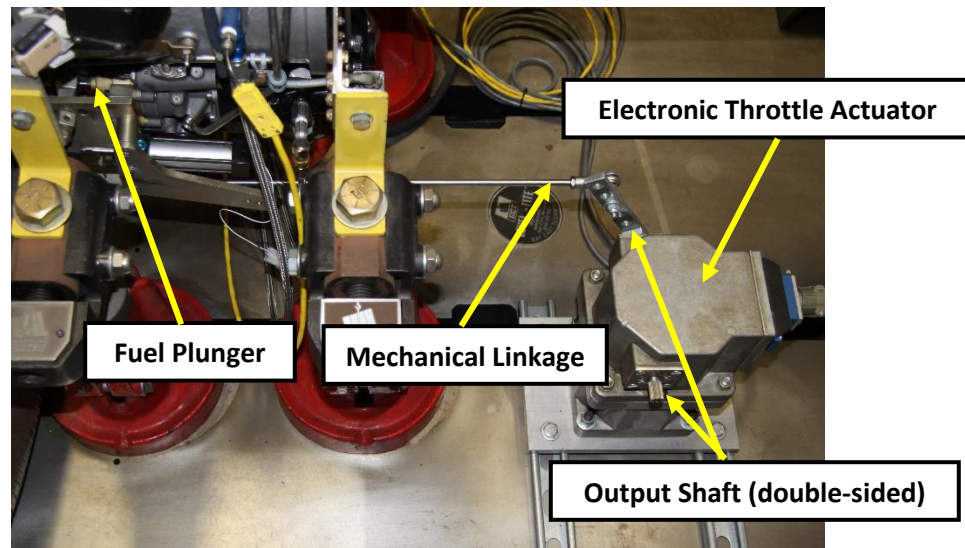


Figure 34. Existing fuel control system

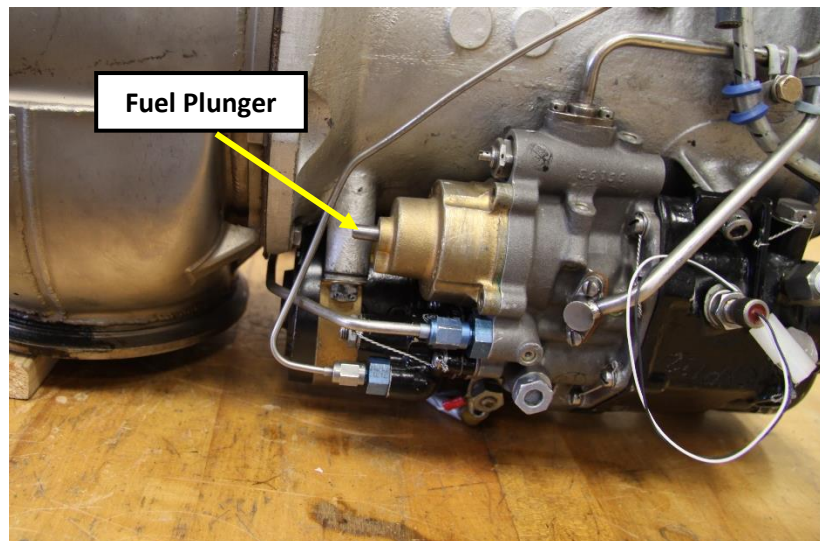


Figure 35. Close-up of fuel plunger

The operator input sends a signal to the electronic throttle actuator, which rotates the output shaft accordingly. This rotation is turned into near-linear motion by the mechanical linkage, which in turn

actuates the fuel plunger. Moving this fuel plunger in and out is what physically meters the amount of fuel entering the engine's combustion chamber.

Once the existing throttle system was understood, the process of designing a redundant position sensor could continue. The first major decision concerned whether to measure rotary position via the output shaft or linear position via the mechanical linkage. Both of these options were considered, however it was ultimately decided that measuring rotary position would require simpler mounting, output a more reliable signal (since the linkage doesn't move in a perfectly linear fashion), and require a less expensive sensor. As shown in Figure 34, the output shaft of the electronic actuator is double-sided (i.e. the same shaft extends out of both sides). This proved extremely convenient, because a rotary position sensor could very easily be mounted on the unused side of the output shaft, providing a reliable signal and very simple mounting. Once it was decided to measure rotary position from the second side of the output shaft, the next step was to determine specifically what kind of sensor should be used. There are multiple ways of measuring rotary position, and an excellent summary of the main technologies can be seen on page 1 of Reference 19. For our specific application, the choice was reduced to two options: a rotary encoder or a potentiometer. Potentiometers have high resolution, are simple to wire, and are very cheap, however are limited by the small range of motion that they can accurately measure. Encoders are more complicated and more expensive, however can often measure multiple rotations and generally have longer lifespans. Because the throttle linkage converts rotary motion to linear motion, the maximum amount of rotation that was necessary for our sensor was only 180 degrees. Additionally, the lifespan requirement was calculated to be approximately 2000 cycles, assuming 5 years of operation in the lab. Both of these requirements are easily met with potentiometers, which are cheap enough that purchasing multiple back-up units in case of premature failure is quite reasonable. For these reasons, a potentiometer was the sensor of choice for the throttle position sensor.

The next decision was how to couple the potentiometer shaft to the output shaft of the electronic throttle actuator. Our preliminary idea involved the use of a soft-jaw coupling (Figure 36), but Jim Gerhardt pointed out that these 3-piece couplings are usually used in extreme shock-loading situations, and would be over-complicated and over-built for our application. He suggested that we investigate helical couplings (Figure 36), which can also tolerate shaft misalignment but are more commonly used in instrumentation and electronics. We heeded his advice, and specified an appropriate helical coupling for our shaft sizes.

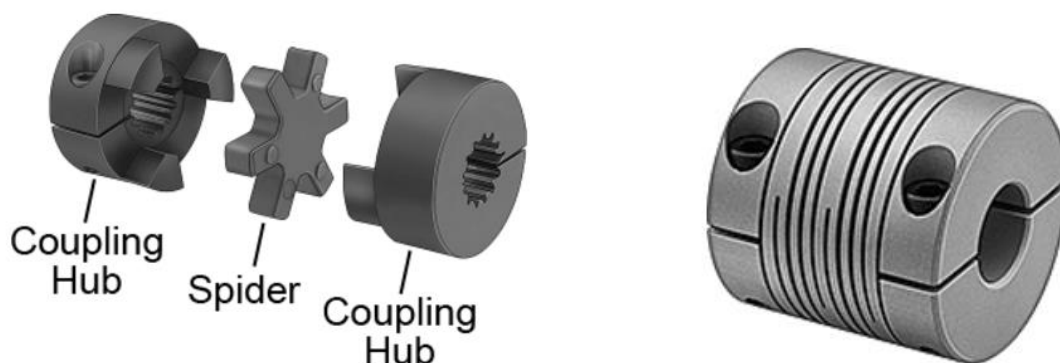


Figure 36. Soft-jaw coupling (left) versus helical coupling (right). [McMaster-Carr]

With the major decisions made, all that was left was to specify a potentiometer and design a mounting bracket. The potentiometer needed to be of appropriate size (1/4"-1/2" diameter input shaft) and be able to output 0-10 volts according to the electrical specifications of the controller. Designing a mounting bracket was fairly straightforward, as the throttle actuator was already mounted on a set of strut channels which allow for linear adjustment in one direction. We decided to mount the bracket in a similar fashion and add a slot to the mounting plate in order to provide linear adjustment in two directions. A detailed description of the final design can be found in Chapter 4.

Laboratory Activity

In order to begin designing the lab activity, customer requirements for this portion of the project needed to be outlined. The primary objectives focus on developing a detailed data collection process, with a safety review, that can be completed in 3 hours, and a lab write-up and analysis that should be easily completed in one week. The lab activity should target students' understanding of the operation of gas turbine engines and the basic thermodynamic principles governing their performance.

From these requirements, the first version of the lab was created. This version focused on collecting data at a single operating point and utilizing that data to perform a comparative analysis of theoretical and experimental calculations. This would allow for students to develop their own computational tool (in Excel or MATLAB) to calculate engine power and efficiency at that single point, and to understand conceptually how the different components of the turbine interact with one another. After much consideration, it was decided that a more in-depth analysis would be required in the lab activity.

The second revision splits the lab into two consecutive activities. The first lab will introduce students to the JFS-100 engine and how to safely operate it on the dyno. They will become familiar with the operating principles of gas turbine engines including specific functions of each component. Then, students will collect data from the JFS at a single operating point, namely the rated engine speed and a pre-determined "baseline" equivalence ratio. This will be considered the "design point." They will use this data to perform a simple one-dimensional thermodynamic analysis to characterize the engine and evaluate component efficiencies. Brayton Cycle T-S and P-V diagrams will be heavily emphasized. A simple energy balance will be performed as a visual aid to help students understand how effective the engine is at converting heat released from combustion to useful work. In addition, a series of conceptual questions will accompany the calculations in order to further theoretical understanding and investigate sources of experimental errors.

The next portion of the lab is still being developed and has yet to be finalized. Currently, the idea is that the activity will build heavily on the first, but be expanded to include investigation of JFS performance at off-design operating points. There will be two primary experiments. Firstly, data will be collected at 4-5 different operating speeds (all tests will be steady-state) below the rated speed of 74000 RPM. This data will be used to investigate engine efficiency, as well as component performance, at these off-design speeds. Secondly, the engine will be maintained at its rated speed, and the equivalence ratio will be varied by means of increasing or decreasing the fuel flow. This will yield corresponding changes in temperatures and pressures downstream of the combustor, and give students insight into the effects that these parameters have on performance. Students will be asked to graph a number of performance parameters as a function of engine speed and equivalence ratio (separately), and to once again answer a set of conceptual questions.

Design Development Summary

Table 6 shows a summary of the major decisions made during the design development phase.

Table 7. Summary of Important Design Decisions

System	Chosen Concept	Reasons
Throttle Position Sensor	Potentiometer	<ul style="list-style-type: none">• Cost• Simplicity• Met requirements for durability, rotation
Throttle Position Sensor Coupling	Helical Coupling	<ul style="list-style-type: none">• Simplicity• Misalignment capability
Instrumentation – Thermocouples	Omega K-Type 1/16” diameter, sheathed	<ul style="list-style-type: none">• Temperature limit• Response time• Cost
Instrumentation – Pressure Transducers	Sensym ICT series (Honeywell)	<ul style="list-style-type: none">• Availability• Cost
Instrumentation – Stage 3	Utilize air-start rakes for both temperature and pressure	<ul style="list-style-type: none">• No machining operations• No risk of gas path leakage
Instrumentation – Stage 4	Direct radial drilling 2-port design (temperature, pressure)	<ul style="list-style-type: none">• Simplicity• Support structure for thermocouple probe• Damage mitigation
Primary Starting Mechanism	Compressed Air	<ul style="list-style-type: none">• Simpler• More reliable

Chapter 4: Description of Final Design

Instrumentation

Stage 1: Compressor Inlet

The first stage is located outside of the turbine, directly before the centrifugal compressor. The current setup for the air intake has an air flow sensor attached to the inlet of the compressor, shown as the gold section in Figures 38 and 39. Below the air flow sensor is an attachment that has a thermocouple and pressure transducer port (Figure 39). This attachment and the airline have already been set up installed by Jim Gerhardt.

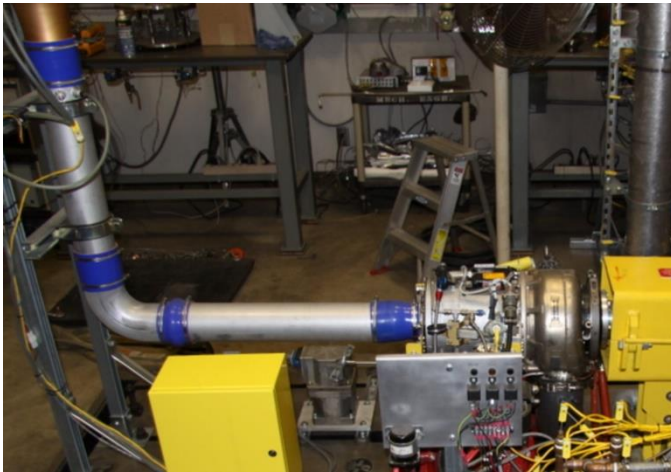


Figure 37. JFS Intake System



Figure 38. Stage 1 Instrumentation

Stage 2: Compressor Exit

The second stage resides directly after the compressor and before the annular combustor. The sensor set-up was pre-determined by Jim Gerhardt when he was working on the previous installation of the JFS-100. There is a small instrumentation port on the outside of the housing wall that gives access to outer wall of the compressor outlet. Using this port and a T-fitting, Jim was able to place thermocouple through one end of the fitting and attach an air line for pressure transducer on the other (Figure 40). This design created a gas path that would flow around the thermocouple through the third end of the fitting, giving an approximation of Stage 2 temperature and pressure.

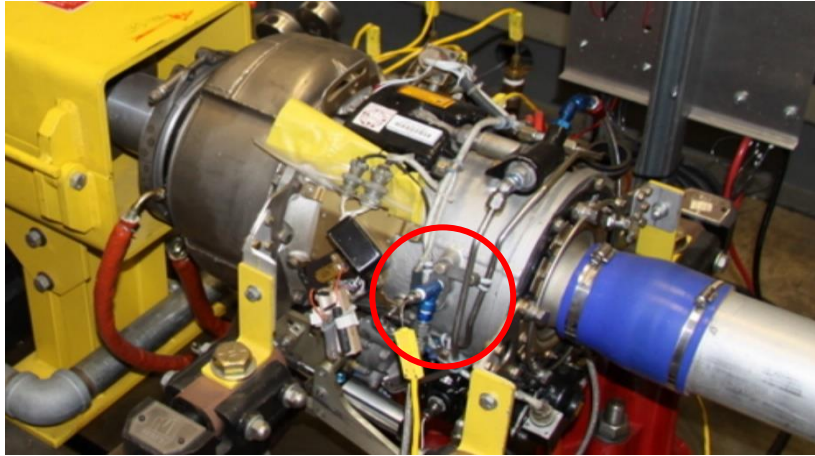


Figure 39. Stage 2 Instrumentation

Stage 3: Gas Generator Turbine Inlet

The temperature and pressure sensors at Stage 3 will be incorporated into the existing air-start port using a T-shaped fitting. For this stage specifically, a thermocouple and pressure transducer will each be connected to a side of the fitting. The third side will connect directly to the first fitting, which will attach to the port, illustrated in Figure 41.

Stage 4: Power Turbine Inlet

After reviewing the model with our project sponsor, Dr. Lemieux, it was decided that the instrumentation design needed to be revised. Our original plan of having two separate stainless steel components, one for the pressure transducer line and one for the thermocouple, was dismissed and the idea of combining them to form one part was adopted.

This design decision was based off the fact that having two different instrumentation housings would require two separate holes to be drilled into the turbine housing. This would increase the chances of an unsuccessful machining operation of a complex part that would be difficult to replace, as well as increase the chances of a gas leak.

The next revision for the instrumentation housing was a single straight piece of 304 stainless steel, 1.5 inches long, that had 1/8 NPT internal male threads on one end for a tee fitting to thread into, and 1/4-28 external male threads on the other end to thread into the containment ring. As can be seen Figure 42, one end of the housing had a small shelf, or groove, cut into it for an O-ring to sit. This O-ring would provide sealing against any escape gases.

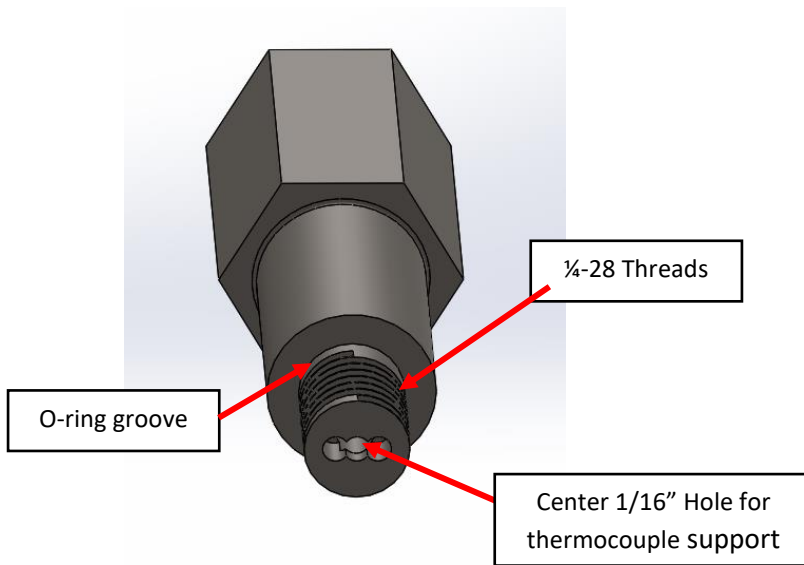


Figure 40. CAD Model of Stage 4 Sensor Housing

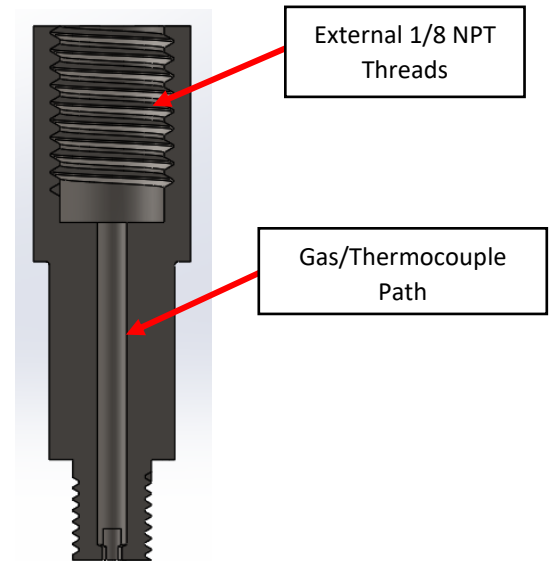


Figure 41. Internal Geometry of the Sensor Housing

The central portion of the housing was designed to hold the thermocouple securely while also providing room around the thermocouple for air to flow to the gas line for the pressure transducer. To accomplish this, three 1/16" holes will be drilled into the end of the housing. The first, and central hole will be used to support the thermocouple and keep it from interfering with the power turbine blades. The other two holes are located on opposite sides of the central hole, and overlap it slightly. The effect is that there are now two small openings for the gas to flow around the supported thermocouple, which provides the static pressure for the pressure transducer to read. The final drawing for this design can be seen in Figure 44 below.

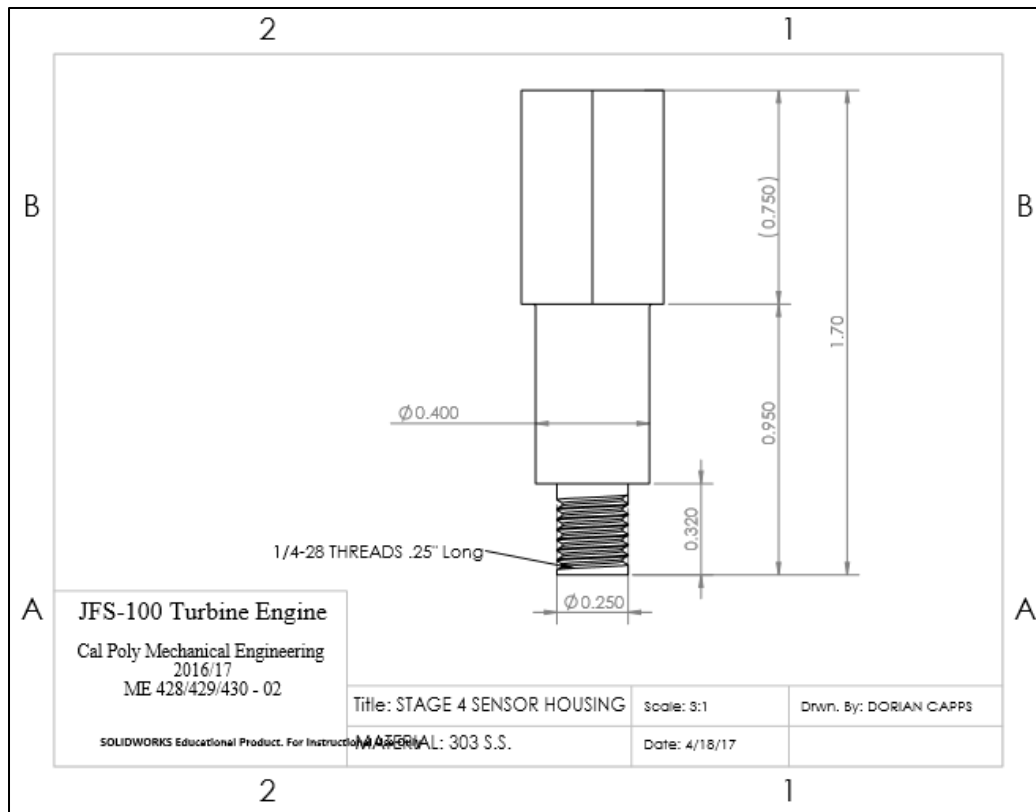


Figure 42. Final drawing of sensor housing for stage 4

Initially, the plan was to use a high temperature silicon O-ring that could take a temperature between 1200°F-1400°F. This temperature range was reasoned from our design point analysis, detailed in Chapter 3. Design Development. It became apparent that using a silicon O-ring would be impractical due to the cost of purchasing an O-ring that could withstand the elevated temperature for a substantial length of time.

During a brief discussion of the issue with Dr. Kean, a professor in the Mechanical Engineering department at Cal poly, metal crush washers were suggested for the application. These washers are typically used on diesel engines to seal spark plugs in cylinder heads, which can reach high temperatures due to their proximity to the combustion chamber. As the name implies, the metal washer forms a seal after being crushed between two surfaces. These are not reusable but are less expensive, less susceptible to heat than polymer O-rings, and fairly easy to replace in comparison.

The incorporation of a metal crush washer called for another revision of the sensor housing. The final design included increasing the length of the shank to 1.7" (allowing more room for a metal crush washer to sit), increasing the diameter of the O-ring shelf at the end of the shank to 1/4", and elongating the hex portion of the housing. The following design changes were made to allow for a better fit of the copper crush washer onto the sensor housing and of the sensor housing into the containment ring.

Stage 5: Engine Exhaust

Stage 5 is the exhaust, located directly after the power turbine. A thermocouple has already been installed in this location, and pressure is assumed to be ambient.



Figure 43. Stage 5 Instrumentation

General Instrumentation Information

There is a control box located above the dynamometer that houses the pressure transducers and thermocouple wiring, Figures 46 and 47. There is a pressure transducer for each stage, which convert the pressure provided pressures into measurable voltages. The thermocouples plug into the same control box, which routes the signal to the Digalog data acquisition and user interface systems outside of the cell.



Figure 44. Inside of dyno control Box



Figure 45. Inputs to dyno control box

JFS Primary Starter

The goal of using the air-start was to increase the reliability of the starting mechanism. Setting up and installing the components for this starter was initially, in theory, a much simpler design, and had more robust components that would be extremely difficult to break even in unfavorable or harmful conditions. This proved not to be feasible, mainly because the compressed air would have to be pressurized to at least 1,000 psi, a fact that was discovered after talking with the turbine enthusiast, George Carey.

Thus, the final design utilizes the original primary electric starter. Our research indicated that the electric motor within the starter was prone to overheating and breaking if the starter was on for over 7

seconds, or had inadequate time to cool off in between starting attempts. To reduce the potential of either of these things happening, two safety backups were incorporated into the final design. First, a thermocouple was attached to the outer casing of the motor to read the casing temperature. This temperature was programmed to be an input into the Digalog software used to control the turbine, and can be used to set over-temperature limits. This will prevent the starter from being turned on if the motor is too warm. Secondly, the starter will only run through a test-controlled setting in the software. This is a subgroup within 'cranking routines', a predesigned subprogram in the Hypercell software that allows us to set various parameters. This includes the runtime of the starter, when it can be turned on (i.e. if the turbine is off, preventing it from being used when the turbine is running), and when the starter will be turned off (i.e. has the turbine reached a predetermined speed). This almost completely eliminates any user input error that could result in the starter being overused and the motor fatigued. The combination of these redundant safety systems will increase the reliability of the starter for the JFS-100.

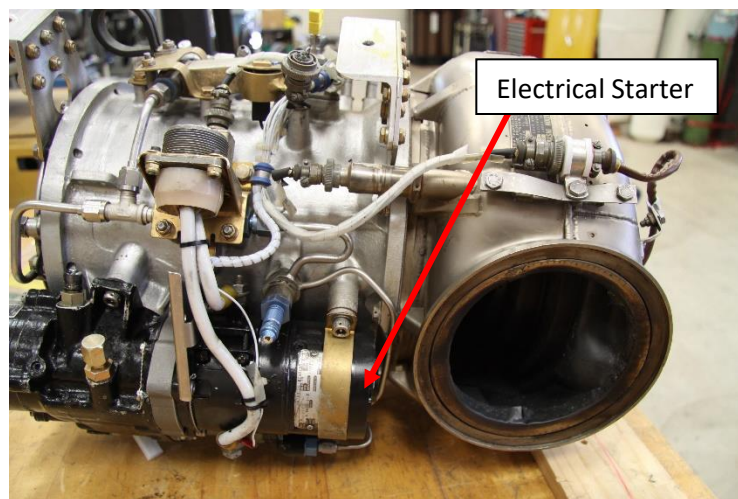


Figure 46. Photo of electrical starter installed on JFS

Software Programming and Shutoff Algorithms

The last part of our final design involves the alarms and limits that we will program into the controller in order to safely shut down the engine if there is any unsafe operating condition. These alarms are programmed into the Hypercell software, which serves as the main user interface program for controlling the engine and dynamometer. Each parameter (temperatures, pressures, etc...) can be set up with two separate alarms:

High Yellow Alarm: This is the first alarm to be triggered, and is generally considered a warning to the operator. It causes a warning message to be displayed on the screen and a loud alarm to sound, however it will not shut off or otherwise control the engine or dyno in any way.

High Red Alarm: Set at a higher threshold than high yellow, this indicates an emergency situation. A different message will be displayed, the engine will be immediately shut off, and the test will be put on hold.

Our task was to decide specifically what values to set these alarms at for each critical parameter. We started with our design point analysis detailed earlier, which describes the steady state operating conditions that we plan to run the engine at. We then chose alarm limits slightly higher than these operating conditions, with a reasonable margin in order to account for small fluctuations while running. As a last check, we repeated our stress analysis calculations at these shutoff conditions in order to ensure that the engine could not be damaged under any circumstances. Table 8 shows a summary of our programmed limits, while Table 9 shows the results of the stress analysis at these worst-case values.

Table 8. Programmed warning and shut-off limits

	T2 [°F]	T3 [°F]	T4 [°F]	T5 [°F]	GG Oil Temp [°F]	PT Oil Temp [°F]	Starter Temp [°F]	G.G. Speed [RPM]	Dyno Speed [RPM]
Design	388	1264	985	932	N/A	N/A	N/A	74000	3497
High Yellow	N/A	1280	1000	1000	250	250	150	74000	3500
High Red	N/A	1350	1100	1100	300	300	200	75000	3550

Table 9. Worst-case stress analysis results at shut-off conditions

G.G. Stress Analysis			P.T. Stress Analysis		
Max Stress	435541888	Pa	Max Stress	596425691	Pa
Temperature	732	degC	Temperature	593	degC
Yield Strength [Mpa]	767654000	Pa	Yield Strength [Mpa]	1053499768	Pa
Factor of Safety	1.7625	-	Factor of Safety	1.766	-

Redundant Throttle Position Sensor

System Overview

The design process detailed in Chapter 3 culminated with the final design depicted in Figures 44 and 45. In these models, the electronic throttle actuator is a rough mockup, but all the dimensions relevant to the TPS system are accurate. The mounting scheme utilizes the same strut channels that the actuator is already mounted to, allowing for simple assembly and adjustability. In reality, the throttle linkage is attached to the left output shaft of the actuator in Figure 44, but it is not shown here (refer to Figure 28 in Chapter 3). Detailed drawings can be found in Appendix B, and vendor specification sheets can be found in Appendix D.

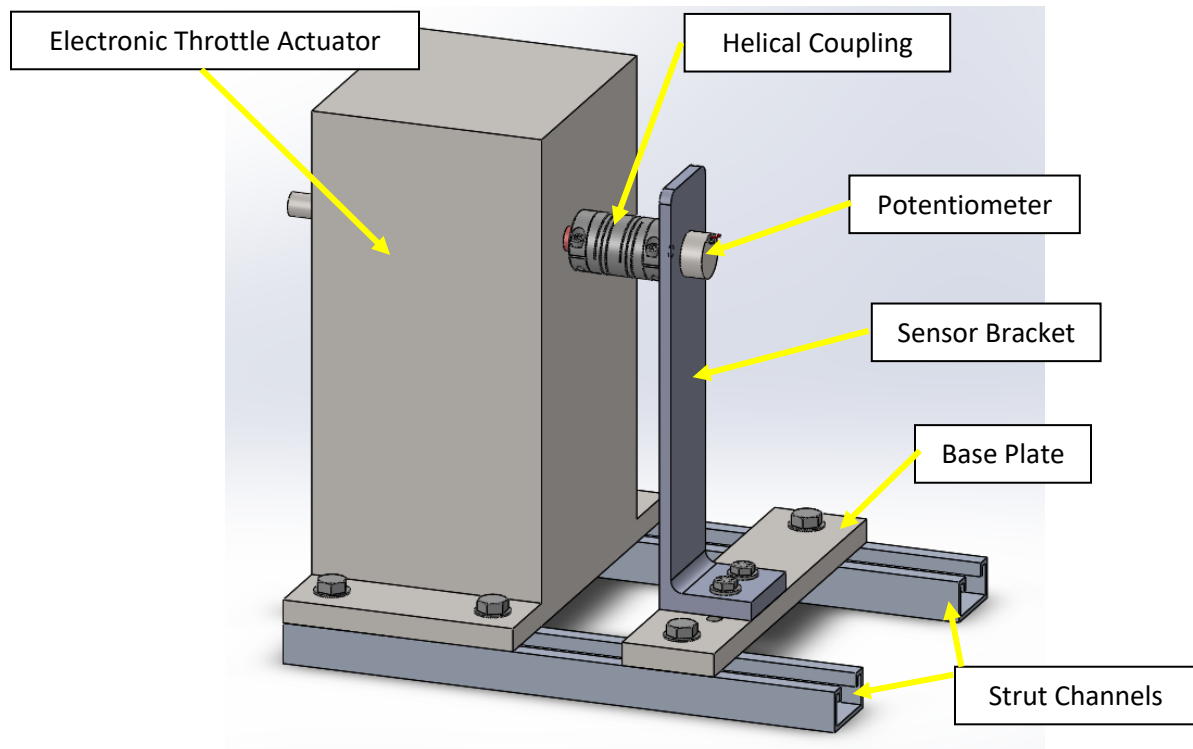


Figure 47. Entire TPS assembly

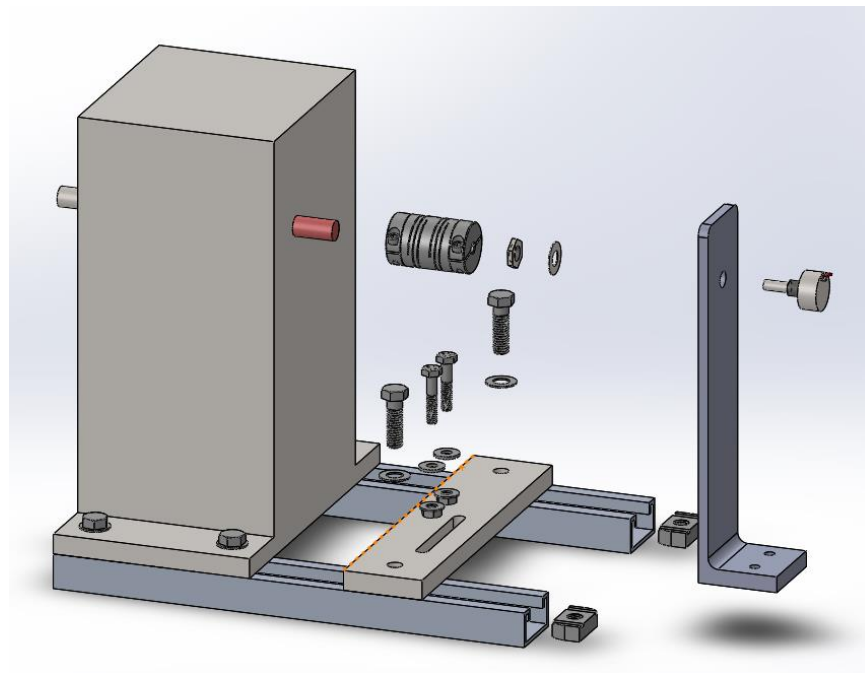


Figure 48. Exploded view of TPS assembly

Position Sensor

The selected rotary position sensor is a Series 026 Rotary Potentiometer manufactured by CTS Electrocomponents and sold by Digikey. The potentiometer is rated to 5 watts, has a linear voltage output, a minimum effective rotational angle of 280 degrees, and is rated to 10,000 cycles. It is a “panel-

mount” style sensor, meaning that the output shaft is inserted through a hole in the Sensor Bracket and secured with the included nut and lock washer, shown in Figure 46.



Figure 49. CTS Series 026 Rotary Potentiometer, Panel-Mount

A simple wiring harness using existing laboratory components will be manufactured and connected to the three electrical terminals on the potentiometer (power, ground, and output). The wires will then be fed into the dyno cell control box which is operated from outside of the cell. The dyno controller has built in functions that assign values (throttle position, in this case) based on a voltage input and a calibration curve. While the engine is off, a simple calibration will be performed by recording the potentiometer output voltage at two throttle positions: fully closed (0%) and fully open (100%). Because it is a linear-output potentiometer, these two values are enough to fully define the calibration curve.

Helical Coupling

The helical coupling is sourced directly from McMaster-Carr, and is sized to fit the $\frac{1}{2}$ " diameter output shaft of the throttle actuator and the $\frac{1}{4}$ " diameter potentiometer shaft. It is tightened onto the shafts via two #8-32 x $\frac{1}{2}$ " socket head cap screws.

Sensor Bracket

One of only two components for the TPS system that we will manufacture ourselves, the Sensor Bracket will be machined on a manual mill from a single piece of AL 6061 U-Channel. The bracket will be bolted to the slot in the Base Plate using two $\frac{1}{4}$ "-20 x 1.25" bolts. Due to the difficulty of perfectly measuring the location of the actuator output shaft relative to the strut channels, the bracket is designed to be fully adjustable in the two lateral directions. This is achieved by means of tee nuts sliding in the strut channels and the bracket mounting bolts sliding in the base plate slot. In order to account for measurement errors in the remaining degree of freedom, height, the locating hole in the Sensor Bracket for the potentiometer will initially be sized approximately $\frac{1}{16}$ " too *high*. The system will then be assembled, and the vertical shaft misalignment will be measured. The bottom face of the Sensor Bracket (the surface that sits on the Base Plate) will then be faced down on a mill by the measured amount to accurately bring the two shafts into alignment. Because the helical coupling can accept up to .015" of parallel misalignment, we are confident that this method will ensure alignment well within specification.

Base Plate

The Base Plate is the second (and last) component that we will be machining, and will be made from 9" x 2" x .5" AL 6061 rectangular bar stock. It will be cut and finish-machined to length, and then drilled and slotted for mounting. The slot for the Sensor Bracket will be machined using a 1/4" end mill. Because of the inherent adjustability, dimensional tolerances on the slot need not be very tight. In fact, the most critical dimension on this part is the distance between the two strut channel mounting holes, a dimension already determined by the existing hardware.

Cost Analysis and BOM

For a comprehensive list of all the parts in our final design, please see the indented BOM in Appendix G. However, the vast majority of the parts in that list have already been acquired, leaving only a select few components that we must buy for this project. Figure 51, below, shows all of our anticipated costs, with components grouped based on relative subsystem.

System	Relevant Part #	Description	Vendor	Quantity	Cost	Total Cost
Instrumentation	ENG0201	OMEGACLAD 1/16" Thermocouple	Omega	2	\$ 25.00	\$ 50.00
Instrumentation	ENG0202	1/8 NPT to AN-4 Adapter	McMaster-Carr	2	\$ 11.30	\$ 22.60
Instrumentation	ENG0303	1/8 NPT Tee Connector	McMaster-Carr	1	\$ 19.47	\$ 19.47
Instrumentation	ENG0204	1/8 NPT OMEGAllok Compression Fitting	Omega	2	\$ 20.50	\$ 41.00
Instrumentation	ENG0205	S.S. 304 1/2" Hex Bar Stock - 1 ft long	McMaster-Carr	1	\$ 10.10	\$ 10.10
Instrumentation	ENG0206	3/32 Cobalt Drillbit	McMaster-Carr	2	\$ 7.78	\$ 15.56
Instrumentation	ENG0207	3/32-3 Flute Jobbers Drill bit	McMaster-Carr	1	\$ 14.68	\$ 14.68
Instrumentation	ENG0208	3/32 4-flute uncoated carbide endmill	MSC	1	\$30.90	\$ 30.90
Instrumentation	ENG0209	1/8 die drill bit	MSC	1	\$27.39	\$ 27.39
Instrumentation	ENG0210	3/32 Die Drill	MSC	1	\$ 26.90	\$ 26.90
Instrumentation	ENG0211	3/32 4-flute carbide endmill	MSC	1	\$ 45.57	\$ 45.57
Instrumentation	ENG0212	1/4-28 Tap for Ti	McMaster-Carr	2	\$ 41.95	\$ 83.90
Instrumentation	ENG0213	3/32 Ultra Duty Drill Bit	McMaster-Carr	1	\$ 27.15	\$ 27.15
Instrumentation	ENG0214	Copper Crush Washers	McMaster-Carr	1	\$ 18.90	\$ 18.90
Instrumentation	ENG0215	KMQXL-062G-6 Thermocouple	Omega	2	\$ 32.00	\$ 64.00
Instrumentation	ENG0216	KMQXL-062G-12 Thermocouple	Omega	2	\$ 33.00	\$ 66.00
Instrumentation	ENG0217	1/4 NPT Tee Fitting	McMaster-Carr	1	\$ 22.79	\$ 22.79
Instrumentation	ENG0218	SSLK-116-18 Thermocouple	Omega	2	\$ 26.00	\$ 52.00
Instrumentation	ENG0219	Aeroquip FBM1011 - Reusable Hose Ends	Summit Racing	2	\$ 10.97	\$ 21.94
Instrumentation	ENG0220	Aeroquip FBM1011 - PTFE Fittings	Summit Racing	2	\$ 7.97	\$ 15.94
Instrumentation	ENG0221	Summit Racing SUM-220490-Summit Racing Hose Ends	Summit Racing	2	\$ 5.97	\$ 11.94
Instrumentation	ENG0222	1/4 NPT to 1/8 NPT Adaptor	McMaster-Carr	1	\$ 2.94	\$ 2.94
Instrumentation	ENG0223	Cobalt End Mill	McMaster-Carr	1	\$ 15.09	\$ 15.09
					Subtotal	\$ 706.76
TPS	TPS0101	CTS Rotary Potentiometer - Panel Mount	DigiKey	1	\$ 5.34	\$ 5.34
TPS	TPS0103	Helical Coupling - 1/2" x 1/4"	McMaster-Carr	1	\$ 58.25	\$ 58.25
TPS	TPS0102	AL 6061 U-Channel, 10" Base x 3-1/2" Leg	McMaster-Carr	1	\$ 28.70	\$ 28.70
TPS	TPS0111	AL 6061 Bar, 1/2" thick x 2" wide x 1' long	McMaster-Carr	1	\$ 8.60	\$ 8.60
					Subtotal	\$ 100.89
Other		Spare JFS-100 P.T. Containment Ring	George Carey	1	\$250.00	\$ 250.00
					Subtotal	\$ 250.00
					Tax (7%)	\$ 77.37
					Est. S&H	\$ 129.29
					TOTAL	\$ 1,264.31

Figure 50. Cost Analysis

As implied earlier, much of the hardware (such as all the nuts and bolts for the TPS system) does not show up on this cost spreadsheet because Jim Gerhardt has a vast selection of such items that we are

able to use for the project. There are no extra machining service costs because all the manufacturing will be completed at Cal Poly. The last line item, the “Spare JFS-100 P.T. Containment Ring,” is an item that was purchased from George Carey, a private seller who is currently our only source of spare parts for the JFS engine. He agreed to sell us a damaged, unusable power turbine containment ring for \$250. Because it is difficult to tell exactly what the inner structure of the containment ring looks like, it seemed risky to drill into ours (which is in excellent condition) without further investigation. We purchased the damaged unit from George, and will cut it apart to be able to clearly see how the various parts of the containment ring interface with each other. We will also be able to “practice” our planned machining operations on the damaged unit, thus minimizing risk when it comes to the final part.

Laboratory Activity

Although developing the lab activity is a central part of our project, it was decided shortly after the Preliminary Design Review that further work on this front should wait until the engine is fully instrumented and operating. Without actually running the engine ourselves, it is difficult to design operating procedures in any degree of detail, and it is unclear how much flexibility we will have regarding safely operating the engine at various operating points. Thus, the laboratory plan laid out in Chapter 3 has not changed. As a review, the primary highlights are:

1. Review safety protocols
2. Introduce students to JFS-100 engine. Include brief overview of component functionality
3. Students will run the engine at its rated design point and collect data
4. This data will be used to perform a simple 1-dimensional thermodynamic analysis to characterize the engine and evaluate component efficiencies
5. An energy balance will be performed on the engine based on the previous analysis
6. Finally, the students will be asked a set of conceptual questions to further understanding

We plan to have the engine running by the beginning of April (see Gantt chart in Appendix F), at which point lab activity development will continue.

Chapter 5: Manufacturing and Assembly

Manufacturing

The vast majority of the manufacturing phase of our project was focused on fabricating the hardware for Stage 4 instrumentation. This proved to be a challenge because it involved machining the titanium containment ring around the power turbine, the power turbine housing itself, and a stainless-steel sensor housing that would hold the thermocouple and pressure transducer line for Stage 4. As discussed earlier in Chapter 3, the majority of the manufacturing processes were carried out in Jim Gerhardt’s shop. This allowed him to supervise and advise us on some of the more delicate and complex machining processes, while still allowing us to be the primary machinists.

Stage 4 Sensor Housing

The sensor housing was designed to hold an OMEGACLAD 1/16” thermocouple and provide a gas path for the pressure transducer line. To accomplish this, two separate machining operations were carried

out. The first involved taking the ½” diameter stock and facing one end to 1.9” on a Haas TL-1 lathe. Using a parting tool, the piece was cut to 1.8 inches and reset into the jaws of the chuck. With Quickcam the shank of the sensor housing was turned down to 0.4”, with a step down to 1/4 “ inch in diameter at the end for the crush washer. Using the tailstock of the lathe, a 1/8” hole was cut 0.75 inches deep into the end of the part and tapped for a 1/8 NPT thread. Once this was completed, the part was removed from the chuck jaws, flipped, and reset. The next step was to manually drill a pilot hole and a 1/16 inch diameter hole. This was cut 0.32” inches into the part, and was designed to loosely hold the thermocouple to allow for a flow path of the gases from stage 4 to the pressure transducer.

The second process was completed on Haas TL-1 CNC mill. The mill was used to precisely locate and drill the other two 1/16” holes into the end of the sensor housing. The final part can be seen in Figures 52 and 54. Figure 53 shows the part with the 1/8 NPT tee fitting attached.

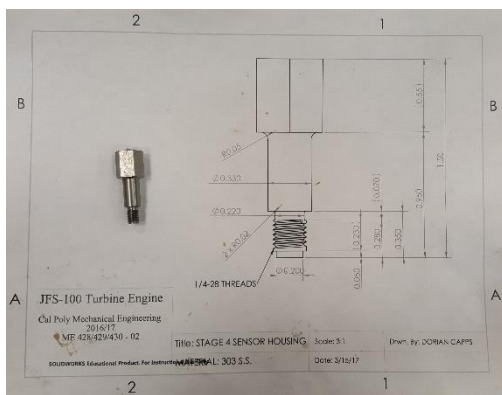


Figure 51. Final Sensor Housing Part with Drawing

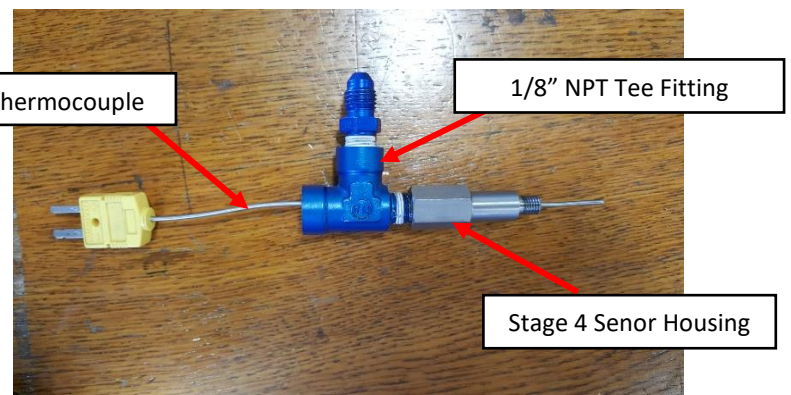


Figure 52. Sensor Housing Installed on Tee fitting w/ Thermocouple

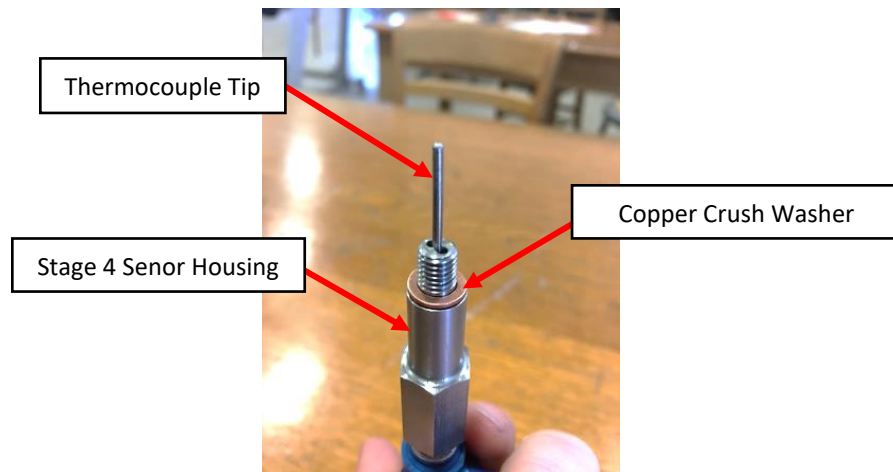


Figure 53. End of sensor housing with the thermocouple and copper crush washer installed

Containment Ring

The containment ring presented two main challenges for us. First, the XRF results showed that the containment ring is made out of Ti-6Al-4V, a high-strength titanium alloy known to be difficult to

machine because it work hardens at low temperatures. Second, it was unknown to us if the containment ring was solid titanium. As can be seen in Figure 55, wear rings are located on the inner diameter. These rings are used to maintain extremely small clearances between the blades of the turbine and the walls that surround it.

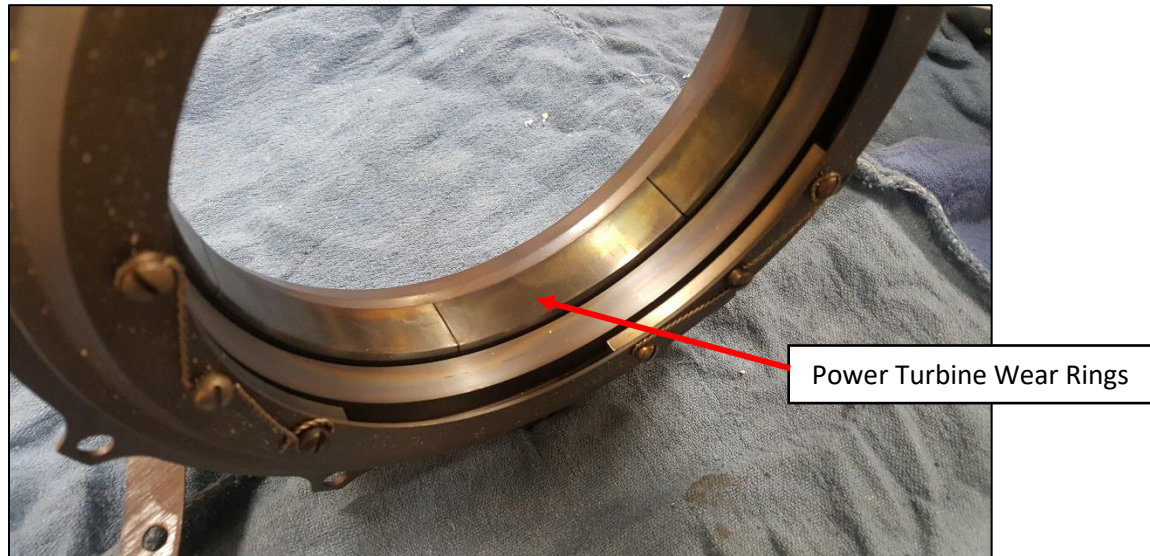


Figure 54. *Power Turbine Containment Ring*

The issue was that there was no clear indication as to what was behind the wear rings, or how they were attached to the titanium portion of the containment ring. Knowing the delicacy of the operation, the large amount of unknowns, and how difficult it would be to machine titanium precisely the first time with no mistakes, we decided to purchase a spare containment ring from George Carey, the turbine enthusiast who is our main source of spare engine parts.

Upon receiving the spare containment ring, a G-code was written for machining the sensor housing instrumentation port on the TM-1 CNC Mill using CamWorks software and the CAD model discussed in the Design Development section, Chapter 3. There were five main tooling operations within this code that needed to be carried out. First, a pilot hole had to be drilled into the outer wall of the containment ring. This would decrease the chances of a drill bit deflecting in the next operation, ensuring a straight drill path through the ring. The next step was to drill a 1/8" through-hole to allow the thermocouple to be inserted through the containment ring and into the gas flow path. Once this had been completed the next two operations were to drill and tap the threads for the sensor housing to screw into. The final machining process was to cut the circular pocket for the crush washer to sit. This involved using a 1/4 inch end mill to cut a 0.45 inch diameter hole, 0.0610 inches in depth.

Unfortunately, there were many complications to this seemingly simple procedure. The first problem became apparent upon drilling the first through-hole. The cobalt drill bit simply snapped after cutting about 1/5 of the way into the containment ring. Thinking that the titanium had been accidentally work hardened, more research was put into the proper feedrates and tool speeds for machining titanium. Another cobalt drill bit was ordered, the practice containment ring was rotated, and the process was repeated. Figure 56 shows the practice containment ring being machined. Looking closely, you can see the multiple machining attempts along the outer wall.



Figure 55. Spare Containment Ring Being Machined on Jim's TM-1

Again, the drill bit snapped early in the machining cycle. Thinking the problem was the tool material, a carbide-coated drill bit was ordered. Once again, the drill bit snapped. The next idea was to use a square-bottom end mill to drill through the containment ring. During this machining cycle, the end mill didn't snap but instead became rounded and lost all of its cutting edges. A

Much to our surprise, the key to (this machining operation) machining this processes was a straight-flute drill bit. Also called die drill bits, these tools are designed for drilling through hardened tool steel often used for stamping and casting dies. With the proper speed and feedrate, a full-retract peck-drill cycle, and a large amount of coolant, this drill bit was able to easily cut through the both the containment ring and the wear plates. A photo of this drill bit can be seen in Figure 57.



Figure 56. Straight-Flute Drill Bit

The next issue was how to properly tap the containment ring. For the first attempt, the HAAS VF-3 CNC mill in Mustang 60 was used. The tap was not sitting correctly in the tool holder which resulted in the tap moving vertically during the machining operation and not threading the hole correctly. In the next attempt, we attempted to hand tap the hole. The reasoning was that we had more control over how fast the hole was tapped, thus be able to ensure that the titanium wasn't being work hardened. The tap ended up snapping about a quarter way through the containment ring, and was in general extremely

difficult to work with manually. It was decided to go back to using Jim's TM-1, with lower feeds and speeds.

This ended up working, and the rest of the machining operation was completed with no problems. The entire process was done repeatedly until we had complete confidence that there were no errors in the code and every operation could be carried out successfully. We then moved on to machining the actual containment ring that would be installed in the engine, shown in Figure 58.



Figure 57. *Final Machining of Actual Containment Ring*

Power Turbine Housing

The last component that needed to be machined for Stage 4 instrumentation was the power turbine housing, which required a clearance hole in order to allow installation of the sensor housing into the containment ring. The power turbine housing is made out of a stainless-steel alloy, and we were able to determine proper cutting tools and parameters easily. The more challenging aspect was how to fixture the turbine housing securely in a vice during machining. Due to the part being asymmetrical and the location of the hole being at a strange angle, we had to make specialized vice jaws and an angle finder. The angle finder was a triangular piece of wood, cut to 18 degrees. The vice jaws were manually milled out of aluminum and can be seen in Figure 59. The final machining set up can be seen in Figure 60, with the turbine housing sitting on top of the original vice jaws because the width was larger than the jaws could be moved to.

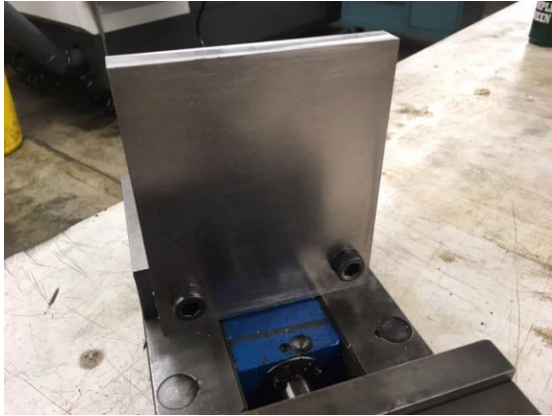


Figure 58. Aluminum vice jaws

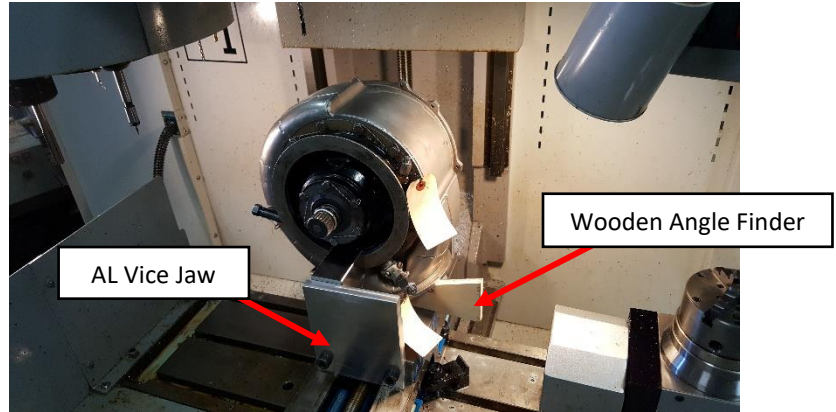


Figure 59. Power Turbine Machining Setup

Throttle Position Sensor

The throttle position sensor has only two components that need to be machined. The first is the base plate that bolts to the rails of the floor, and is what the sensor bracket is mounted to. The base plate was machined in Mustang 60' on the manual mill (Figure 61). The first step was to use the aluminum chop saw to cut the 12 inch aluminum stock down to 9 inches. Next, the part was faced down to the appropriate length on the mill using a $\frac{1}{4}$ inch end mill and the DRO. Two $\frac{3}{8}$ inch holes were drilled with a $\frac{3}{8}$ inch center-cutting end mill. The final step was to mill out the 0.3" diameter, 2.5"-long slot.



Figure 60. Base plate machining setup

The second part that needs to be machined is the sensor bracket. This will only require two machining operations to be completed. The first is to cut the aluminum stock to length using the aluminum chop saw. After this has been completed, two slots will be machined on the base portion of the bracket to allow for lateral adjustment of the part. Currently, this component has yet to be machined.

Assembly

With manufacturing complete, we began installing the instrumentation and reassembling the engine. The first step was to install the Stage 3 instrumentation into the air-start port, shown in Figures 62 and 63.

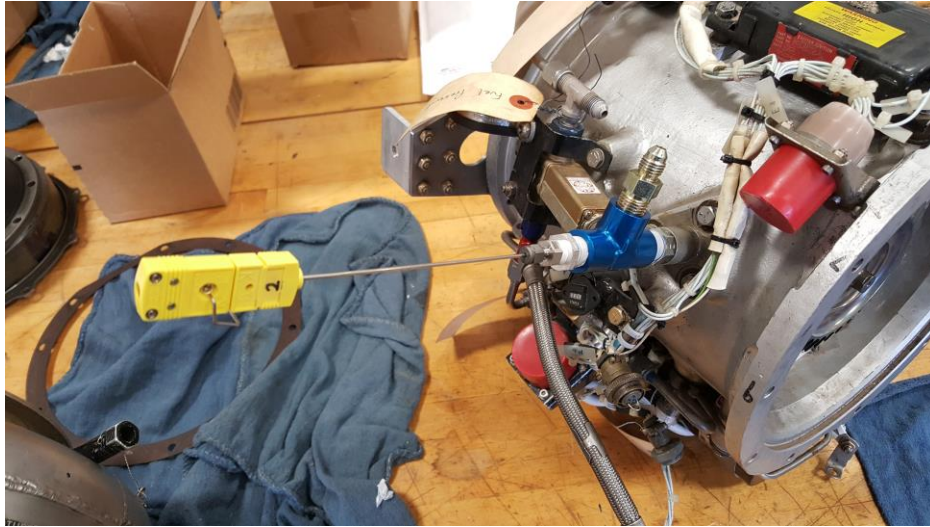


Figure 61. Stage 3 instrumentation port



Figure 62. Stage 3 thermocouple inserted through the air-start rakes

The power turbine IGV ring was then installed, with a layer of high-temperature silica sealant applied to the mating surface (Figure 64).



Figure 63. Power turbine IGV ring ready for installation

Following aerospace standards, the screws that fasten the IGV ring to the gas generator assembly were safety-wired to prevent them from loosening due to vibration (Figure 65).



Figure 64. IGV ring installed in the gas-generator assembly, with the bolts safety-wired

The next step was to install the power turbine containment ring into the power turbine housing, thus completing the power turbine assembly. During disassembly, we had noticed a significant amount of white thermal insulation installed in the space between the containment ring and the housing. Accordingly, we purchased sheets of 1/32"-thick ceramic insulation from McMaster-Carr and wrapped it

around the containment ring prior to installation, as shown in Figure 66. We cut out a small hole in this insulation to accommodate the Stage 4 sensor housing.



Figure 65. Thermal insulation wrapped around containment ring prior to installation

The containment ring was then slid into the power turbine, and the Stage 4 instrumentation holes on both parts were checked for alignment. Figure 67 shows these two components mated together.



Figure 66. Containment ring installed in power turbine housing

Next, the Stage 4 instrumentation assembly, including the sensor housing, thermocouple, and compression fitting, were inserted through the clearance hole in the power turbine housing and threaded into the containment ring, shown in Figure 68.



Figure 67. Stage 4 instrumentation installed in power turbine

The depth of the thermocouple was adjusted to the desired point: extending as far into the flow path as possible without interfering with the power turbine blades. When the desired position was achieved, the compression fitting was tightened around the thermocouple, fixing it in place. Figure 69 shows the final Stage 4 thermocouple location.



Figure 68. Stage 4 thermocouple location

With the power turbine and gas generator both assembled, the last step was to mate them together. The large flange shown in Figure 70 provides the mating surface, and ten screws are installed through the gas generator housing and are threaded into the power turbine housing. Figure 71 shows the fully assembled engine.

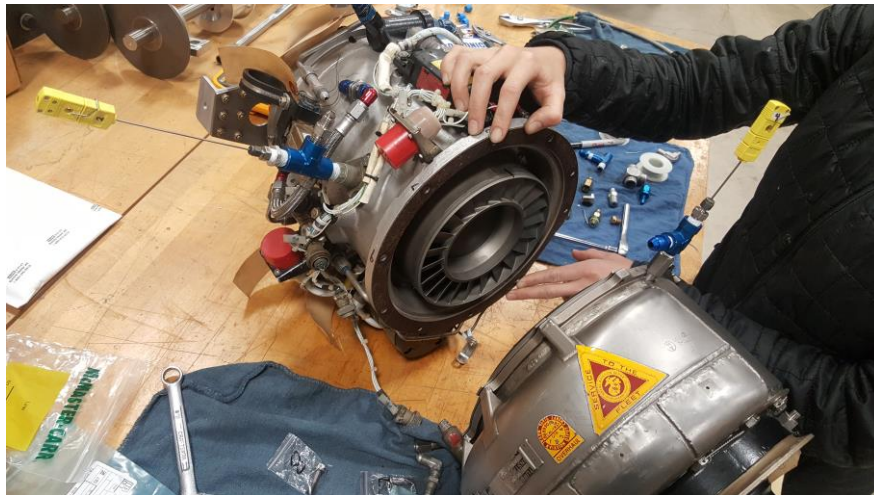


Figure 69. Preparing to mate the gas generator and power turbine assemblies



Figure 70. Fully assembled and instrumented engine

During the entire process of reassembly, we would repeatedly spin the turbine by hand to ensure that there was no interference with any part of the rotating assembly. We were very careful to keep things clean and organized, as a small oversight here could have been very costly. One of the challenges we faced was that none of the manuals for the engine included torque specifications for any of the fasteners. We considered calculating some rough torque values ourselves, using the type and size of fastener as well as the materials that they interface with. However due to the exotic materials used in the engine and our complete lack of knowledge regarding grade or material of the fasteners themselves, we soon realized that any attempt at such an analysis would be primarily guesswork. Thus, under the direction of Jim Gerhardt, we tightened everything using a small handle ratchet until they were quite firm, and left it at that.

Installing the engine on the dynamometer was the next task, and included many small hardware details that needed attention, many of which were initially unforeseen. Because it had been many years since the hardware was used, numerous components had to be installed, tested, and in some cases, repaired or replaced. In the interest of brevity, we will not discuss each and every one of these tasks in depth, however what follows is a brief outline of the dyno installation process. The engine was carried over to the dyno, attached the dyno coupling, and bolted to the four main mounting points as shown in Figure 72.

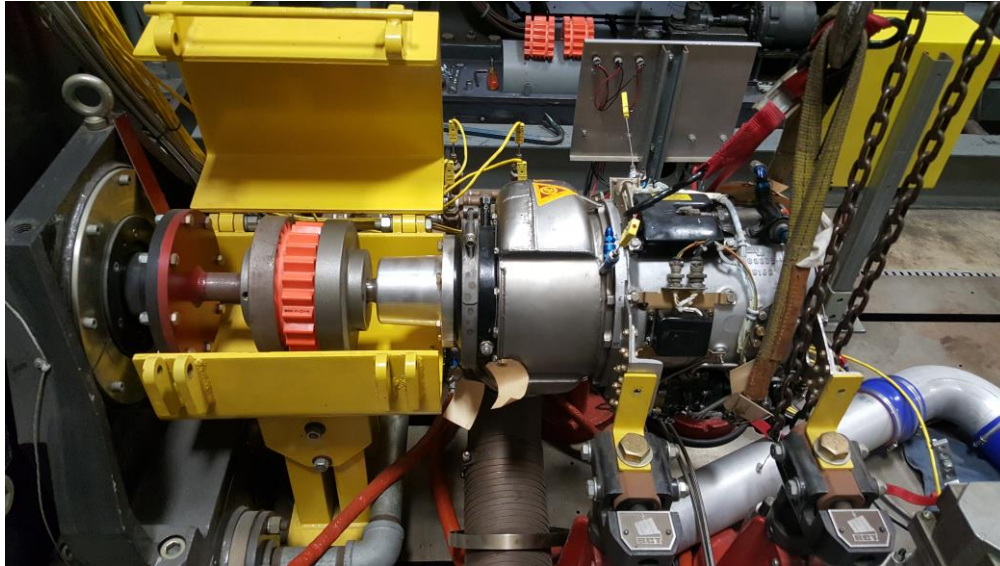


Figure 71. *Installing the engine on the dynamometer*

The alignment of the coupling was checked to ensure that there was no more than 1 degree of misalignment in any direction. Because this had been set up and aligned before, no further adjustment was necessary. We attached the intake and exhaust pipes, and connected hoses from the pressure ports on the engine to the pressure transducers located in the control box in the dyno cell. The engine was filled with oil, and the oil circulation pumps were turned on to ensure proper operation. In fact, one of these pumps had corroded and seized, and was subsequently replaced. We tested the water supply system, which circulates cooling water both through the dyno and through the oil heat exchangers, and had to flush the system and replace the water filter. The new instrumentation was wired to the control box, which was already set up to output the required channels to the controller and data acquisition system outside of the test cell. All of the sensors were calibrated (see Chapter 8), and the wires and hoses were bundled and organized to make sure they did not touch any hot engine components. The fuel supply system (running through the Fuel Balance that measures fuel flow when the engine is running) was reattached and flushed with fresh Jet-A fuel. The completed engine/dyno assembly is shown in Figure 73.

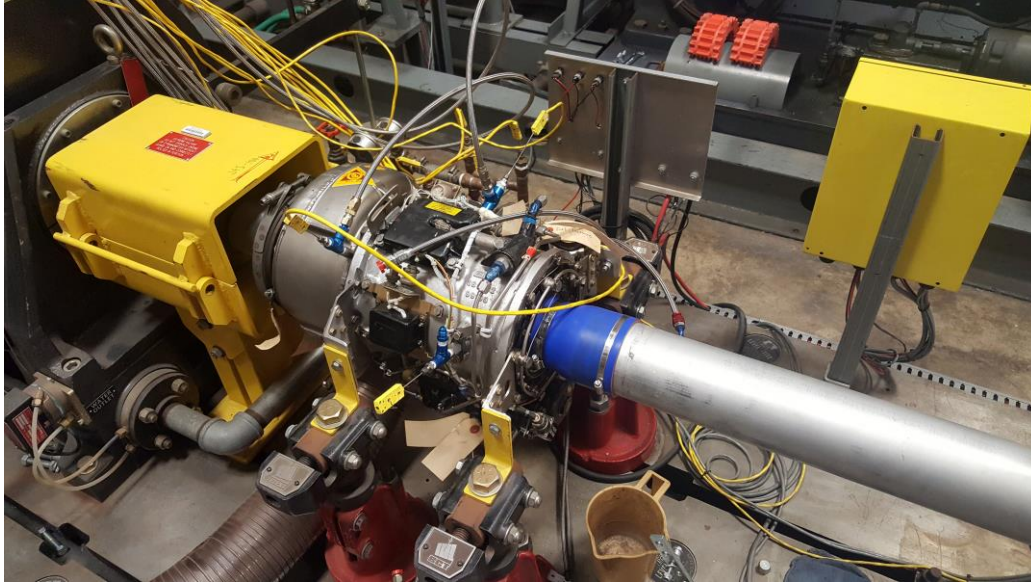


Figure 72. Engine fully installed and hooked up to the dynamometer

Chapter 8: Testing and Design Verification

Thermocouple Testing

Although we purchased the thermocouples from Omega, a highly regarded instrumentation company, small thermocouples tend to be rather fragile and can easily break during shipping/transportation. As such, we decided to test all of the thermocouples we purchased to make sure they function properly. This testing process involved submersing each thermocouple in both an ice bath and a reservoir of boiling water, and ensuring that they measured 32 °F and 210 °F respectively. The key piece of equipment we used for this testing was a Fluke Thermocouple Calibrator provided by Jim Gerhardt. This handheld calibrator can be directly plugged into the thermocouple connector and measures temperature output. For each thermocouple, we repeated the experiment three times. The results are shown in Table 10.

Table 10. Results from preliminary thermocouple testing

	Ice Bath			Boiling Water		
	Trail 1 [°F]	Trial 2 [°F]	Trail 3 [°F]	Trail 1 [°F]	Trial 2 [°F]	Trail 3 [°F]
Thermocouple 1	33.0	33.0	33.0	208.9	209.1	209.2
Thermocouple 2	33.1	33.0	33.1	209.1	209.0	209.0
Thermocouple 3	33.0	33.0	33.0	208.5	209.0	209.0
Thermocouple 4	33.0	33.1	33.1	209.0	209.1	209.2

Each thermocouple accurately measured the desired temperature within 2 °F for each of the three trials. We concluded that all of the thermocouples were accurate and functioning properly.

Sensor Calibration

With all of the sensors installed in the engine and wired into the controller, the next step was to calibrate them in the Digalog data acquisition system, using the Hypercell user interface software (Figure 74). Because the entire system hadn't been used in 5-6 years, we decided to calibrate *all* of the thermocouples and pressure transducers used to monitor the engine, not just the ones that we added ourselves. The thermocouples are calibrated using a linear conversion through the Hypercell "Calibration" menu. First, the Fluke Thermocouple Calibrator was plugged into one of the thermocouple channels and set to "Output" mode. This mode allows the calibrator to imitate a temperature input to the channel. The calibration interface requires a "low value" and a "high value", which it uses to create the linear calibration curve. We used a low value of 0 °F, and a high value of the design point temperature for each thermocouple (e.g. 1264 °F for T₃). After calibrating all the thermocouples, with the engine off they all displayed the proper ambient temperature within 2 °F.

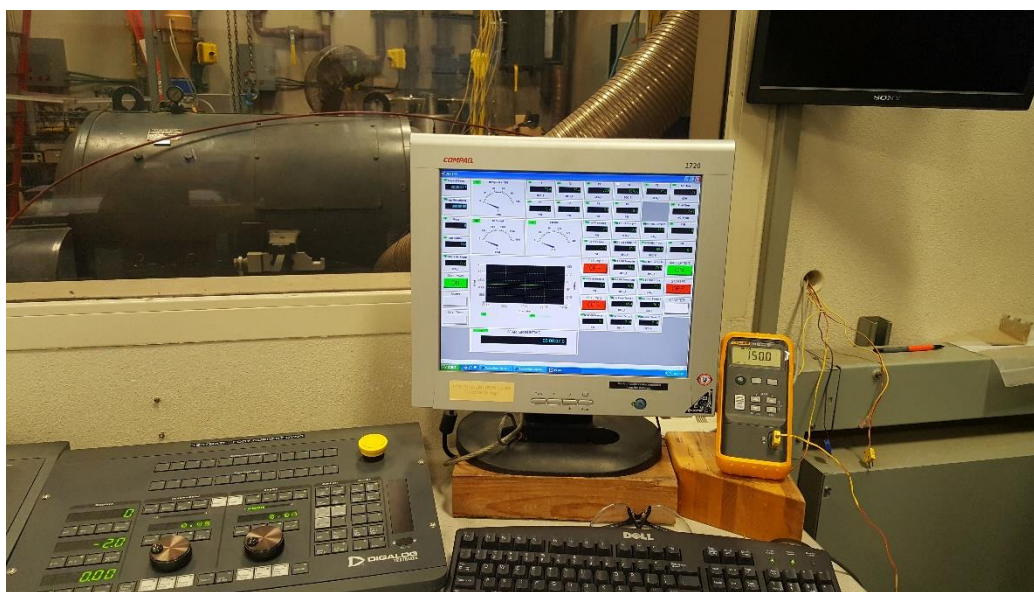


Figure 73. Controller interface including Hypercell display

A similar procedure was followed to calibrate the pressure transducers, this time using a Fluke Pressure Calibrator. This equipment contains a small hand pump, pressure display, and supply hose that allows you to apply the desired pressure to a transducer or other pressure sensor. Like the thermocouples, the transducers are linear output sensors, and thus a linear calibration curve was used. We used a low value of 0 psig and a high value of 100psig, which covers the entire operating range of the Sensym ICT pressure transducers. After calibration and with the engine and subsystems off, the pressure transducers all displayed within .5 psig of the expected atmospheric pressure of 0 psig.

Another critical component that required recalibration was the Laminar Flow Element that is used to measure the volumetric air flow into the engine. Also a linear output sensor, the LFE uses the differential pressure across a laminar flow-inducing restriction to characterize the flowrate, and was thus easily calibrated using the Fluke Pressure Calibrator. A low value of 0 inH₂O differential pressure was used,

corresponding to a flowrate of 0 CFM. A high value of 407 CFM at 8 inH₂O differential pressure was provided by the equipment manufacturer.

Shutoff Algorithms

After programming the alarms and limits into Hypercell, it was necessary to verify that they functioned properly before starting the engine itself. This was done using two methods. The first method was to use the thermocouple calibrator described earlier to “fake” an over-temperature condition. For example, with the T4 limits set at 1000 °F (high yellow) and 1100 °F (high red), the calibrator was set in “output” mode and the output slowly increased until it reached 1000 °F. At this point, the high yellow alarm would be tripped and a warning message would appear, accompanied by the Testmate alarm sound. After acknowledging the alarm, we continued to increase the calibrator output until it reached 1100 °F. This would trip the high red alarm, causing the engine power to be shut off and the test to be put on hold. In this manner, we verified that the alarms and shutoff actions for each critical temperature performed properly.

A different method was used to test the over-speed software limits, which were programmed to shut off the engine if either the engine or the dyno speed limits were exceeded. Similar to the temperature testing described previously, we needed to fake a speed signal to the controller in order to test the alarm protocols. This was accomplished by using a signal generator and an oscilloscope, shown in Figure 75. We programmed the signal generator to output a 1 V_{pp} square wave, the same type of signal output by the hall-effect speed sensors. By varying the frequency of the signal generator, we could imitate different speeds to the controller. Using this method, we were able to verify that the high yellow and high red alarms based on speed inputs were properly activated, and that the engine power was indeed shut off in the high red alarm state.

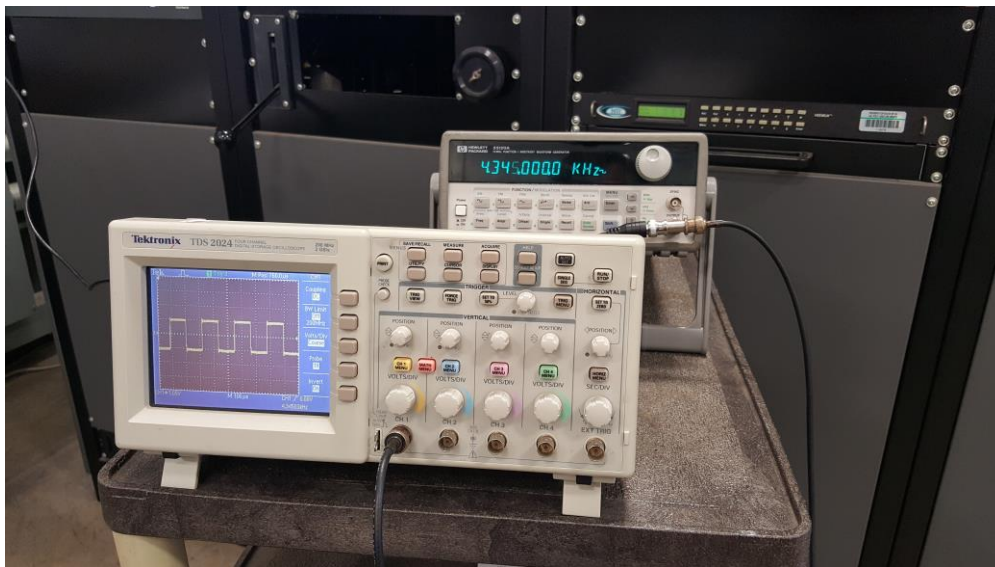


Figure 74. Testing over-speed shutoff conditions using a signal generator

Engine Startup

With all of the sensors calibrated and programming complete, the final step is to actually start the engine. This will allow us to thoroughly verify our design point analysis and instrumentation hardware under real operating conditions. Regrettably, at the time of this writing, we are still working through the

last safety checks and engine operating procedures with Dr. Lemieux and Jim Gerhardt, and thus have not yet ran the engine. We are planning on completing this crucial step in the final week of the project.

Chapter 9: Conclusions and Recommendations

By now it should be fairly clear to the reader that we did not complete all of the objectives that were stated at the outset of the project. Throughout the manufacturing and assembly processes, we took extreme care to make sure that parts were made correctly and no details were overlooked. As we were integrating the engine back onto the dyno, numerous small projects would arise that needed to be completed, mostly due to the fact that none of the hardware had been used in more than five years. We spent many hours simply troubleshooting the network system that allows the user interface software to communicate to the engine and dyno controllers. Even more time was spent learning how to program the software, which affords the user a large amount of control and customization, at the cost of a very steep learning curve. Although frustrating at times, this lengthy process was necessary to ensure that we could confidently run the engine without fear of malfunction or damage. We were constantly reminded by Dr. Lemieux, our sponsor, and Jim Gerhardt to work through the details slowly and methodically to avoid costly mistakes. Unfortunately, however, this means that there is still work to be done before the engine is ready for use as part of a class. The remaining items that still require development are: engine startup and design point verification, final manufacturing and integration of the redundant TPS, and detailed design of the laboratory activity. Jim Gerhardt and Dr. Lemieux will continue working to complete these objectives in the coming months.

Special thanks to Jim Gerhardt, Dr. Patrick Lemieux, and Dr. Peter Schuster for their advice and support!



Figure 75. The dream team (From left: Dr. Lemieux, Dorian, Jim, Zoe)

APPENDIX A

House of Quality

Customer Description		Importance	▲	▲	▲	▲	▼	▲	▼	▲	○	○	▲	Customer Ratings						
1. Dr. Patrick Lemieux 2. Students of ME444 3. Jim Gerhardt			Accurate Mech. Interface with Digalog Dyno	Instrumentation Interface with Digalog Controller	Automatic Shut off System	Temperature and Pressure Instrumentation @ Stages 1-5	Instrumentation capable of accurate measurements at local conditions	Externally-Cooled Oil System	Reliable Air Start Mechanism operable from outside test cell	Reliable Fuel Flow system	Thermocouples installed throughout oil circuit	Engine intake interfaces with mass flow air sensor	Subsystems Durability 10 years	Bad	1	2	3	4	5	Good
1	Safety		○	○	○	○	○	○	△	○	△	○	○	1	□	2	○	3	△	5
2	Reliable		○	△	○	○	○	○	○	○	○	○	○		□	○	○	△		
3	Ease of operation		○	○	△	○	○	○	○	○	○	○	○		□	○	○	△		
4	Cost Efficient (Inexpensive)		△	○	△	○	△	△	○	△	△	○	△	△	△	□	○	○	△	
5	Servicable		△	○	○	○	○	○	○	△	△	○	△		□	△	○			
6	Educational		○	○	△	○	○	△	△	△	△	△	○	○	□	○			△	
Strong - ○ Medium - ○ Weak - △		5	△		△	△		△	△	△	△	△								
		4		△				△					△	△						
		3									○									
		2							□		□		○							
		1	□	○	□	○	□	○	○	□	○	□	○	□						
Targets		1 deg. Misalignmmt Max																		
		Yes/No																		
		Within +/- 10 deg. C of limit																		
		Yes/No																		
		Yes/No																		
Relationship Strength		Min. Rated Start Speed																		
		Yes/No																		
		Yes/No																		
		Yes/No																		
		10 Years																		

△TurboGen
○Zenith Air
□Homebuilt TurboKart

△TurboGen
 ○Zenith Air
 □Homebuilt TurboKart

Design Safety Hazard Checklist

ME 428/429/430 Senior Design Project

2016-2017

DESIGN HAZARD CHECKLIST		
Team:	<u>Turbine Team</u>	Advisor: <u>Peter Schuster</u>
Y N		
<input checked="" type="checkbox"/> <input type="checkbox"/>	1. Will any part of the design create hazardous revolving, reciprocating, running, shearing, punching, pressing, squeezing, drawing, cutting, rolling, mixing or similar action, including pinch points and sheer points?	
<input checked="" type="checkbox"/> <input type="checkbox"/>	2. Can any part of the design undergo high accelerations/decelerations?	
<input checked="" type="checkbox"/> <input type="checkbox"/>	3. Will the system have any large moving masses or large forces?	
<input type="checkbox"/> <input checked="" type="checkbox"/>	4. Will the system produce a projectile?	
<input type="checkbox"/> <input checked="" type="checkbox"/>	5. Would it be possible for the system to fall under gravity creating injury?	
<input type="checkbox"/> <input checked="" type="checkbox"/>	6. Will a user be exposed to overhanging weights as part of the design?	
<input type="checkbox"/> <input checked="" type="checkbox"/>	7. Will the system have any sharp edges?	
<input type="checkbox"/> <input checked="" type="checkbox"/>	8. Will any part of the electrical systems not be grounded?	
<input type="checkbox"/> <input checked="" type="checkbox"/>	9. Will there be any large batteries or electrical voltage in the system above 40 V?	
<input checked="" type="checkbox"/> <input type="checkbox"/>	10. Will there be any stored energy in the system such as batteries, flywheels, hanging weights or pressurized fluids?	
<input checked="" type="checkbox"/> <input type="checkbox"/>	11. Will there be any explosive or flammable liquids, gases, or dust fuel as part of the system?	
<input type="checkbox"/> <input checked="" type="checkbox"/>	12. Will the user of the design be required to exert any abnormal effort or physical posture during the use of the design?	
<input type="checkbox"/> <input checked="" type="checkbox"/>	13. Will there be any materials known to be hazardous to humans involved in either the design or the manufacturing of the design?	
<input checked="" type="checkbox"/> <input type="checkbox"/>	14. Can the system generate high levels of noise?	
<input checked="" type="checkbox"/> <input type="checkbox"/>	15. Will the device/system be exposed to extreme environmental conditions such as fog, humidity, cold, high temperatures, etc?	
<input checked="" type="checkbox"/> <input type="checkbox"/>	16. Is it possible for the system to be used in an unsafe manner?	
<input type="checkbox"/> <input checked="" type="checkbox"/>	17. Will there be any other potential hazards not listed above? If yes, please explain on reverse.	
<p>For any "Y" responses, add (1) a complete description, (2) a list of corrective actions to be taken, and (3) date to be completed on the reverse side.</p>		

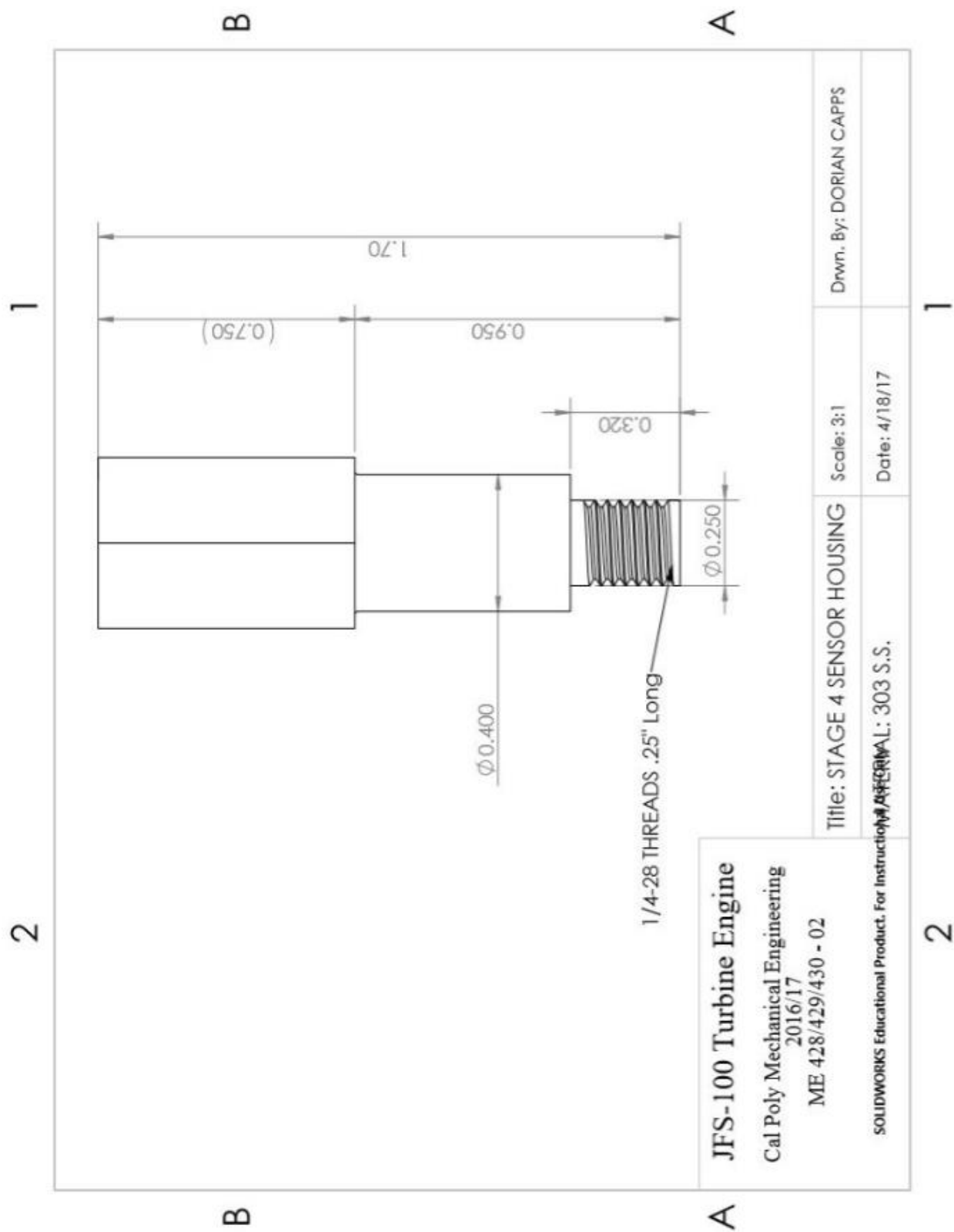
Description of Hazard	Planned Corrective Action	Planned Date	Actual Date
Turbine Blades, Output Shaft coupled to Dynamometer	Students will be required to be outside of test cell during turbine operation	Winter 2017	N/A
Fuel System	Thermocouples will be installed within fuel system to monitor temperature	Completed	N/A
Dynamometer Shaft	A metal case will be locked over coupled shaft	Completed	N/A
Exhaust Temperature	Temperature sensors will be installed in the turbine at this location to monitor combustor outlet temperature	01/09/2017	N/A
Gas Turbine Engine	Students will be required to wear ear protection during turbine operation	Winter 2017	N/A

2

Part Number	Part Name
1	POWER TURBINE HOUSING
2	POWER TURBINE ROTATOR
3	POWER TURBINE DIFFUSER
4	POWER TURBINE CONTAINMENT RING
5	POWER TURBINE IGV RING
6	POWER TURBINE GASKET
7	GAS GENERATOR TURBINE
8	GAS GENERATOR ASSEMBLER

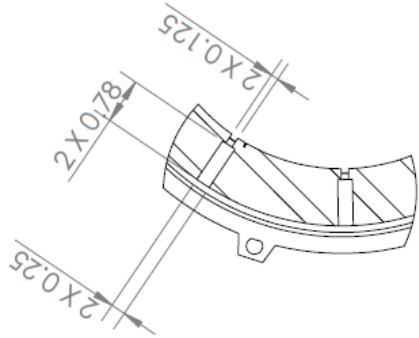
Chkd. By: ZOE TUGGLE

△

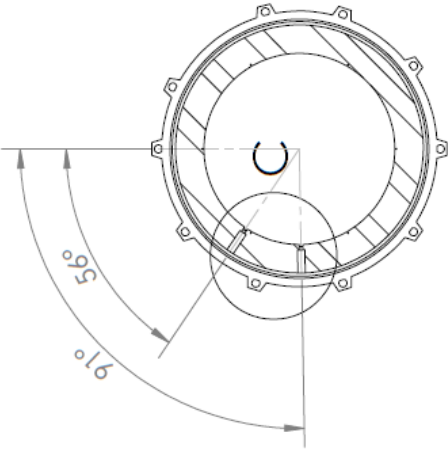
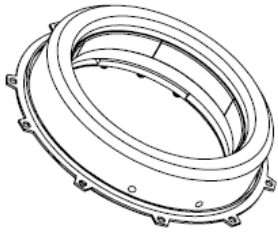


2

1



DETAIL C
SCALE 2:5



- NOTES**
TWO HOLES ARE IDENTICAL
UNLESS OTHERWISE SPECIFIED:
- 1. ALL DIMS. IN INCHES
 - 2. TOLERANCES:
X=±1
X.XX=±0.1
X.XXX=±0.005
ANGLES=±2°
 - 3. MATERIAL: TI-6AL-4V

B

B

A

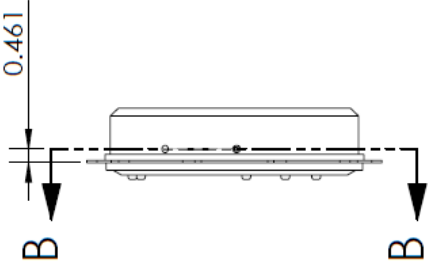
A

JFS-100 Turbine Engine
Cal Poly Mechanical Engineering
2016/17
ME 428/429/430 - 02

SOLIDWORKS Educational Product. For Instructional Use Only

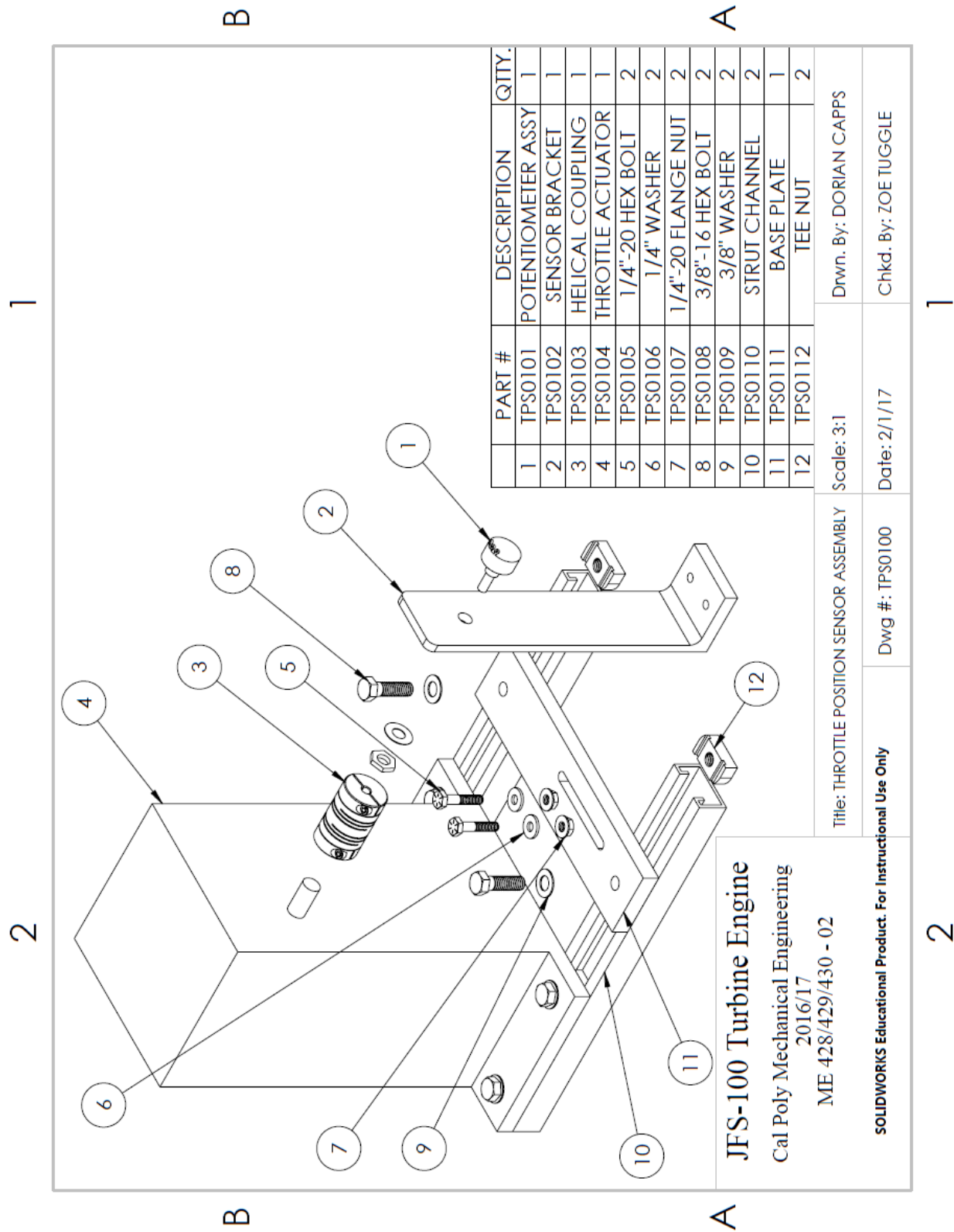
Title: POWER TURBINE CONTAINMENT RING		Scale: 1:5	Drwn. By: DORIAN CAPPS
Dwg #: ENG0104		Date: 2/9/17	Chkd. By: ZOE TUGGLE

SECTION B-B



2

1



2

1

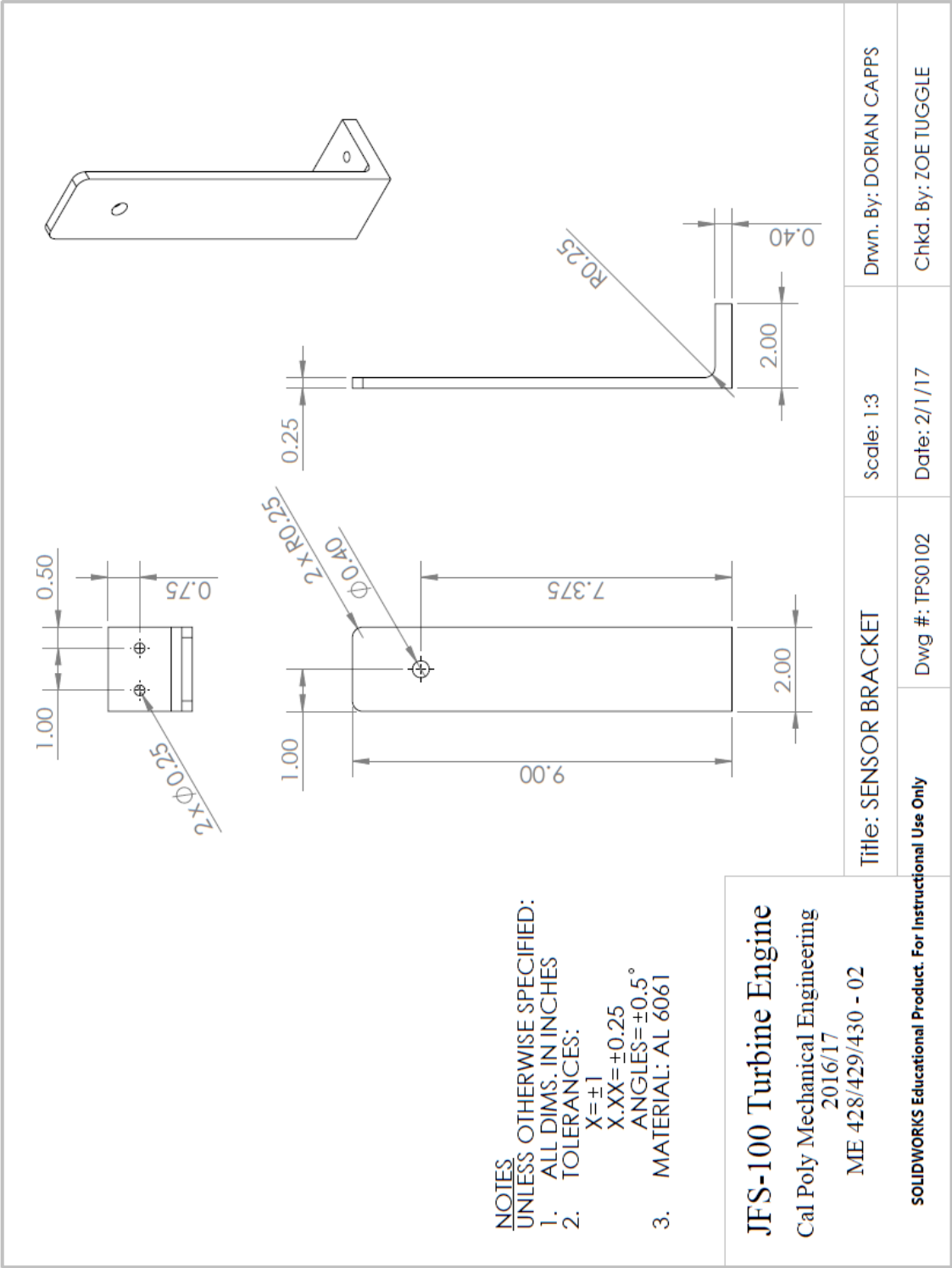
B

B

- NOTES**
UNLESS OTHERWISE SPECIFIED:
1. ALL DIMS. IN INCHES
2. TOLERANCES:
X=±1
X.XX=±0.25
ANGLES=±0.5°
3. MATERIAL: AL 6061

A

A



2

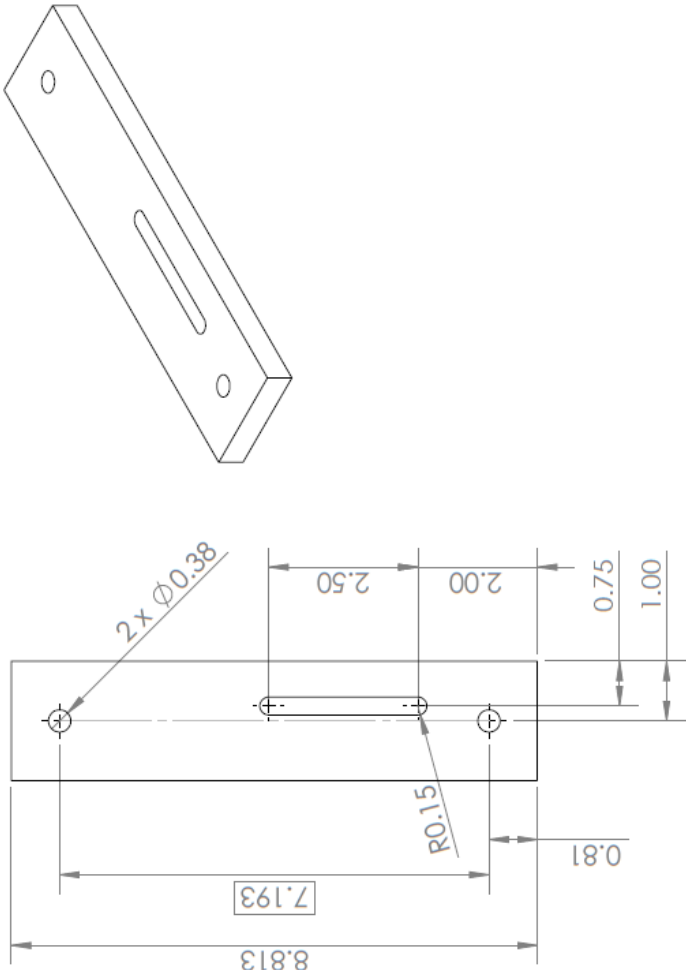
1

2

1

B

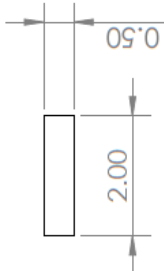
B



- NOTES
UNLESS OTHERWISE SPECIFIED:
1. ALL DIMS. IN INCHES
2. TOLERANCES:
X = ±1
X.XX = ±0.25
ANGLES = ±0.5°
3. MATERIAL: AL 6061

A

A



JFS-100 Turbine Engine

Cal Poly Mechanical Engineering
2016/17
ME 428/429/430 - 02

SOLIDWORKS Educational Product. For Instructional Use Only

Title: BASE PLATE

Dwg #: TPS0111

Scale: 2:3

Chkd. By: ZOE TUGGLE

Drwn. By: DORIAN CAPPS

Date: 2/1/17

2

1

APPENDIX C

Vendor List

McMaster-Carr

<https://www.mcmaster.com/>

(562) 692-5911

(562) 641-2800

DigiKey

<http://www.digikey.com/>

1-800-344-4539

Omega

<http://www.omega.com/>

1-800-826-6342

Grainger

<https://www.grainger.com/>

1-800-472-4643

Honeywell Sensing

<https://sensing.honeywell.com/>

800-537-6945

APPENDIX D

Vendor Specification Sheets

Thermocouples

Super OMEGACLAD® XL Thermocouple Probes

A Technological Advance in Temperature Measurement



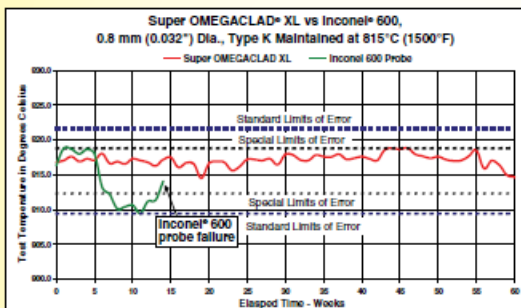
KQXL-18U-12, shown smaller than actual size.

- ✓ Thermocouple Technology from OMEGA for K and N Calibrations Only
- ✓ Super Stable Temperature Drift—Less than 2.8°C (37°F) in 25 weeks
- ✓ Better Performance at a Smaller Size—0.8 mm (0.032") Probe Withstands 815°C (1500°F) for 3 Years
- ✓ Probe Life Expectancy up to 10 Times Greater than Competing Devices*
- ✓ Handles Temperatures Up to 1335°C (2400°F)

OMEGA brings you the Super OMEGACLAD® XL Thermocouple Probe family, the exclusive innovation in thermocouple technology. Manufactured using state-of-the-art processes for mineral insulated (MI) thermocouple cable and finished thermocouple probe assemblies, these temperature sensors maximize performance, even at extremely small diameters. The devices resist carburization, oxidation, and chlorination in tough environments.

High
Performance!

An Exclusive
OMEGA
Manufactured
Innovation



* Tests conducted using ungrounded probes in an open-air, electric, muffle furnace versus a Type "T", NIST traceable standard. Individual results may vary depending on customer application. Inconel® is a registered trademark of Special Metals Corporation.

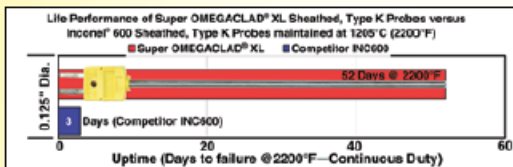
Small Size, Big Performance!

Typical 0.8 mm (0.032") Dia. Type K probes have a maximum temperature of 700°C (1260°F). Our Super OMEGACLAD® XL 0.8 mm (0.032") Dia. probe took on 815°C (1500°F) for 3 years and even reached 1000°C (1832°F) for 2 months!

Probes shown ~50% smaller than actual size.

6.4 mm (0.250")	2.25 sec**
3.2 mm (0.125")	0.55 sec**
1.6 mm (0.062")	0.3 sec**
0.8 mm (0.032")	~0.25 sec**

** Approx. response time—ungrounded in water



1204°C (2200°F) replace 17 of theirs in 52 days or just one of ours!

In life-cycle lab testing, the OMEGACLAD XL sheathed, 3 mm (0.125") Type K Probe operated continuously for 52 days at 1204°C (2200°F) while competitors' 3 mm (0.125") Inconel 600 sheathed, Type K probes lasted 3 days.

* Results will vary on application and operating environment.

Long Life, Low Maintenance!

If your application operates at the punishing temperature of nearly 1204°C (2200°F), changing out failed thermocouples costs money in excessive maintenance, slows or cuts production, and can cause inconsistent product quality.

In head-to-head tests, Super OMEGACLAD XL thermocouple probes consistently post the best performance results. Our innovative temperature sensors last upwards of 10 times or longer when compared to competitors' Inconel 600 sheathed probes of equal or larger diameters. Let OMEGA's leading edge products help engineer **your next innovation!**

SPT Series

Low Cost, Stainless Steel Pressure Transducers



0-3 psi to 0-5000 psi

The SPT stainless steel devices are designed for pressure applications that involve measurement of hostile media in harsh environments and will accommodate any media that will not adversely attack 304 or 316 stainless steel wetted parts.

This SPT Series is calibrated and compensated for three styles of output: 4-20 mA (mA version), 1-5 Vdc (4V version), and 0-100 mV (mV version). All versions feature a variety of pressure connections to allow use in a wide range of OEM equipment.

The SPT stainless steel devices are rugged and reliable transducers for use in a wide variety of pressure sensing applications where corrosive liquids or gases are monitored. Contact your local SenSym ICT representative, the factory, or go to Sensym ICT's Web site at www.sensym-ict.com for additional details.

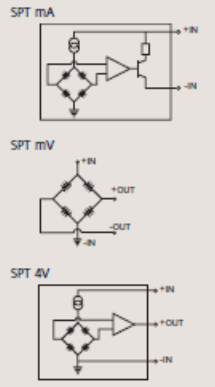
APPLICATIONS

Industrial Automation and Flow Control
Pressure Instrumentation
Hydraulic Systems
Process Control

FEATURES

Reliable Semiconductor Technology
Calibrated and Temperature Compensated
Rugged Stainless Steel Package
NEMA 4 Design
Small Size
Absolute, Gauge, Sealed Gauge, Vacuum Gauge Pressures

EQUIVALENT BASIC CIRCUIT



**invensys**
Sensor Systems

SPT Series

PRESSURE TRANSDUCER CHARACTERISTICS

Environmental Specifications

Compensated: -10°C to +85°C Vibration: 10G at 20-2000 Hz
Operating: -40°C to +125°C Shock: 100G for 11 msec
Storage: -40°C to +125°C Life: 1 Million cycles minimum
Insulation Resistance: 100 MΩ at 50 Vdc

Recommended Supply Range

SPT mA: Supply Voltage $V_S = +12.5$ Vdc to +30 Vdc
SPT 4V: Supply Voltage $V_S = +12$ Vdc to +30 Vdc
Quiescent Current $I_{QSC} = 5$ mA
Short Circuit Current $I_{SC} = 18$ mA
SPT mV: Supply Voltage $V_S = +10$ Vdc

Maximum Supply Ratings

SPT mV: Supply Voltage $V_S = +15$ Vdc
SPT mA and SPT 4V: Supply Voltage $V_S = +30$ Vdc

PRESSURE RANGE SPECIFICATIONS (all devices)

SenSym ICT Part No. *	Pressure Range	Proof Pressure ⁽¹⁾	Burst Pressure ⁽¹⁾
SPT(mA,mV,4V) 0003P G (4,5,6,7,9) (B/WXO)	0-3 psig	9 psig	15 psig
SPT(mA,mV,4V) 0005P G (4,5,6,7,9) (B/WXO)	0-5 psig	15 psig	25 psig
SPT(mA,mV,4V) 0010P G (4,5,6,7,9) (B/WXO)	0-10 psig	30 psig	50 psig
SPT(mA,mV,4V) 0015P (A,G,V) (4,5,6,7,9) (B/WXO)	0-15 psi	45 psi	75 psi
SPT(mA,mV,4V) 0030P (A,G,V) (4,5,6,7,9) (B/WXO)	0-30 psi	90 psi	150 psi
SPT(mA,mV,4V) 0050P (A,G,V) (4,5,6,7,9) (B/WXO)	0-50 psi	150 psi	250 psi
SPT(mA,mV,4V) 0100P (A,G,V) (4,5,6,7,9) (B/WXO)	0-100 psi	300 psi	500 psi
SPT(mA,mV,4V) 0200P (A,G,V) (4,5,6,7,9) (B/WXO)	0-200 psi	600 psi	1000 psi
SPT(mA,mV,4V) 0300P (A,G,V) (4,5,6,7,9) (B/WXO)	0-300 psi	900 psi	1500 psi
SPT(mA,mV,4V) 0500P (A,G,V) (4,5,6,7,9) (B/WXO)	0-500 psi	1200 psi	2400 psi
SPT(mA,mV,4V) 1000P (A,S) (4,5,6,7) (B/WXO)	0-1000 psi	3000 psia	5000 psia
SPT(mA,mV,4V) 2000P (A,S) (4,5,6,7) (B/WXO)	0-2000 psi	6000 psia	10000 psia
SPT(mA,mV,4V) 3000P (A,S) (4,5,6,7) (B/WXO)	0-3000 psi	9000 psia	10000 psia
SPT(mA,mV,4V) 5000P (A,S) (4,5,6,7) (B/WXO)	0-5000 psi	10000 psia	10000 psia

* Note: Vacuum gauge units (V option) allow you to pull a hard vacuum on the gauge units. Vacuum gauge parts are only available on the mV version in 15 through 500 psig. As sold, this package design is not submersible. In order to make the package design submersible, package needs to be sealed.

SPT mV Series PERFORMANCE CHARACTERISTICS⁽¹⁾

Characteristic	Min	Typical	Max	Units
Zero Pressure Offset	-2	0	+2	mV
Full-Scale Span (0-3 to 0-5 psig only) ⁽¹⁾	48	50	52	mV
Full-Scale Span (0-10 to 0-3000 psi only) ⁽¹⁾	98	100	102	mV
Full-Scale Span (0-5000 psi only) ⁽¹⁾	148	150	152	mV
Pressure Non-Linearity ⁽¹⁾	-	±0.1	±0.25	%FSS
Pressure Hysteresis ⁽¹⁾	-	±0.015	±0.030	%FSS
Repeatability	-	±0.010	±0.030	%FSS
Temp. Effect on Span ⁽¹⁾	-	±0.5	±1.0	%FSS
Temp. Effect on Offset ⁽¹⁾	-	±0.5	±1.0	%FSS
Temp. Effect on Span (0-3 and 0-5 psi only) ⁽¹⁾	-	±1	±2.0	%FSS
Temp. Effect on Offset (0-3 and 0-5 psi only) ⁽¹⁾	-	±1	±2.0	%FSS
Thermal Hysteresis (-10 to +85°C)	-	±0.1	±0.3	%FSS
Long Term Stability of Offset & Span ⁽¹⁾	-	±0.1	±0.3	%FSS
Response Time ⁽¹⁾	-	0.1	-	mS
Common Mode Voltage (Voltage Version "K") ⁽¹⁾	.5	1.25	2.0	Vdc
Input Resistance	8.0	25	50	kΩ
Output Resistance	3.0	4.5	6.0	kΩ

SPT mV SERIES SPECIFICATION NOTES

Note 1: Reference Conditions (unless otherwise noted):
 $T_A = 25^\circ\text{C}$
Supply
 $V_S = 10$ Vdc ± 0.01 Vdc

Note 2: Full-Scale Span is the algebraic difference between the output voltage at full-scale pressure and the output at zero pressure. Full-Scale Span (FSS) is ratiometric to the supply voltage.

Note 3: Pressure Non-Linearity is based on best-fit straight line from the zero to the full-scale pressure. Pressure Hysteresis is the maximum output difference at any point within the operating pressure range for increasing and decreasing pressure.

Note 4: Maximum error band of the offset voltage or span over the compensated temperature range, relative to the 25°C reading.

Note 5: Long term stability over a six month period.

Note 6: Response time for 0 psi to FSS pressure step change, 10% to 90% rise time.

Note 7: The maximum pressure that can be applied without changing the transducer's performance or accuracy.

Note 8: The maximum pressure that can be applied to a transducer without rupture of either the sensing element or transducer case.

Note 9: Common Mode Voltage as measured from output to ground.

SPT mA Series PERFORMANCE CHARACTERISTICS⁽¹⁾

Characteristic	Min	Typical	Max	Units
Zero Pressure Offset	3.84	4.0	4.16	mA
Full-Scale Span ⁽²⁾	15.84	16.0	16.16	mA
Pressure Non-Linearity ⁽³⁾	—	±0.1	±0.25	%FSS
Pressure Hysteresis ⁽⁴⁾	—	±0.015	±0.03	%FSS
Repeatability	—	±0.010	±0.030	%FSS
Temp. Effect on Span ⁽⁵⁾	—	±0.5	±1.5	%FSS
Temp. Effect on Offset ⁽⁶⁾	—	±0.5	±1.5	%FSS
Temp. Effect on Span (0-3psi and 0-Spsi only) ⁽⁶⁾	—	±1.5	±2.5	%FSS
Temp. Effect on Offset (0-3psi and 0-Spsi only) ⁽⁶⁾	—	±1.5	±2.5	%FSS
Thermal Hysteresis (-10 to +85°C)	—	±0.1	±0.3	%FSS
Long Term Stability of Offset & Span ⁽⁷⁾	—	±0.1	±0.3	%FSS
Response Time ⁽⁸⁾	—	5	—	mS

SPT 4V Series PERFORMANCE CHARACTERISTICS⁽¹⁾

Characteristic	Min	Typical	Max	Units
Zero Pressure Offset	0.96	1.0	1.04	Volts
Full-Scale Span ⁽²⁾	3.96	4.0	4.04	Volts
Pressure Non-Linearity ⁽³⁾	—	±0.1	±0.25	%FSS
Pressure Hysteresis ⁽⁴⁾	—	±0.015	±0.03	%FSS
Repeatability	—	±0.010	±0.030	%FSS
Temp. Effect on Span ⁽⁵⁾	—	±0.5	±1.5	%FSS
Temp. Effect on Offset ⁽⁶⁾	—	±0.5	±1.5	%FSS
Temp. Effect on Span (0-3psi and 0-Spsi only) ⁽⁶⁾	—	±1.5	±2.5	%FSS
Temp. Effect on Offset (0-3psi and 0-Spsi only) ⁽⁶⁾	—	±1.5	±2.5	%FSS
Thermal Hysteresis (-10 to +85°C)	—	±0.1	±0.3	%FSS
Long Term Stability of Offset & Span ⁽⁷⁾	—	±0.1	±0.3	%FSS
Response Time ⁽⁸⁾	—	5	—	mS

SPT mA AND SPT 4V SERIES SPECIFICATION NOTES

Note 1: Reference Conditions
(unless otherwise noted):
 $T_A = 25^\circ\text{C}$
Supply
 $V_S = 24\text{ Vdc} \pm 0.01\text{ Vdc}$

Note 2: Full-Scale Span is the algebraic difference between the output voltage at full-scale positive pressure and the output at zero pressure.

Note 3: Pressure Non-Linearity is based on best-fit straight line from the zero to the full-scale pressure. Pressure Hysteresis is the maximum output difference at any point within the operating pressure range for increasing and decreasing pressure.

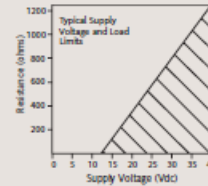
Note 4: Maximum error band of the offset voltage or span over the compensated temperature range, relative to the 25°C reading.

Note 5: Long term stability over a six month period.

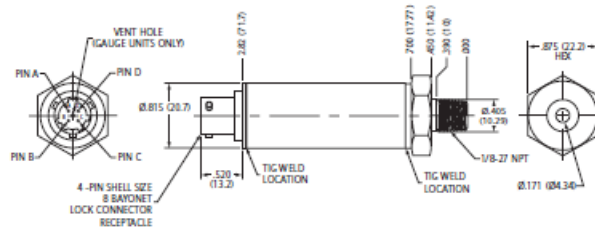
Note 6: Response time for a 0 psi to FSS pressure step change, 10% to 90% rise time.

Note 7: The maximum pressure that can be applied without changing the transducer's performance or accuracy.

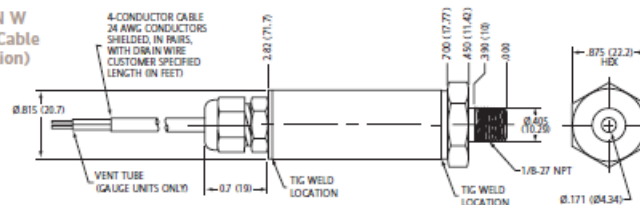
Note 8: The maximum pressure that can be applied to a transducer without rupture of either the sensing element or transducer case.

SPT mA SERIES EXTERNAL LOAD LINE**PHYSICAL DIMENSIONS****PACKAGE 4
1/8 NPT PORT**

VERSION B
(Bayonet
Connector)



VERSION W
(Pigtail Cable
Connection)



THE FOLLOWING
TABLES APPLY TO ALL
DRAWINGS

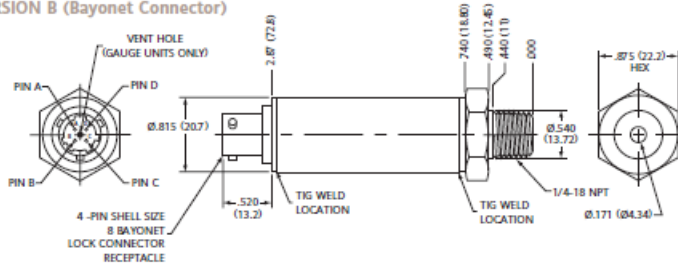
PIN DESIGNATIONS			
PIN	LTR	mA	4V
A	+IN	+IN	+IN
B	N/C	+OUT	+OUT
C	N/C	N/C	-OUT
D	-IN	-IN	-IN

WIRE CODE			
Color	mA	4V	mV
RED	+IN	+IN	+IN
BLACK	-IN	-IN	-IN
GREEN	N/C	+OUT	+OUT
WHITE	N/C	N/C	-OUT
BARE	SHIELD	SHIELD	SHIELD

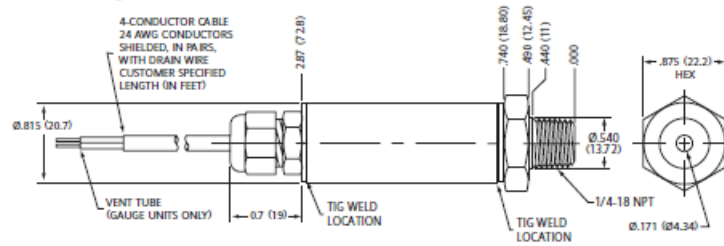
PHYSICAL DIMENSIONS (con't)

PACKAGE 5
1/4 NPT PORT

VERSION B (Bayonet Connector)

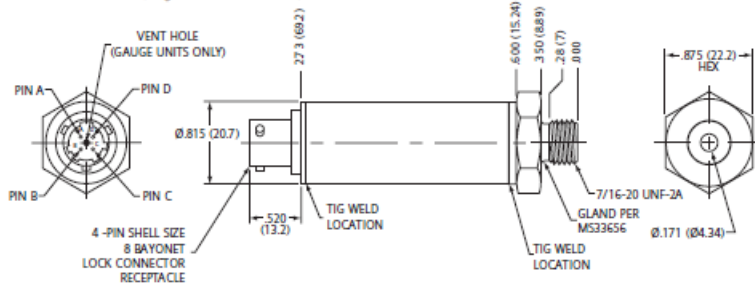


VERSION W (Pigtail Cable Connection)

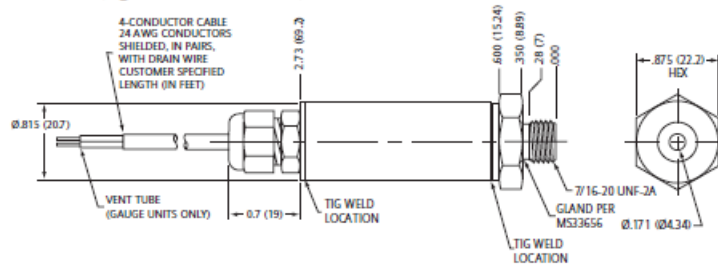


PACKAGE 6
7/16-20 UNF PORT

VERSION B (Bayonet Connector)



VERSION W (Pigtail Cable Connection)

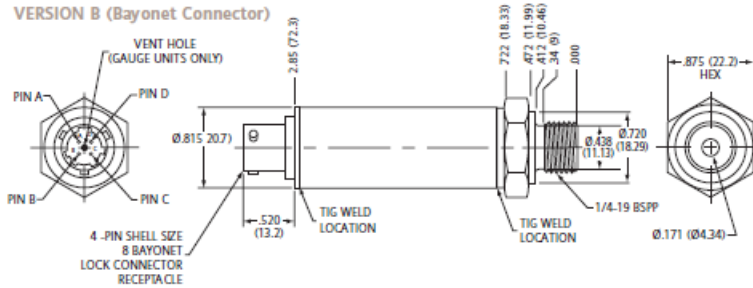


SPT Series

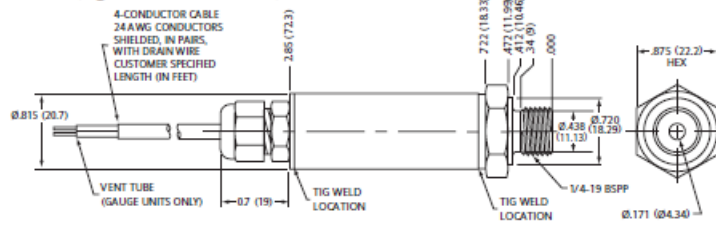
PHYSICAL DIMENSIONS (con't)

PACKAGE 7 1/4-19 BSPP PORT

VERSION B (Bayonet Connector)

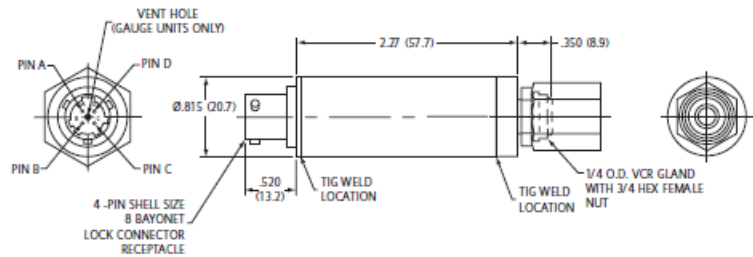


VERSION W (Pigtail Cable Connection)

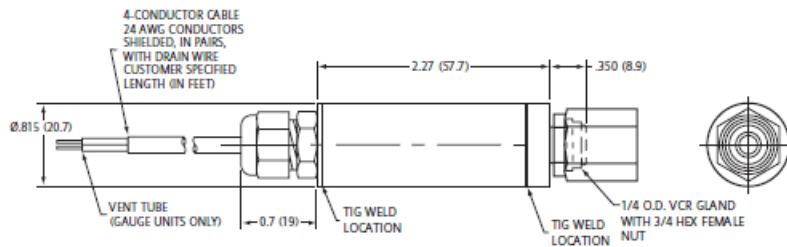


PACKAGE 9 VCR PORT

VERSION B (Bayonet Connector)



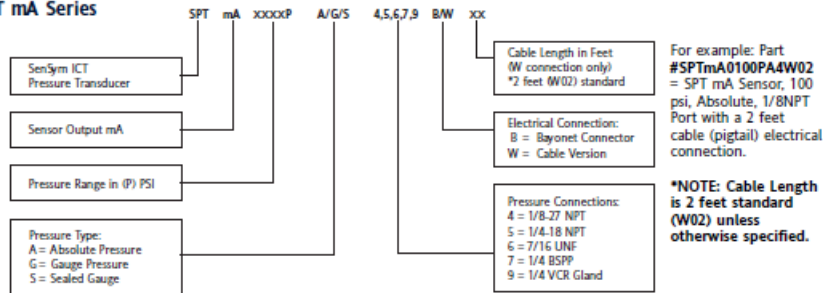
VERSION W (Pigtail Cable Connection)



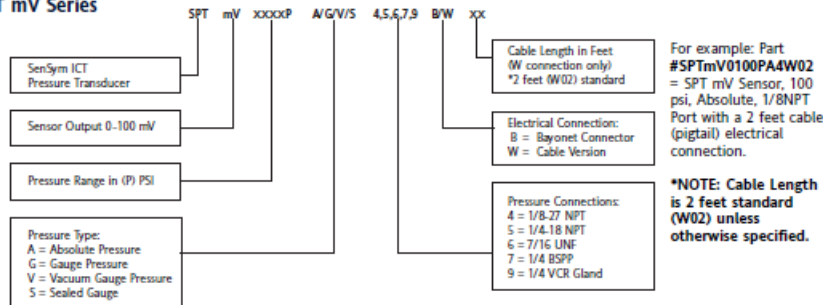
SPT Series Low Cost, Stainless Steel Pressure Transducers

ORDERING INFORMATION - PART # DESCRIPTION

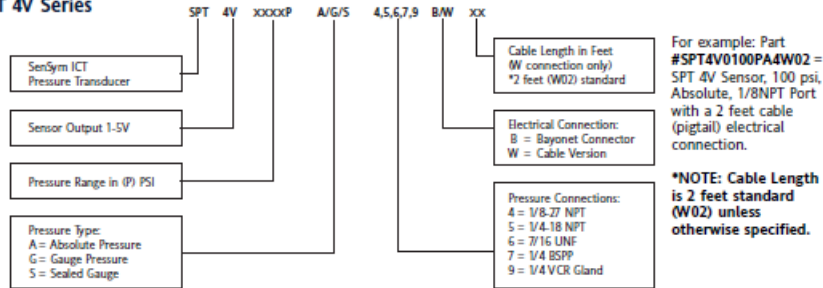
SPT mA Series



SPT mV Series



SPT 4V Series



1 408 954 6700
FAX: 408 954 9458
SenSym ICT
1804 McCarthy Boulevard
Milpitas, CA 95035
www.sensym-ict.com

GENERAL DISCLAIMER: Invensys Sensor Systems reserves the right to make changes to its products and their specifications at any time, without prior notice to anyone. Invensys Sensor Systems has made every effort to ensure accuracy of the information contained herein but can assume no responsibility for inadvertent error, omissions, or subsequent changes. Invensys Sensor Systems does not assume any responsibility for the use of any circuit or other information described within this document, and further, makes no representations of any kind that the circuit and information described herein is free of infringement of any intellectual property right or any other right of third parties. No express or implied licenses of any Invensys Sensor Systems intellectual property right is granted by implication or otherwise.

SEN0107_3000_6/02 REF#121801R02



Series 026 Data Sheet Rotary Potentiometer

Industrial 24mm Diameter 5 Watt, Wirewound Rotary Potentiometer

Features

- Dust-proof construction
- Precision linearity
- 5 watt power rating
- Superior resistance stability in temperature and environment change
- Tandem constructions available
- Bushing or twist tab mounting
- Available with pull-push and rotary power switches
- RoHS compliant



Electrical and Mechanical Specifications

Resistance Range

Linear : 1 ohm through 25K ohms
Audio : 20 ohms through 10K ohms

Resistance Tolerance

±20%, ±10%, ±5%

Power Rating

5 watts @ 25°C

Dielectric Strength

1,000 VAC for 1 minute

Maximum Operating Voltage

500 VDC

Insulation Resistance

100 Megohms minimum @ 250 VDC

Rotational Angle

Mechanical Angle: 300°±5°
Effective Angle:
Without switch: 280°
With switch: 240°

Rotational Torque

3/4 to 8 in. oz. (54 - 432 gf-cm)

Linearity (linear curve only)

Standard: 3% linearity
Special : 2% linearity

Mounting Information

Bushing Mount
Twisted Tab

Power Switch

Rotary Switch-SPST, DPST, SPDT
Pull-Push Switch-SPST (Pull-ON, Push-OFF)

Rotational Life

standard : 10,000 cycles
special : 50,000 , 100,000 cycles

Solder Heat Resistance

Maximum 350°C for 3 sec

Operating Temperature

-30°C to +105°C

APPENDIX E
Supporting Analysis

Compressor					G.G. Turbine					Power Turbine				
P_1	0.101	Mpa	W_{comp}	87.6	kW	P_3	0.101	Mpa						
T_1	25.00	degC	h_1	825.5	kJ/kg	T_3	500	degC						
h_1	298.45	kJ/kg	h_2	998.7	kJ/kg	h_3	793	kJ/kg						
P_2	0.262344132	MPa	P_3	0.82	Mpa	W_{out}	16.4	kW						
T_2	186.0288931	degC	T_3	683	degC	$C_{p,3}$	1.095	kJ/kg.K						
h_2	475.74	kJ/kg	P_4	2.32	degF	T_4	805	K						
W_{in}	87.84	kW	H	897.2	kJ/kg	T_{max}	1257	-						
W_{out}	117.44	hp	T_{min}	1.3456238	degC	η	32.42	kJ/kg						
					$C_{p,3}$	1.17151468	kJ/kg.K	P_4	1.122	-				
					η	0.85944429	-	P_5	0.113	Mpa				

Working Fluid		Air		-	
Stoichiometric Air/F	14.7	-			
m_{air}	0.5	kg/s			
m_{fuel}	0.0061	kg/s			
m_{mix}	0.5061	kg/s			
ϕ	0.179	-			
P_{inlet}	20	hp			
P_{out}	14.9	kW			
$\eta_{isentro}$	0.9	-			

P ₁ Estimate (From geometry)										P ₂ Estimate (From test data trendline)										P ₃ Estimate (From test data trendline)										P ₄ Estimate (From test data trendline)										P ₅ Estimate (From test data trendline)									
Impeller Dia										74										74										74										74									
Impeller Tip Speed										442.9										442.9										442.9										442.9									
Power Input Factor										1.040										1.040										1.040										1.040									
Slip Factor										0.900										0.900										0.900										0.900									
η_{mech}										0.34										0.34										0.34										0.34									
η_{mech}										1.000										1.000										1.000										1.000									
$C_{p,3}$										1.091										1.091										1.091										1.091									
P_1 (abs)										298.1										298.1										298.1										298.1									
P_1 (gag)										298.1										298.1										298.1										298.1									
P_2										2.60										2.60										2.60										2.60									
T_1										173.03										173.03										173.03										173.03									
T_2										471.03										471.03										471.03										471.03									
P_1 (abs)										0.262										0.262										0.262										0.262									

Waxalway Field Strength										Waxalway Field Strength										Waxalway Field Strength										Waxalway Field Strength										Waxalway Field Strength									
Temperature [C]										Temperature [F]										Temperature [C]										Temperature [F]										Temperature [C]									
13										13										13										13										13									
15										15										15										15										15									
21										21										21										21										21									
427										427										427										427										427									
538										538										538										538										538									
649										649										649										649										649									
760										760										760										760										760									
780										780										780										780										780									
Yield Strength [ksi]										Yield Strength [ksi]										Yield Strength [ksi]										Yield Strength [ksi]										Yield Strength [ksi]									
1003.7										1003.7										1003.7										1003.7										1003.7									
1318.6										1318.6										1318.6										1318.6										1318.6									
1726.9										1726.9										1726.9										1726.9										1726.9									
126.8										126.8										126.8										126.8										126.8									
120										120										120										120										120									
124.5										124.5										124.5										124.5										124.5									
117.5										117.5										117.5										117.5										117.5									
102.7										102.7										102.7										102.7										102.7									
708.5										708.5										708.5										708.5										708.5									
708.5										708.5										708.5										708.5										708.5									

Yield Strength [ksi] vs Temperature [C]

Equation: $y = 4.3805x + 1003.3$

Yield Strength [ksi] vs Temperature [F]

Equation: $y = 4.3805x + 1003.3$

Waxalway Field Strength										Waxalway Field Strength										Waxalway Field Strength										Waxalway Field Strength										Waxalway Field Strength									
Temperature [C]										Temperature [F]										Temperature [C]										Temperature [F]										Temperature [C]									
13										13										13										13										13									
15										15										15										15										15									
21										21										21										21										21									
427										427										427										427										427									
538										538										538										538										538									
649										649										649										649										649									
760										760										760										760										760									
780										780										780										780										780									
Yield Strength [ksi]										Yield Strength [ksi]										Yield Strength [ksi]										Yield Strength [ksi]										Yield Strength [ksi]									
1003.7										1003.7										1003.7										1003.7										1003.7									
1318.6										1318.6										1318.6										1318.6										1318.6									
1726.9										1726.9										1726.9										1726.9										1726.9									
126.8										126.8										126.8										126.8										126.8									
120										120										120										120										120									
124.5										124.5										124.5										124.5										124.5									
117.5										117.5										117.5										117.5										117.5									
102.7										102.7										102.7										102.7										102.7									
708.5										708.5										708.5										708.5										708.5									
708.5										708.5										708.5										708.5										708.5									

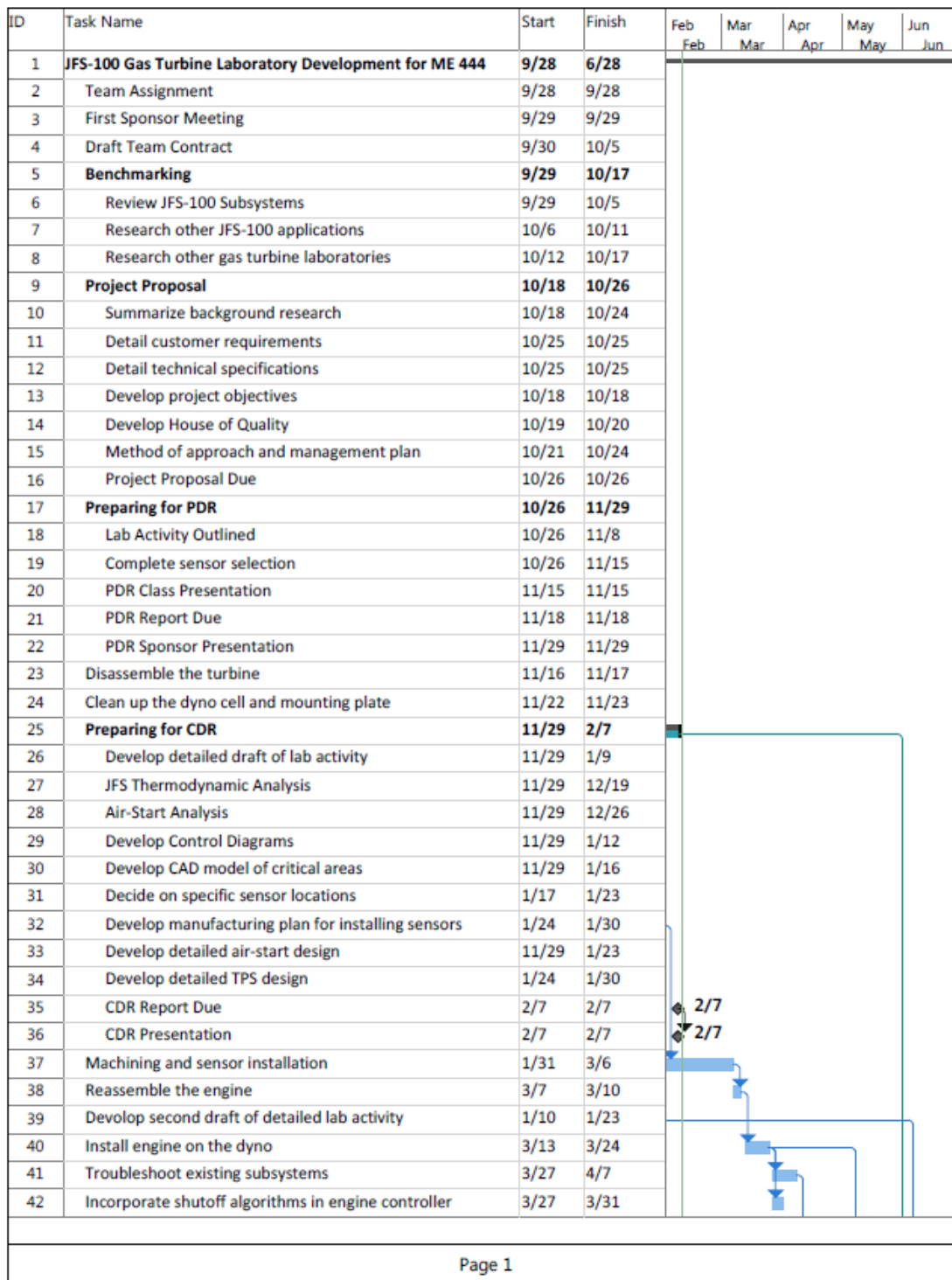
Test Data

Notes		Elapsed Time	Air Flow	P ₁	T ₁	P ₂	m _{air}	m _{fuel}	Φ	Brake Power	A Speed	P ₂	PR _{comp}
		[s]	m ³ /s	Mpa	°C	kg/m ²	kg/s	kg/s	-	[HP]	[RPM]	Mpa	-
TEST NO : CalPoly		00:00.0	-0.0002	0.098	22.7	1.16	0.000	0.0000	0.560	0.00	2000.00	0.099	1.007
Project No : JF3100		00:01.0	-0.0002	0.098	22.6	1.16	0.000	0.0000	0.560	0.00	2000.00	0.099	1.007
Engine Serial No : 000		00:02.0	-0.0002	0.098	22.7	1.16	0.000	0.0000	0.560	0.00	2000.00	0.099	1.007
Dry Temperature : 60.000000		00:03.0	-0.0002	0.098	22.8	1.16	0.000	0.0000	0.187	0.00	2000.00	0.099	1.007
Operator : P. Lemieux		00:04.0	-0.0002	0.098	22.7	1.16	0.000	0.0000	0.000	0.00	2000.00	0.099	1.007
Engine Family : Garrett Turbine		00:05.0	-0.0002	0.098	22.8	1.16	0.000	0.0000	0.187	0.00	2000.00	0.099	1.007
: 3-20-2011		00:06.0	-0.0002	0.098	22.6	1.16	0.000	0.0000	0.000	0.00	2000.00	0.099	1.007
Barometric Pressure : 99.000000		00:07.0	-0.0002	0.098	22.6	1.16	0.000	0.0002	-15.69	0.00	2000.00	0.099	1.007
: 52.8		00:08.0	-0.0002	0.098	22.7	1.16	0.000	0.0009	-63.33	0.00	2000.00	0.099	1.007
Analysis		00:09.0	-0.0001	0.098	22.6	1.16	0.000	0.0008	-75.44	0.00	2000.00	0.099	1.007
Stoichiometric A/F	14.7	-	0.0236	0.098	22.7	1.16	0.027	0.0030	1.59	0.00	1000.00	0.100	1.014
Stoichiometric F/A	0.06802721	-	0.0533	0.098	23.0	1.15	0.061	0.0089	2.13	0.00	11000.00	0.101	1.035
Peak Torque	70.4	ft*lb	0.0679	0.098	23.2	1.15	0.078	0.0110	2.07	0.00	15000.00	0.105	1.071
Peak Power	30.54	hp	0.0907	0.098	23.3	1.15	0.104	0.0106	1.50	0.00	22000.00	0.111	1.134
Atmospheric Pressure	99	kPa	0.1213	0.097	23.3	1.14	0.138	0.0108	1.15	0.00	27926.80	0.120	1.242
			0.1654	0.096	23.1	1.13	0.187	0.0115	0.900	0.47	17946.40	0.136	1.408
			0.2330	0.095	22.6	1.12	0.260	0.0104	0.589	0.88	19361.70	0.153	1.611
			0.2729	0.094	22.2	1.11	0.303	0.0097	0.471	1.20	18567.10	0.162	1.717
			0.2947	0.093	22.0	1.10	0.325	0.0092	0.414	1.44	15309.70	0.167	1.782
			0.3074	0.093	21.6	1.11	0.340	0.0088	0.380	1.53	13113.70	0.169	1.811
			0.3153	0.093	21.7	1.10	0.346	0.0085	0.363	1.67	11631.40	0.171	1.840
			0.3197	0.093	21.9	1.10	0.350	0.0084	0.351	1.80	10606.60	0.171	1.847
			0.3211	0.093	21.5	1.10	0.352	0.0083	0.345	1.83	9911.20	0.171	1.847
			0.3220	0.093	21.6	1.10	0.353	0.0082	0.343	1.85	9435.40	0.171	1.847
			0.3223	0.093	21.4	1.10	0.354	0.0082	0.341	1.91	9106.00	0.172	1.854
			0.3230	0.093	21.4	1.10	0.355	0.0082	0.338	1.88	8868.10	0.172	1.854
			0.3218	0.093	21.6	1.10	0.353	0.0081	0.339	2.05	8740.00	0.172	1.854
			0.3221	0.093	21.5	1.10	0.353	0.0081	0.339	3.35	8758.30	0.171	1.847
			0.3221	0.093	21.6	1.10	0.353	0.0082	0.339	5.43	9472.00	0.171	1.847
			0.3216	0.093	21.5	1.10	0.353	0.0082	0.341	7.70	10441.90	0.171	1.847
			0.3199	0.093	21.9	1.10	0.351	0.0082	0.345	12.33	12637.90	0.171	1.847
			0.3177	0.093	22.2	1.09	0.348	0.0083	0.351	15.85	15950.20	0.171	1.847
			0.3161	0.093	22.6	1.09	0.346	0.0084	0.356	14.77	19372.30	0.171	1.847
			0.3146	0.093	23.2	1.09	0.343	0.0085	0.363	11.97	21476.80	0.171	1.847
			0.3132	0.093	23.5	1.10	0.344	0.0085	0.364	9.01	21769.60	0.171	1.826
			0.3113	0.093	24.0	1.10	0.341	0.0086	0.369	7.48	20580.10	0.171	1.826
			0.3105	0.093	24.2	1.10	0.340	0.0086	0.371	8.77	19628.50	0.171	1.826
			0.3082	0.093	24.2	1.10	0.338	0.0087	0.378	9.37	19372.30	0.171	1.826
			0.3095	0.093	24.3	1.09	0.339	0.0086	0.375	9.54	19335.70	0.171	1.826
			0.3090	0.093	24.3	1.09	0.338	0.0087	0.376	9.57	19335.70	0.171	1.826
			0.3079	0.093	24.6	1.09	0.337	0.0087	0.378	9.60	19335.70	0.171	1.826
			0.3082	0.093	24.7	1.09	0.337	0.0087	0.378	8.64	19244.20	0.171	1.826
			0.3075	0.093	24.7	1.09	0.336	0.0087	0.380	4.54	17597.20	0.170	1.819
			0.3082	0.093	24.9	1.09	0.337	0.0087	0.380	4.82	15657.40	0.170	1.819
			0.3085	0.093	25.4	1.09	0.337	0.0087	0.380	5.99	14541.10	0.170	1.819
			0.3078	0.093	25.6	1.09	0.336	0.0087	0.381	6.80	14065.30	0.170	1.819
			0.3067	0.093	25.9	1.09	0.336	0.0087	0.380	7.15	13955.50	0.170	1.819
			0.3083	0.093	26.2	1.09	0.335	0.0087	0.381	7.26	13937.20	0.170	1.819
			0.3081	0.093	26.0	1.09	0.335	0.0087	0.381	7.33	13937.20	0.170	1.819
			0.3081	0.093	26.4	1.09	0.335	0.0087	0.381	7.29	13955.50	0.170	1.819
			0.3073	0.093	26.6	1.09	0.334	0.0087	0.384	7.26	13955.50	0.169	1.811
			0.3077	0.093	27.1	1.08	0.334	0.0100	0.440	9.99	11631.40	0.176	1.885
			0.3562	0.092	27.6	1.07	0.380	0.0126	0.487	24.40	13129.60	0.200	2.168
			0.3929	0.091	28.4	1.06	0.415	0.0142	0.502	30.51	21928.30	0.216	2.358
			0.4148	0.091	28.9	1.05	0.437	0.0149	0.501	30.54	24312.60	0.224	2.448
			0.4248	0.091	29.3	1.04	0.444	0.0153	0.505	29.51	24660.30	0.228	2.512
			0.4330	0.091	29.6	1.04	0.452	0.0155	0.503	30.21	23404.10	0.231	2.550
			0.4394	0.091	30.1	1.04	0.458	0.0156	0.500	30.39	24276.00	0.233	2.573
			0.4506	0.090	30.5	1.03	0.465	0.0157	0.495	29.42	25081.20	0.233	2.593
			0.4073	0.091	30.7	1.05	0.427	0.0107	0.369	11.87	27992.10	0.206	2.252
			0.3576	0.092	30.9	1.06	0.377	0.0107	0.416	8.21	14705.80	0.188	2.041
			0.3340	0.093	31.1	1.06	0.355	0.0097	0.403	7.33	14815.60	0.178	1.921
			0.3209	0.093	31.6	1.06	0.340	0.0092	0.398	7.13	14724.10	0.173	1.869
			0.3134	0.093	31.8	1.07	0.335	0.0090	0.394	7.16	14614.30	0.171	1.826
			0.3106	0.093	32.0	1.07	0.331	0.0088	0.391	7.20	14577.70	0.169	1.811
			0.3093	0.093	32.3	1.07	0.330	0.0087	0.389	7.20	14559.40	0.169	1.804
			0.3088	0.093	32.6	1.07	0.329	0.0087	0.389	7.17	14559.40	0.168	1.797
			0.3087	0.093	32.9	1.06	0.328	0.0087	0.387	7.16	14577.70	0.168	1.797
			0.3096	0.093	33.4	1.06	0.329	0.0086	0.386	7.16	14614.30	0.167	1.789
			0.3103	0.093	34.0	1.06	0.329	0.0087	0.391	7.31	14413.00	0.168	1.797
			0.3155	0.093	34.1	1.06	0.334	0.0089	0.393	7.90	14992.10	0.170	1.819
			0.3213	0.093	34.3	1.05	0.338	0.0090	0.391	8.32	15772.50	0.172	1.854
			0.3255	0.093	34.5	1.05	0.342	0.0090	0.387	8.53	15681.00	0.173	1.862
			0.3286	0.093	34.4	1.05	0.345	0.0090	0.383	8.68	15662.70	0.173	1.869
			0.3306	0.093	34.8	1.05	0.347	0.0090	0.381	8.64	15681.00	0.174	1.877
			0.3311	0.093	34.9	1.05	0.347	0.0090	0.380	8.63	15717.60	0.174	1.877
			0.3316	0.093	35.3	1.05	0.348	0.0090	0.381	8.59	15717.60	0.174	1.877
			0.3346	0.093	35.7	1.05	0.350	0.0094	0.396	9.55	14875.80	0.177	1.906
			0.3598	0.092	36.1	1.04	0.373	0.0106	0.416	14.02	15716.40	0.188	2.041
			0.3888	0.091	36.7	1.03	0.401	0.0110	0.403	17.22	18966.10	0.197	2.154
			0.4062	0.091	37.4	1.03	0.417	0.0111	0.393	17.79	20130.80	0.202	2.207
			0.4199	0.091	37.8	1.02	0.421	0.0110	0.394	16.75	20679.80	0.202	2.214
			0.4291	0.091	38.1	1.02	0.419	0.0108	0.380	15.83	20064.10	0.201	2.199
			0.4060	0.091	38.1	1.02	0.415	0.0107	0.380	15.34	19247.10	0.200	2.184
			0.4037	0.091	38.6	1.02	0.412	0.0107	0.381	14.99	19283.70	0.199	2.177
			0.4024	0.091	38.9	1.02	0.411	0.0107	0.381	14.87	19302.00	0.198	2.169
			0.4022	0.091	39.2	1.02	0.410	0.0106	0.381	8.56	18570.00	0.198	2.161
			0.4027	0.091	39.6	1.02	0.410	0.0106	0.380	4.11	15825.00	0.198	2.161

01:28.0	0.4047	0.091	39.8	1.02	0.412	0.0106	0.378	2.69	13244.70	0.198	2.161
01:29.0	0.4061	0.091	40.1	1.02	0.413	0.0108	0.375	2.43	11231.70	0.198	2.161
01:30.0	0.4081	0.091	40.4	1.02	0.414	0.0108	0.373	2.46	9731.10	0.198	2.169
01:31.0	0.4128	0.091	40.8	1.01	0.419	0.0104	0.367	2.49	9090.60	0.196	2.139
01:32.0	0.3366	0.093	41.2	1.03	0.346	0.0066	0.279	2.13	7469.60	0.161	1.736
01:33.0	0.2365	0.095	41.4	1.05	0.248	0.0033	0.195	1.98	-15206.30	0.134	1.414
01:34.0	0.1620	0.096	41.3	1.07	0.173	0.0016	0.132	1.75	-24973.70	0.118	1.229
01:35.0	0.1111	0.097	40.9	1.08	0.119	0.0005	0.060	1.58	-28887.50	0.109	1.128
01:36.0	0.0769	0.098	41.1	1.08	0.083	-0.0005	-0.081	1.46	-30892.80	0.105	1.071
01:37.0	0.0542	0.098	40.9	1.08	0.059	-0.0011	-0.278	1.35	-30989.60	0.102	1.042
01:38.0	0.0390	0.098	40.9	1.09	0.043	-0.0015	-0.529	1.21	-33177.90	0.100	1.021
01:39.0	0.0292	0.098	40.9	1.09	0.032	-0.0018	-0.820	1.11	-31421.10	0.100	1.014
01:40.0	0.0229	0.098	40.9	1.09	0.025	-0.0016	-0.929	1.02	-29737.50	0.099	1.007
01:41.0	0.0188	0.098	40.6	1.09	0.021	-0.0012	-0.872	0.91	-28127.10	0.099	1.007
01:42.0	0.0159	0.098	40.7	1.09	0.017	-0.0009	-0.755	0.83	-26553.30	0.099	1.007
01:43.0	0.0138	0.098	40.6	1.09	0.015	-0.0006	-0.614	0.76	-25034.40	0.099	1.007
01:44.0	0.0121	0.098	40.7	1.09	0.013	-0.0004	-0.491	0.69	-23581.70	0.099	1.007
01:45.0	0.0108	0.098	40.6	1.09	0.012	-0.0003	-0.400	0.60	-22179.60	0.099	1.007
01:46.0	0.0097	0.098	40.6	1.09	0.011	-0.0002	-0.325	0.54	-20825.40	0.099	1.007
01:47.0	0.0087	0.098	40.5	1.09	0.009	-0.0002	-0.280	0.47	-19507.80	0.099	1.007
01:48.0	0.0078	0.098	40.4	1.09	0.009	-0.0001	-0.250	0.44	-18263.40	0.099	1.007
01:49.0	0.0071	0.098	40.2	1.09	0.008	-0.0001	-0.232	0.39	-17055.60	0.099	1.007
01:50.0	0.0064	0.098	40.3	1.09	0.007	-0.0001	-0.229	0.33	-15894.40	0.099	1.007
01:51.0	0.0058	0.098	40.2	1.09	0.006	-0.0001	-0.234	0.31	-14786.40	0.099	1.007
01:52.0	0.0052	0.098	40.3	1.09	0.006	-0.0001	-0.223	0.27	-13706.70	0.099	1.007

APPENDIX F

Gantt Chart



ID	Task Name	Start	Finish	Feb	Mar	Apr	May	Jun
				Feb	Mar	Apr	May	Jun
43	Fabricate/install redundant throttle position sensor	4/10	4/21					
44	TPS Calibration Test	4/24	4/24					
45	Fabricate/install air start mechanism	4/24	5/5					
46	Air-Start Pressure Test	5/8	5/8					
47	Air-Start Speed Test	5/9	5/11					
48	Start-time Warning Test	5/8	5/8					
49	Test and verify modifications and new subsystems	5/8	5/12					
50	TPS Fuel Flow Correction Test	5/15	5/18					
51	Overspeed Shutoff Test	5/15	5/18					
52	Overtemp Shutoff Test	5/19	5/22					
53	Characterize the engine at multiple operating points	5/23	6/5					
54	Perform the planned lab activity	6/6	6/7					
55	Preparing for FDR	6/2	6/28					
56	Develop final draft of detailed lab activity	6/8	6/21					
57	Develop necessary safety documents	6/22	6/28					
58	FDR Report Due	6/2	6/2					6/2
59	Senior Project Expo	6/2	6/2					6/2
60	Final Team Evaluations Due	6/8	6/8					6/8

APPENDIX G

Indented BOM

Indented Bill of Material (BOM)						
JFS-100 Engine						
Assy Level	Part Number	Description	Matl	Vendor	Qty	Ttl Cost
		Lvl0 Lvl1 Lvl2 Lvl3				
0		Engine System				
1	ENG0100	JFS-100 Engine				
2	ENG0101	Power Turbine Housing	Nitronic 40	-----	1	\$ - \$ -
2	ENG0102	Power Turbine Rotor	Waspalloy	-----	1	\$ - \$ -
2	ENG0103	Power Turbine Diffuser	347 S.S.	-----	1	\$ - \$ -
2	ENG0104	Power Turbine Containment Ring	Ti-6Al-4V	-----	1	\$ - \$ -
2	ENG0105	Power Turbine IGV Ring	L605	-----	1	\$ - \$ -
2	ENG0106	Power Turbine Gasket	-----	-----	1	\$ - \$ -
2	ENG0107	Gas Generator Turbine Rotor	Waspalloy	-----	1	\$ - \$ -
2	ENG0108	Gas Generator Assembly	-----	-----	1	\$ - \$ -
1	ENG0200	Stage 4 Instrumentation Assembly				
2	ENG0201	1/16" Dia. Sheathed Thermocouple	-----	Omega	1	\$ 25.00 \$ 25.00
2	ENG0202	SENSYM ICT Pressure Transducer	-----	Honeywell	1	\$ - \$ -
2	ENG0203	1/8 NPT to AN-4 Adapter	316 S.S.	McMaster-Carr	1	\$ 11.30 \$ 11.30
2	ENG0204	1/8 NPT OMEGALok Compression Fitting	316 S.S.	Omega	1	\$ 20.50 \$ 20.50
2	ENG0205	Stage 4 Thermocouple Port	304 S.S.	-----	1	\$ - \$ -
2	ENG0206	Stage 4 Pressure Port	304 S.S.	-----	1	\$ - \$ -
1	ENG0300	Stage 3 Instrumentation Assembly				
2	ENG0301	1/16" Dia. Sheathed Thermocouple	-----	Omega	1	\$ 25.00 \$ 25.00
2	ENG0302	SENSYM ICT Pressure Transducer	-----	Honeywell	1	\$ - \$ -
2	ENG0303	1/8 NPT Tee Connector, Anodized AL	Aluminum	McMaster-Carr	1	\$ 19.47 \$ 19.47
2	ENG0304	1/8 NPT OMEGALok Compression Fitting	316 S.S.	Omega	1	\$ 20.50 \$ 20.50
2	ENG0305	1/8-1/4 NPT Male Reducer	316 S.S.	McMaster-Carr	1	\$ - \$ -
2	ENG0306	1/8 NPT to AN-4 Adapter	316 S.S.	McMaster-Carr	1	\$ - \$ -
0		Air-Starter System				
1	AIR0100	Air-Starter Assembly				
2	AIR0101	Solenoid Valve	-----	Grainger	1	\$ 96.03 \$ 96.03
2	AIR0102	Solenoid Mounting Plate	Aluminum	-----	1	\$ - \$ -
2	AIR0103	1/4 NPT Tee Connector, Anodized AL	Aluminum	McMaster-Carr	1	\$ 22.79 \$ 22.79
2	AIR0104	1/4 NPT to AN-6 Adapter	-----	-----	1	\$ - \$ -
2	AIR0105	AN-5 Male to 1/4 NPT Male Adapter	-----	-----	1	\$ - \$ -
2	AIR0106	1/4"-20 Hex Bolt - 1in	-----	McMaster-Carr	4	\$ - \$ -
2	AIR0107	1/4"-20 Hex Nut	-----	McMaster-Carr	4	\$ - \$ -
2	AIR0108	Air-Start Mounting Plate	-----	McMaster-Carr	1	\$ - \$ -
2	AIR0109	Solenoid Support Bracket	-----	McMaster-Carr	1	\$ - \$ -
0		Throttle Position Sensor System				
1	TPS0100	Throttle Position Sensor Assembly				
2	TPS0101	Potentiometer	-----	DigiKey	1	\$ 5.34 \$ 5.34
2	TPS0102	Sensor Bracket	AL 6061	-----	1	\$ - \$ -
2	TPS0103	Helical Coupling	-----	McMaster-Carr	1	\$ 58.25 \$ 58.25
2	TPS0104	Throttle Actuator	-----	-----	1	\$ - \$ -
2	TPS0105	1/4"-20 Hex Bolt	Steel	McMaster-Carr	2	\$ - \$ -
2	TPS0106	1/4" Washer	Steel	McMaster-Carr	2	\$ - \$ -
2	TPS0107	1/4"-20 Flange Nut	Steel	McMaster-Carr	2	\$ - \$ -
2	TPS0108	3/8"-16 Hex Bolt	Steel	McMaster-Carr	2	\$ - \$ -
2	TPS0109	3/8" Washer	Steel	McMaster-Carr	2	\$ - \$ -
2	TPS0110	Strut Channel	Steel	McMaster-Carr	2	\$ - \$ -
2	TPS0111	Base Plate	AL 6061	-----	1	\$ - \$ -
2	TPS0112	Tee Nut	Steel	McMaster-Carr	2	\$ - \$ -

Purchased Parts Total: \$ 304.18

Design Verification Plan

Turbine Team DVP&R												
Report Date: 6/15/2017		Sponsor:		Patrick Lemieux			Component/Assembly:	JFS-100 Engine	REPORTING ENGINEER:	Dorian Capps, Zoe Tuggle		
TEST PLAN								TEST REPORT				
Item No	Specification or Clause Reference	Test Description	Acceptance Criteria	Test Responsibility	Test Stage	SAMPLES		TIMING		TEST RESULTS		NOTES
						Quantity	Type	Start date	Finish date	Quantity	Pass	
1	Thermocouple Accuracy	Connect thermocouple to calibrator and Insert into ice bath. Repeat using boiling water. Perform for each new thermocouple.	Thermocouple output should be 32±2°F and 210±2°F for ice bath and boiling water, respectively	Dorian Capps	DV	3	B	5/5/2017	5/8/2017	Pass	All	N/A
7	Overtemp Shutoff	Connect the calibrator to each critical thermocouple port, and input temperature values that exceed the shutoff threshold of each channel.	Main power to the engine should be shut off immediately	Dorian Capps	DV	3	B	5/28/2017	6/4/2017	Pass	All	N/A
2	Overspeed Shutoff	Slightly lower G.G. speed threshold, purposely overspeed the engine. Repeat for dyno speed.	Main power to the engine should be shut off immediately	Dorian Capps	DV	3	B	6/2/2017	6/8/2017	Pass	All	N/A
3	Start-time warning	Slightly lower the start-time threshold, run the starter for longer than the threshold without injecting fuel to ensure the engine doesn't start	Warning light should illuminate immediately	Zoe Tuggle	DV	3	B	6/2/2017	6/8/2017	Pass	All	N/A
6	TPS Calibration	Operate throttle throughout full range (0-100%)	Both TPS measurements should remain within 0.5% of each other throughout entire range of actuation	Dorian Capps	DV	5	B	Unknown	Unknown	Incomplete	N/A	N/A

APPENDIX H

JFS100 Operator's Manual

Start-up Procedure

1. Inside Test Cell

- Connect two 12V batteries to the 24V connector
- Turn on cooling water valve
- Turn on exhaust vent fan
- Turn on fuel pump
- Open HEX water supply
- Open HEX water return
- Fuel selector valve: set to 'diesel'

2. Outside Test Cell

- Turn on cooling tower switch
- Verify that fuel tank is full (Jet A only)
- Verify tank quick disconnect
- Record atmospheric pressure
- Turn on Cellmate
- Turn on lower Testmate
- Turn ON breaker for dyno field
- Verify "AC Dyno Power" red light on Testmate rear panel is ON
- Turn on right remote Testmate control panel
- Turn on right dyno computer.
- Open HCmain.exe
- Reset N1 channel
- Open/start history file (Calpoly.his, z: drive)
- Open JFS100 display

3. On Remote Testmate Control Panel

- Turn on Panel Enable
- Turn on Aux. Power
- Turn on Throttle Power
- Toggle on "Diesel" control button
- Set Dyno Control to Absorb and Torque
- Set Engine Control to "%Throt Position"
- Set 40% throttle position

4. To Run

- Turn on two oil pump switches on display; verify HEX oil pressure (approx.. 2psig)
- Toggle on Ignition (master)
- Toggle on Fuel (Run/Abort)

References

- [1] Hill, P., Petersen, C., 1992. "Mechanics and Thermodynamics of Propulsion." Addison Wesley Publishing Company, Inc.
- [2] Leone, D., "A-7 Corsair II and the Val Program." <https://theaviationist.com/2013/08/07/a-7-program/>
- [3] Allied Signal, "Gas Turbine Engine Power Unit Maintenance Manual, Parts Catalog, JFS-100-13A, Jet Fuel Starter Unit," Allied Signal, Dist. Jim Vos
- [4] <http://jfs100jets.com/>
- [5] Kurz, R., 2005. "Gas Turbine Performance," *Proceedings of the Thirty-Fourth Turbomachinery Symposium*, Turbomachinery Laboratory, Texas A&M University
- [6] Korakianitis, T., Wilson, D. G., 1998. "The Design of High-Efficiency Turbomachinery and Gas Turbines." Prentice Hall, Upper Saddle River, NJ.
- [7] Glaser, A. J., Caldwell, N., Gutmark, E., 2007. "Performance of and Axial Flow Turbine Driven by Multiple Pulse Detonation Combustors," American Institute of Aeronautics and Astronautics, NV
- [8] Glaser, A. J., Caldwell, N., Gutmark, E., 2006. "Performance Measurements of a Pulse Detonation Combustor Array Integrated with an Axial Flow Turbine," American Institute of Aeronautics and Astronautics, Reno, NV
- [9] *Turbokart.com*. N.p., n.d. Web. 10 Feb. 2017.
- [10] "Garrett JFS 100-13A Turboshift engine (Zodiac powerplant - kit airplane)." *Garrett JFS 100-13A Turboshift engine (Zodiac powerplant - kit airplane)*. N.p., n.d. Web. 10 Feb. 2017.
- [11] Smith, K., 2012. "Gas Turbine Governing Dynamics and Control," California Polytechnic State University, San Luis Obispo
- [12] Turbine Technologies, LTD., 2010. "TurboGen, Gas Turbine Electrical Generation System Sample Lab Experiment Procedure," Turbine Technologies, LTD., Chetek, Wisconsin
- [13] Witkowski, T., White, S., Ortiz Duenas, C., Strykowski, P., Simon, T., 2003. "Characterizing the performance of the SR-30 Turbojet Engine," University of Minnesota.
- [14] Perez-Blanco, H., "ACTIVITIES AROUND THE SR-30 MINILAB at PSU," Mechanical and Nuclear Engineering – The Pennsylvania State University
- [15] "TEMPERATURE AND PRESSURE MEASUREMENTS IN A TURBINE ENGINE," Georgia Institute of Technology – Daniel Guggenheim School of Aerospace Engineering
- [16] Myre, D., "EA429 Course Objectives," United States Naval Academy
- [17] "XL-PMI - Retired Product." *GE Digital Solutions*. N.p., 23 Mar. 2016. Web. 10 Feb. 2017.
- [18] "Waspaloy Tech Data." *Waspaloy Tech Data*. N.p., n.d. Web. 10 Feb. 2017.
- [19] Cain, P., "Pot vs. Sensor," Piher International, Libertyville, IL